IN-29
J6016
119P

NASA Technical Memorandum 103775

An Examination of Anticipated g-Jitter on Space Station and Its Effects on Materials Processes

Emily S. Nelson
Lewis Research Center
Cleveland, Ohio

September 1994

National Aeronautics and
Space Administration

Executive Summary

The development of a viable materials science laboratory for use in the space environment is not a trivial task. There are a host of engineering intricacies associated with the design of such a quiet low-gravity environment on an inhabited mechanical space platform. Furthermore, the fundamental issues associated with the use of such an environment are not yet fully understood. Unfortunately, the level of sophistication and specificity necessary to adequately address either of these aspects of the problem makes it difficult to acquire perspective of the broad issues involved. In this report, the focus is on the role of the time-dependent variation of the body force in orientation and magnitude in the low-gravity environment. Commonly known as g-jitter, this residual acceleration arises from the contributions of aerodynamic and aeromechanical forces, routine crew activity, and equipment operation. The goal of this work is to describe the likely acceleration environment aboard Space Station Freedom based on current specifications and our space experience to date; to review what we currently know about the effects of gravity modulation on various classes of materials processing problems; to identify areas in which our knowledge about the effects of g-jitter are deficient; and to recommend actions which will allow us to scientifically approach the role of the acceleration environment on materials processing.

This work attempts to compile within a single document the current state of knowledge regarding g-jitter. Consequently, it does not presume to be fully comprehensive regarding subjects which have been the focus of scholarly attention for decades, but rather hopes to indicate the basic issues, findings and recommendations specific to g-jitter. In keeping with the objective of providing an easy-to-use reference for a broad audience, each section is designed to stand alone, causing some inevitable redundancy. Appendices provide definitions of important nondimensional numbers, a bibliography by subject, a discussion of analytical techniques, and a brief review of some available accelerometers.

Although some of the information contained in this document is specific to the baseline configuration for Space Station Freedom (hereafter SSF), the bulk of this work is intended to be qualitative and therefore applicable to any space structure. All such platforms will be subject to structural oscillation; once-per-orbit variation in residual acceleration sources such as atmospheric drag; and the disturbances engendered by thruster firings, mass translations, facility operations, and, when inhabited, by crew activities. In addition, the information and conclusions of this work are applicable not only to materials science but, due to their fundamental nature, also have direct relevance to fluid physics and some life sciences experimentation.

The current theoretical/experimental database is insufficient for specific predictions for a given process, because it lacks adequate environment characterization and explicit correlation to particular processes. However, the growing body of knowledge is large enough to indicate general qualitative trends which are by now indisputable. Important highlights of this work include the following (refer to the cited sections for additional details):

- SSF environment specification of tolerable residual acceleration levels as a function of frequency is inadequate to assure a quality low-gravity environment because it:
  - is based on an oversimplified order-of-magnitude analysis which limits its applicability to single-frequency harmonic disturbances;
  - does not address the deleterious and potentially disastrous effects of multifrequency summation (2.1, 2.2.2.1, 3.1.2.2);
  - does not resolve the contribution of impulsive transients (2.1, 2.2.3, 3.1.3);
  - lacks sufficient experimental validation at this time.
- To meet even current specifications for the low-gravity environment aboard SSF, it will be necessary to:
  - prohibit thruster firings during time allotted to low-gravity research (2.1, 2.2.3.1, 2.5);
  - limit the large-magnitude impulsive disturbances caused by crew activity (2.1, 2.2.3.2);
  - require vibration isolation of major sources of disturbance, particularly the exercise equipment and centrifuge, as well as isolation of some of the experiments themselves since some acceleration sources, such as structural oscillation, cannot themselves be isolated (2.1, 2.2.2.2, 2.2.2.3, 2.4).
- The orientation of g, which may be a critical determinant of sensitivity for certain processes, will likely be unpredictable due to the wide variety of disturbance sources (2.1, 2.3).
- Examination of the sources of residual acceleration (2.2) indicates that scaling down SSF may provide a more beneficial residual acceleration environment *if* it reduces atmospheric drag due to a more compact structure (2.2.1.2); utilizes a higher-frequency structural resonance regime (2.1, 2.2.2.1, 3.1.2, 3.2.2); and places the laboratory spaces closer to the center of mass. However, smaller free flyers placed in higher polar orbits would likely provide an even better platform, strictly from g-jitter considerations alone.
- Based on a limited database, some processes, particularly those with large density gradients such as crystal growth from the melt, may not be successfully performed in the relatively noisy environment of a large inhabited space structure (3.1.1.1, 3.1.1.2, 3.1.3.6).
- Impulses which are of short duration relative to the characteristic fluid diffusion time cause predictable behaviors in buoyancy-driven fluid systems (3.1.3.1, 3.1.3.2, 3.1.3.5) and can be directly related to process sensitivity:
  - Maximum disturbance to momentum field was found to be proportional to the integrated (time-dependent) acceleration input;

- Long-term behaviors of momentum, solute and thermal fields were not dependent on the shape of the pulse, but rather on its integrated acceleration input and the fluid properties.

- Fluid systems subject to buoyancy-driven flows have been shown to exhibit an additive response to multiple-frequency disturbances (except perhaps near resonance conditions) (3.1.2.2).

Recommendations for future work include:

- A large-scale, highly coordinated and intensive research effort geared at specifically addressing the development of practical experiment-specific sensitivity requirements in a timely manner for SSF designers. This effort can be based on existing work, but requires close collaboration among researchers, SSF designers and equipment contractors, and furthermore, must be given the appropriate priority to result in timely, relevant and meaningful specifications.

- Well-resolved acceleration measurements on both the Orbiter and SSF in the vicinity of the experiments must be made frequently and routinely. Such data will be critical for:
  - Correlation of g-jitter effects to specific experiments;
  - Accurate numerical modeling and physical understanding of same;
  - Monitoring of the process to assure integrity of the experiment;
  - The possibility of tailoring experiments to the environment (rather than vice versa).

- Tightly coupled space experiments and numerical analysis specifically designed to provide a greater understanding of this topic.

- Use of a free flyer for critical materials experiments which cannot be performed on SSF or on the Orbiter.

- More sophisticated numerical modeling, including detailed *three-dimensional transient* analysis with nontrivial effects such as radiation heat transfer and surface-tension driven flows when appropriate, and accurate quantification of physical properties.

The potentially profound effects of g-jitter on materials processing have not been *fully* appreciated until recently. Nevertheless, our physical understanding has increased dramatically through the use of numerical modeling and even limited space experimentation. This author feels that it is not sufficient to dismiss the current knowledge as too sparse and subjective and to simply wait until SSF is built for definitive data. Optimal use of this unique environment requires the intelligent design of both experiments and experimental platforms and must consider more fully the time- and direction-varying properties of the acceleration environment.

This page intentionally left blank

Table of Contents

Nomenclature

a_d - acceleration arising from atmospheric drag

a_t - acceleration arising from tidal forces

A_p - projected area of space vehicle

$\underline{b}$ - body force

Bo - Bond number = $\rho g L^2/\sigma$

c_i - concentration of species i

C_d - drag coefficient

C_p - heat capacity

D - diffusion coefficient

e - energy

f - frequency

g_o - gravitational acceleration at sea level = 9.81 m/s^2

Gr - Grashof number = $g\beta\Delta T L^3/\nu^2$

L - characteristic length

m - mass

Ma - Marangoni number = $\sigma\Delta T L \left(\frac{\partial\sigma}{\partial T}\right)/\rho\nu^2$

p - pressure

Pr - Prandtl number = ν/κ

R - radius of cylinder

Ra - Rayleigh number = $g\beta\Delta T L^3/\nu\kappa$

Sc - Schmidt number = ν/D

t - time

T - temperature

$\underline{V}$ - velocity

V_p - pulling rate

Greek Symbols

α - coefficient of solutal expansion

β - coefficient of thermal expansion

ρ - density

ν - kinematic viscosity

μ - absolute viscosity

κ - thermal diffusivity

σ - surface tension

1. Objective

In some quarters, it has become accepted as almost axiomatic that performing materials science in any space environment will automatically enhance the quality of convection-dominated materials processes, from the solidification of semiconductors to the growth of exotic organic molecules. It is also clear that, despite the significant efforts in applied microgravity science over the past 20 years, relatively few unambiguous success stories can be told. While many factors contribute to a success or failure of a space experiment, experience and analyses are beginning to address even more fundamental questions, especially as regards the adequacy of these environments for all such applications. Here, we consider specifically the effects of g-jitter, i.e., the time-dependent variation of the body force in magnitude and orientation. This residual acceleration arises from the contributions of aerodynamic and aeromechanical forces, routine crew activity, and equipment operation. The goal of this work is to describe the likely acceleration environment aboard Space Station Freedom based on current specifications and our space experience to date (although the conclusions are general enough to be valid for any large space structure); to review what we currently know about the effects of gravity modulation on various classes of materials processing problems; and to identify areas in which our knowledge about the effects of g-jitter are deficient.

This topic is by its nature immensely broad, leapfrogs across disparate engineering and scientific disciplines, and continues to provoke controversy among the scientific community. Consequently, this work does not presume to be fully comprehensive, but rather serves to provide some fundamental background, to gather much of the available knowledge into one report, to highlight some of the important issues and to raise some questions which ought to be considered carefully. The objective of providing an easy-to-use reference on the subject of g-jitter requires some redundancy in the information presented here.

The paper describes the realities of the low-gravity environment in section 2, as recorded on the Orbiter and other low-earth orbit facilities, and outlines the expectations for Space Station Freedom; next, a review of what is currently known about the effects of g-jitter on a variety of materials processes in section 3; followed by conclusions and recommendations in section 4.

2. Characterization of the low-gravity environment

To date, a low-gravity environment can be realized for a couple of seconds in a drop tower; tens of seconds on a Learjet or KC-135; several minutes aboard a sounding rocket; or several hours, possibly days, aboard the Orbiter and the anticipated Space Station Freedom (SSF). However, even aboard the Shuttle, this is not the quiescent environment with an unchanging and benevolently low-level gravitational field originally envisioned by space processing advocates. In addition to the residual acceleration arising from aerodynamic and orbital mechanical forces, other disturbances such as the firing of rocket thrusters for positional orientation or reboost; mass translations; impulsive crew motions, their respiration and exercise; and the background vibration of machinery and structural vibration all combine to produce a broad spectrum of body forces at any given location in the space vehicle. It is not out of line to presume that the variation in the instantaneous body force will vary significantly with amplitudes of up to 10^{-2} g_0 (where g_0 is the gravitational acceleration at sea level), will be comprised of both multiple-frequency oscillatory components as well as impulsive transients, and will significantly deviate in terms of orientation. This complex and highly unsteady acceleration field will likely play a dominant role in many materials processes and in fluid physics. It is therefore imperative that the consequences of *g*-jitter be carefully considered when designing or numerically modeling a space experiment.

2.1 The total environment

In their compilation of experimentally obtained acceleration characteristics, Chassay and Schwaniger (1986) (hereafter C&S) routinely document acceleration levels of 10^{-3} g_0 in the low-gravity environment of Skylab and Shuttle missions. The largest accelerations are due to the primary thruster firings on the order of 10^{-2} g_0, as can be seen in figure 1, which represents an orbital maneuvering system (OMS) burn on the D1 mission. Note that there are appreciable components of body force generated in all three dimensions, up to the saturation level of 1×10^{-2} g_0. Table 1 documents the acceleration peaks in all three primary directions due to various sorts of disturbances which were recorded on Spacelab 1, both on the experimental pallet and in the module. These represent typical results from the Shuttle (see, e.g., C&S, Hamacher et al., 1986a-c, 1987; Rogers and Alexander, 1991a, b; Dunbar and Thomas, 1990; Schoess, 1990). Even during quiet time, the mean measured body force levels were found to be about 10^{-4} g_0 (C&S). The "best" recorded environment of all the low-*g* vehicles surveyed by C&S was aboard the June 1983 SPAR-X free flyer with typical accelerations of order 10^{-5} g_0 with peaks of 10^{-4} g_0. It should be noted that this vehicle operated in low-earth orbit; free flyers which are located at higher altitudes may pro-

FIGURE 1. Temporal accelerometer record from Spacelab 1 Orbital Maneuvering System (OMS) burn (after Hamacher et al., 1986a)

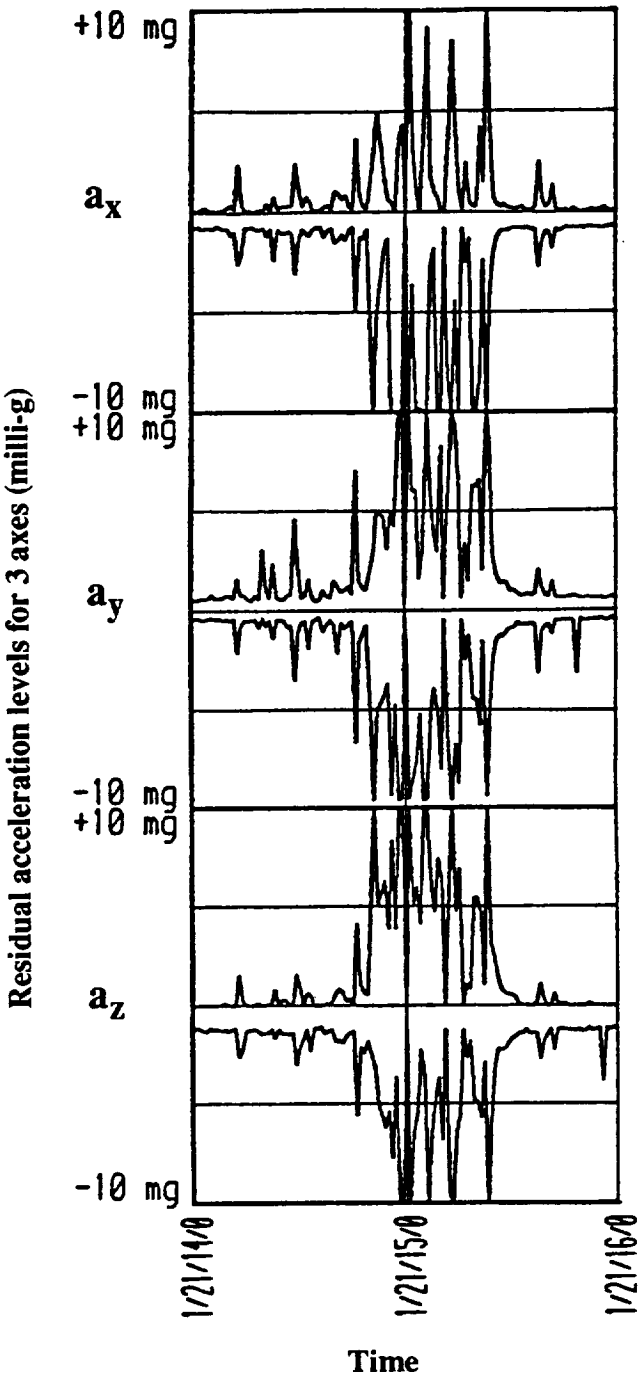

TABLE 1. Experimentally measured peak accelerations on Spacelab 1 (after Chassay and Schwaniger, 1986)

	MODULE			PALLET		
	X–DIRECTION	Y–DIRECTION	Z–DIRECTION	X–DIRECTION	Y–DIRECTION	Z–DIRECTION
"QUIET TIME" 11.18–11.23 HRS AMPLITUDE (mg) FREQUENCY (Hz)	0.35 – 0.4 20 –35	0.25 22 – 40	0.5 – 0.65 17 – 40	0.13 – 0.26 22	0.2 – 0.45 22	0.13–0.25 8 – 16
COUGH TEST 11.314 – 11.315 HRS AMPLITUDE (mg) FREQUENCY (Hz)	1.0 10	1.0 11	2.8 9	0.2 10	0.3 8	0.7 10
X–PUSH–OFF 11.340 – 11.355 HRS AMPLITUDE (mg) FREQUENCY (Hz)	2.8 12	3.0 21	2.5 9	0.6 12	1.0 6	1.2 8
Y–PUSH–OFF 11.375 – 11.385 HRS. AMPLITUDE (mg) FREQUENCY (Hz)	0.1 16	1.0 21	2.4 8	0.3 18	0.5 15	0.5 8
Z PUSH–OFF 11.404–11.406 HRS. AMPLITUDE (mg) FREQUENCY (Hz)	1.1 12	1.0 20	1.7 16	0.7 15	1.1 17	1.0 9
VERNIER THRUSTER FIRING 202050–202110 SEC. (111 NEWTONS) AMPLITUDE (mg) FREQUENCY (Hz)	0.3 – 0.5 17	0.3 – 0.6 25	0.5 – 1.0 18	NOT AVAILABLE	NOT AVAILABLE	NOT AVAILABLE
PRIMARY THRUSTER FIRING 188.870–188.930 HRS. (3,870 NEWTONS) AMPLITUDE (mg) FREQUENCY (Hz)	25 – 29 9	20 – 29 9	2.5 – 2.9 9	10 – 15 8	10–15 16	20 – 29 16
TUNNEL TRUNNION DISTURBANCE 188.431 – 188.435 HRS. AMPLITUDE (mg) FREQUENCY (Hz)	12 13	6.0 20	9.0 15	2.5 12	2.4 25	3.0 12

vide an even better environment. Other clever concepts to minimize the quasisteady residual acceleration levels have been developed, such as flying a free-floating mass within a cavity at the center of mass and actually flying the surrounding spacecraft centered to this reference. Very low mean background levels can thereby be realized, but the presence of g-jitter may remain an issue in the quality of the residual acceleration environment.

As shown in table 2, the relative importance of the following sources of residual acceleration can be roughly ranked in terms of magnitude as: thruster firings (10^{-2} g_0); crew activities (10^{-2} to 10^{-5} g_0); atmospheric drag (10^{-5} to 10^{-8} g_0); gravity-gradient accelerations (10^{-5} to 10^{-8} g_0); fluid dumps (10^{-5} to 10^{-6} g_0); structural vibration (predicted to be of order 10^{-7} g_0 at the fundamental structural frequency of about 0.17 Hz); and solar radiation pressure (10^{-8} to 10^{-9} g_0). In addition, there is an enormous variability in the net orientation of the gravitational vector, as was apparent from figure 1. This will be discussed further in section 2.3.

Disturbances are classified into three categories for the purposes of Space Station Freedom (SSF) specifications: quasisteady, oscillatory and transient. *Quasisteady* disturbances are residual accelerations which are maintained for tens of minutes and arise from drag, tidal, and Keplerian accelerations. *Oscillatory* body-force components are harmonic and periodic in nature and can include the effects of repetitive crew activity; rotating and reciprocating equipment for fluid, attitude, and environmental control, experiment operations, and the payloads themselves; and steady structural oscillations arising from SSF itself as well as individual structural components, e.g., communication and tracking devices. *Transient* disturbances include all other time-dependent disturbances to the low-gravity environment such as thruster firings, latch opening and closing, mass translations, impulsive crew activities, etc.

The specification of the allowable residual acceleration field has been part of an ongoing process of collaboration between potential users of the low-gravity environment and SSF designers. This has been an enormously difficult task, partly because SSF is required to perform a multitude of tasks in addition to providing a quality low-gravity environment for materials science and fluid physics. These include servicing and launch of satellites, accommodation of Shuttle dockings (or berthings), monitoring the planet earth, providing a laboratory facility for life sciences experiments, etc. Another tremendous complication is that the ramifications of working in a low-gravity environment are not fully understood by materials scientists at present because space processing is still at a relatively immature stage in its development.

TABLE 2. Comparison of residual acceleration sources aboard the Orbiter and on Space Station Freedom (disturbance types are classified as Q.S. = quasisteady; O = oscillatory; T = transient)

Body Force	Type	Shuttle	Space Station
Tidal	Q.S.	$4 \times 10^{-7}\ g_0$ / m	$4 \times 10^{-7}\ g_0$ / m
-gravity gradient			
-centrifugal			
Euler $(\frac{\partial \Omega}{\partial t})$	Q.S.	usu. neglected	$10^{-7}\ g_0$ at 10^{-4} Hz
Atmospheric drag	Q.S.	$3 \times 10^{-6}\ g_0$ at 170 km $2 \times 10^{-8}\ g_0$ at 560 km	10^{-8} to $10^{-5} g_0$
Altitude control	T		
-primary thruster firings		$3 \times 10^{-2}\ g_0$*	5x per year
- vernier thruster firings		10^{-3} - $10^{-4}\ g_0$	
Gas and fluid dumps	T	$10^{-5}\ g_0$	‡
Structural vibration	O	app. 5, 7, and 11 Hz	fundamental 0.17 Hz
- KU band antenna	O	$10^{-2}\ g_0$ at 17 Hz*	‡
Crew motion	T, O	10^{-2} - $10^{-5}\ g_0$*	‡
Machinery	T, O	$10^{-4}\ g_0$ at >100 Hz*	‡
Centrifuge	T, O	‡	$10^{-5}\ g_0$ at 0.3 Hz †
Solar radiation pressure	Q.S.	$4 \times 10^{-9}\ g_0$	$1 \times 10^{-8}\ g_0$
TOTAL		10^{-3} - $10^{-4}\ g_0$	

* Experimentally measured acceleration peaks
† Estimate from calculation for 1.8 ft. dia. centrifuge (Searby, 1986)
‡ Unknown or not applicable

Although it would be ideal to have the SSF acceleration environment at true microgravity acceleration levels (i.e., 10^{-6} g_0) or less over the entire frequency range, this is simply not possible from a design standpoint. It may not be mandatory from the standpoint of heat and mass transport either (with some provisos). Since there is a finite fluid response time associated with a disturbance, in general, the tolerance to single-frequency harmonic residual acceleration to a a given materials process increases with increasing frequency. (This will be discussed in further detail in section 3; see, e.g., sections 3.1.2 .) This understanding forms the basis for a specification in the form of a design curve of allowable residual acceleration level as a function of frequency.

Figure 2 shows the design curves for maximum frequency-dependent residual acceleration levels of a portion of the SSF laboratory experiment spaces (see, e.g., Space Station Freedom Microgravity Environment Definition, 1988). The lower curve (solid line; the so-called "microgravity vibration requirement") attempts to characterize the desirable residual acceleration limits during the quiet time allotted to materials science experimentation.

FIGURE 2. Allowable g-levels as a function of frequency for Space Station Freedom

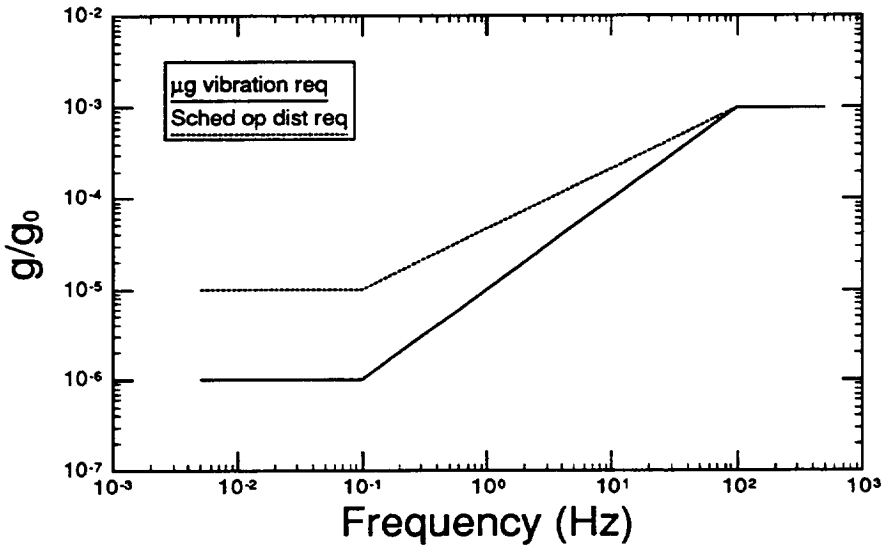

The upper curve (dashed line; the "schedulable operations disturbances requirement") represents a (probably) more realistic depiction of the design environment, subjected to disturbances such as crew exercise. The presumption is that the former curve can be adhered to when necessary for sensitive experiments by scheduling routine disturbances around these quiet times, but at no time should residual acceleration levels exceed the upper curve. Both curves are restricted to fairly low levels of allowable residual acceleration below the structural resonance frequency regime (for SSF configuration, the fundamental

structural vibration was calculated to be 0.17 Hz; Sullivan, 1990). Below 0.1 Hz, the maximum tolerable residual acceleration is less than 10^{-5} g_0. Above this value, the allowable g-level increases with frequency to a maximum value of 10^{-3} g_0 at 10^2 Hz.

The specifications for allowable residual acceleration levels are currently interpreted in the following manner: over a given time interval, the power spectral density of the laboratory environment can be determined as a function of frequency (e.g., in units of acceleration squared per Hz). The tolerable *g*-level for any given frequency increment Δf (the magnitude of which is seen in figure 2) is then the square root of the local value of the power spectral density curve integrated over the appropriate frequency range. This is a much less stringent requirement than looking at instantaneous magnitudes of the residual acceleration. For example, Rogers and Alexander (1991b) find that, for their discretization, the acceleration environment on Spacelab 3 produced frequency components in the range of 4.5×10^{-3} to 50 Hz of magnitude 1×10^{-3} g_0 or less, as compared with absolute magnitudes of residual acceleration of up to 2.5×10^{-2} g_0.

However, without additional constraints, this interpretation does not guarantee a low-gravity environment suitable for materials processing. For example, the instantaneous *g*-level is *unbounded* without a fixed value for Δf and for the upper and lower limits on the frequency range. Another consideration is that the effects of impulsive transients are not adequately addressed with this form of the specifications. (It should be noted that the integrated acceleration with respect to time, which is related to the momentum input to the system, might be one reasonable means of incorporating the effects of transient disturbances into the environment definition; see sections 2.2.3 and 3.1.3).

Figure 3 shows the calculated acceleration environment on SSF resulting from two disturbances considered separately. The microgravity vibration requirement is also provided for easy reference. The hab soar[1] by a crew member in the laboratory module, shown in figure 3(a), indicates that a large peak is generated at 0.34 Hz (twice the fundamental structural frequency). In figure 3(b), the operation of one version of the life sciences centrifuge under the chosen operating conditions will yield significant contributions at about 0.6 Hz and at other peaks in the range of 0.2 - 4.0 Hz. In order to allocate allowable *g*-levels to various disturbance sources, SSF designers compute similar spectra for anticipated residual acceleration sources considered individually. At any given frequency, the linear sum of the resultant spectra should not exceed the design curve of figure 2. The difficulty with this interpretation of the specifications is that at any given moment in time, the low-gravity ex-

1. A hab soar is a pushoff by a crew member from the habitat wall to translate to a new position.

periment will "feel" the effects of all of the frequencies. The body force which modulates

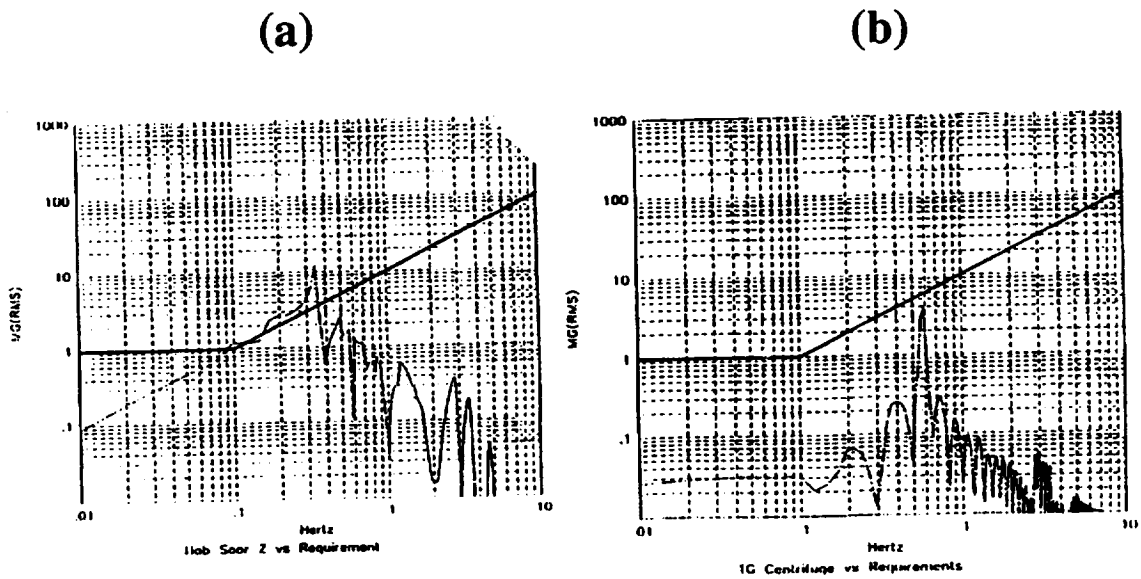

FIGURE 3. Acceleration environment resulting from (a) hab soar; and (b) operation of centrifuge (after Lindenmoyer, 1989)

at 0.17 Hz must be combined with the residual acceleration contribution of the centrifuge at 0.2 Hz, for example, in addition to all of the other frequency-dependent accelerations. Granted, the phase relationship between the various signals will mean that some frequency components will detract from the net resultant body force, but, just as surely, some components will augment each other at some point in time. This requires that the sensitivity analysis used to develop the tolerance criterion *must* consider the effects of multifrequency disturbances.

However, at the time these specifications were written, the potentially profound effects of *g*-jitter were just beginning to be recognized by the materials science community. The early qualitative analysis of materials science and fluid physics experiments used to determine this form of the specification considered the body force to be represented by a *single*-frequency axially directed harmonic modulation; that analysis did *not* address the combined effects of multiple-frequency and impulsive disturbance inputs. This is now understood to be a major shortcoming.

It should be noted that only half of the laboratory experiment spaces would be subject to these requirements; the residual acceleration levels in the other 50% of the laboratory spaces would have an undefined, but almost certainly more noisy, acceleration environ-

ment. One would expect that the particular 50% which are subject to the requirement would not change during the course of an experiment. In any case, it is obvious that care will need to be given in assigning laboratory space, especially since these spaces may vary in accessibility and power availability.

The existing SSF specifications were derived from analysis which considered the response to a single-frequency axially directed harmonic disturbance. However, this does not adequately represent the complex, multifrequency and transient acceleration inputs which will undoubtedly be inherent in any version of SSF. The response of materials processes and fluid physics experiments to impulses and transient disturbances, discussed in section 3.1.2.2, may be quite different from the response to steady sinusoidal disturbances; thus the specifications, based only on steady sinusoidal disturbances, offer limited value. Unfortunately, little information on transient disturbances was available when the specifications were written. One sensible approach might be to consider the integrated acceleration with respect to time which is input into the system. This will be discussed further in sections 2.2.3, 3.1.3 and 3.2.3.

It is absolutely essential that the overall g level, the total integrated acceleration content of transients, and the effects of multiple-frequency and impulsive disturbances be addressed in order for the specifications to fully address problems pertinent to materials science, life sciences and fluid physics community.

2.2 The sources of residual acceleration

Examination of the individual components of residual acceleration which combine to produce the often noisy and variable residual acceleration environment follows. For consistency with Space Station designers, this paper is arranged to address the low-*g* environment and its concomitant effects on materials processes with their classification of quasisteady, oscillatory and transient forces as a framework. For additional and complementary discussion:

- on the sources of residual acceleration, see Alexander (1990); Alexander and Lundquist (1988); Ostrach (1982); Knabe and Eilers (1982); Feuerbacher et al. (1988); Hamacher et al. (1986a-c; 1987); and Naumann (1988b).
- on the recorded space environment, see Dunbar and Thomas (1990); Dunbar et al. (1991a, b); Schoess (1990); Rogers and Alexander (1991a, b); Hamacher et al. (1986a-c, 1987); and Chassay and Schwaniger (1986).

2.2.1 Quasisteady forces

Quasisteady forces can be expected to remain essentially constant for tens of minutes. Consequently, forces which vary periodically in a single-frequency fashion over the course of an orbit fall in this category, for Space Station Freedom, about once every 90 minutes or approximately 1.9 x 10^{-4} Hz.

2.2.1.1 Tidal accelerations

Only when an object is placed physically upon the space vehicle/structure's center of mass (CM) will centrifugal and gravitational forces exactly cancel each other. On the other hand, if the object is located closer to or farther from the earth, its Keplerian orbit will be slightly different, and consequently a slightly different period will ensue, so that without an additional imposed acceleration on the object, it would slowly drift away from the CM. Many of the earliest low-*g* experiments, e.g., on board the Apollo spacecraft, located the experiment nearly at the CM due to the vehicle's small size. With the advent of larger space structures, this force becomes of increasing importance, because this force varies proportionally with distance from the CM, as well as altitude above the earth.

The residual gravitational acceleration imposed by off-CM location is the tidal acceleration, itself comprised of contributions from gravity-gradient and centrifugal forces. This tidal acceleration acts in both directions normal to the vehicle velocity. Hamacher et al. (1987) calculates contours of constant tidal acceleration in a plane normal to the velocity at an altitude of 300 km in figure 4. These contours are elliptical because the centrifugal force, which cancels the gravity-gradient force in the flight direction ($\underset{\sim}{x}$ in the figure), actually enhances the gravity-gradient acceleration in the local vertical direction.

FIGURE 4. Contours of constant tidal acceleration in the yz-plane at 300 km for the gravity-gradient mode (after Hamacher et al., 1987)

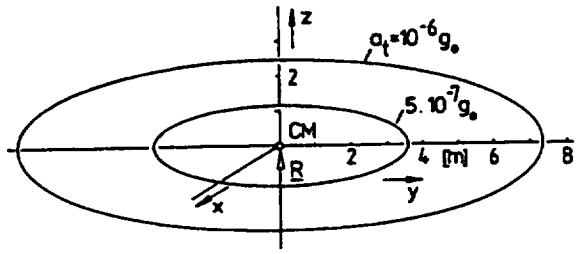

There are a couple of choices for the orbital mode of space vehicles, as shown in figure 5. The vehicle can remain fixed relative to some external celestial object, e.g., the sun, in the

inertial mode as shown in figure 5(a). Alternatively, in the gravity-gradient stabilized mode (figure 5(b)), the position of the vehicle remains fixed along a radius emanating from the earth's center of mass. The advantage of the inertial mode is that the vector sum of the induced acceleration from quasisteady tidal and drag forces (represented in the figure by a_t and a_d, respectively) at some location in the space vehicle would theoretically net to zero over one orbit (if a_d were constant in magnitude). However, this means that the orientation of the imposed gravitational field due to this component would continuously vary. The gravity-gradient stabilized mode requires fewer thruster firings for positional

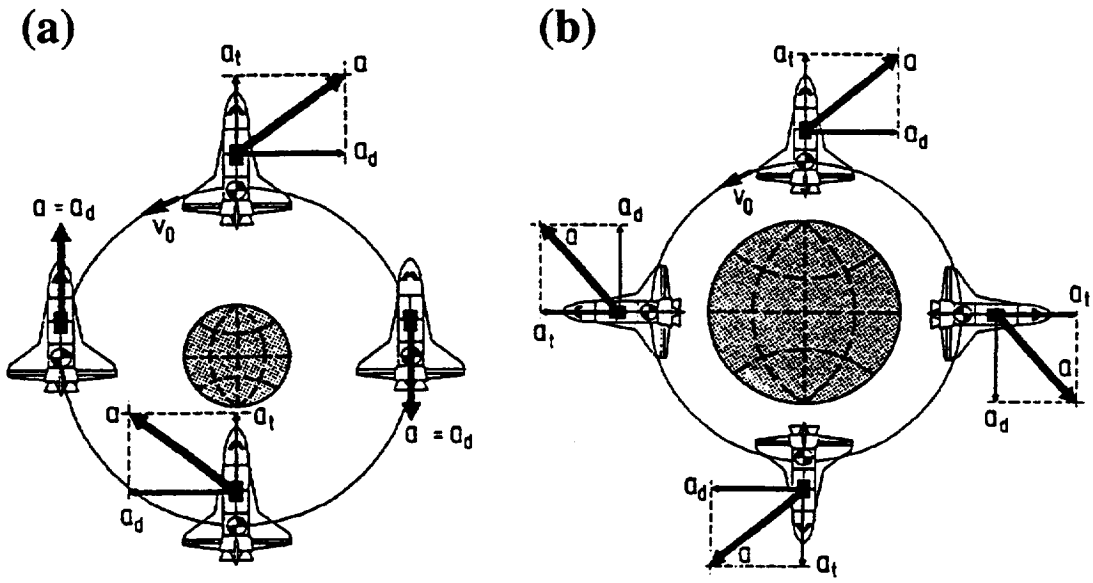

FIGURE 5. Comparison of Orbiter orientation for (a) inertial; and (b) gravity-gradient flight modes (after Feuerbacher et al., 1988)

correction, and in addition the orientation of the vector sum of these two forces is less variable, both of which are desirable from a materials processing standpoint.

In addition to altitude, tidal forces are related to location from the center of mass; so if the location of the CM changes due to mass translation or addition, some variation will appear. The advantage of the gravity-gradient stabilized flight mode is that the relative orientation of the net acceleration resulting from drag and tidal forces is less variable.

2.2.1.2 Aerodynamic drag

The magnitude of the quasisteady body force component due to aerodynamic drag, a_d, is a function of the density of the atmosphere, ρ (and therefore, the altitude, the time of year and solar flux levels), the vehicle velocity V, the projected area of the vehicle A_p, and the

vehicle mass m:

$$a_d = \frac{1}{2}\frac{A_p}{m} C_d \rho V^2 \qquad (1)$$

where C_d is the drag coefficient. Drag acts in the direction opposing vehicle velocity. Local atmospheric density typically decreases with increasing altitude. SSF is expected to orbit the earth in the range of 190 - 210 n.m. (or about 350 - 390 km); it is limited by the van Allen radiation belt on the high end. In addition, the earth's atmosphere exhibits a diurnal bulge on the day side of the planet due to solar heating so that density varies at a given altitude over an orbital period.

Based on a drag coefficient of 2 and a mass of 9.1×10^4 kg for the Orbiter, Hamacher et al. (1987) calculate deceleration due to atmospheric drag on the Shuttle as a function of altitude, shown in figure 6. This is close to Ostrach's (1982) calculations of 3×10^{-6} g_0 at an

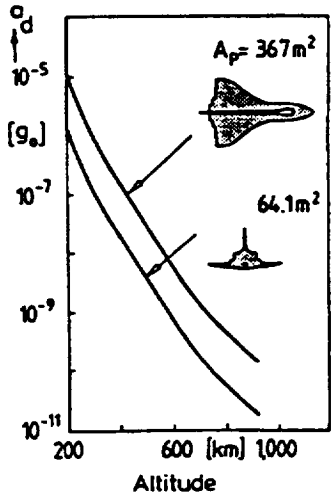

FIGURE 6. Calculated deceleration due to atmospheric drag as a function of altitude for the Orbiter (after Hamacher et al., 1987)

altitude of 170 km to 2×10^{-8} g_0 at 560 km for the Shuttle oriented in the gravity-gradient mode. Alexander and Lundquist's (1988) calculations also fall within this range with a worst-case and best-case scenario based on cited values of drag coefficient, shown in table 3.

At a given altitude, the structural complexity and larger surface area-to-mass ratio of Space Station Freedom will induce even larger drag than the Shuttle. The design goal is

for the atmospheric drag be in the range of $2\text{-}4 \times 10^{-7}$ g_0 and to vary by no more than a factor of 6 over one orbit. The atmospheric drag will vary through the course of an orbit for a variety of reasons. The projected area of SSF will change in an orbital period since the orientation of the solar panels will vary in response to SSF's orientation to the sun. Also, the

TABLE 3. Calculated drag for (1) the Orbiter and (2) Space Station Freedom based on (a) worst and (b) best estimated drag coefficients as a function of altitude (after Alexander and Lundquist, 1988)

Altitude (km)	Drag (μg) Shuttle C_D=0.059	Drag (μg) Shuttle C_D=0.01	Drag (μg) SSF C_D=0.3	Drag (μg) SSF C_D=0.09
275	2.10	0.360	10.6	3.1
300	1.20	0.210	6.1	1.8
325	0.69	0.120	3.6	1.1
350	0.41	0.070	2.1	0.6
400	0.24	0.025	0.7	0.2
450	0.05	0.009	0.4	0.1
500	0.02	0.001	0.8	0.02

attitude of SSF will vary somewhat within some tolerance range. In figure 7, Hamacher et al. (1987) calculate the deceleration of SSF caused by atmospheric drag resulting from changes of aspect angle, diurnal cycle, and variable solar activity at an altitude of 450 km over one orbit. Alexander and Lundquist (1988), on the basis of best and worst estimates

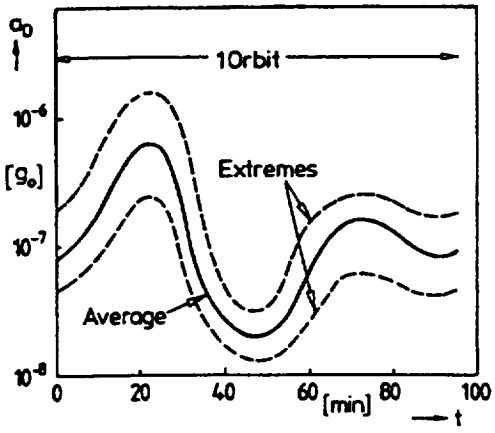

FIGURE 7. Calculated deceleration of Space Station Freedom due to atmospheric drag at 450 km (after Hamacher et al., 1987)

for drag coefficient and at varying altitudes tabulate a range of values for atmospheric drag on SSF from 1×10^{-5} g_0 to 2×10^{-8} g_0, as was shown in table 3. In the worst case, the

contribution of aerodynamic drag alone can put us out of the range of true "micro"gravity. A scaled-down version of SSF might decrease the magnitude of this residual acceleration source if it had a more favorable projected area-to-mass ratio. On the other hand, small platforms with large arrays of solar panels, such as EURECA and MEM, have larger A_p/m ratios than either the Orbiter or current version of SSF.

Calculation by SSF designers of atmospheric drag variation over an orbit, which includes more of the specifics of the SSF configuration OF-2, is shown in figure 8 (see Space Station program report, 1988). Notice that, while atmospheric drag is expected to be periodic,

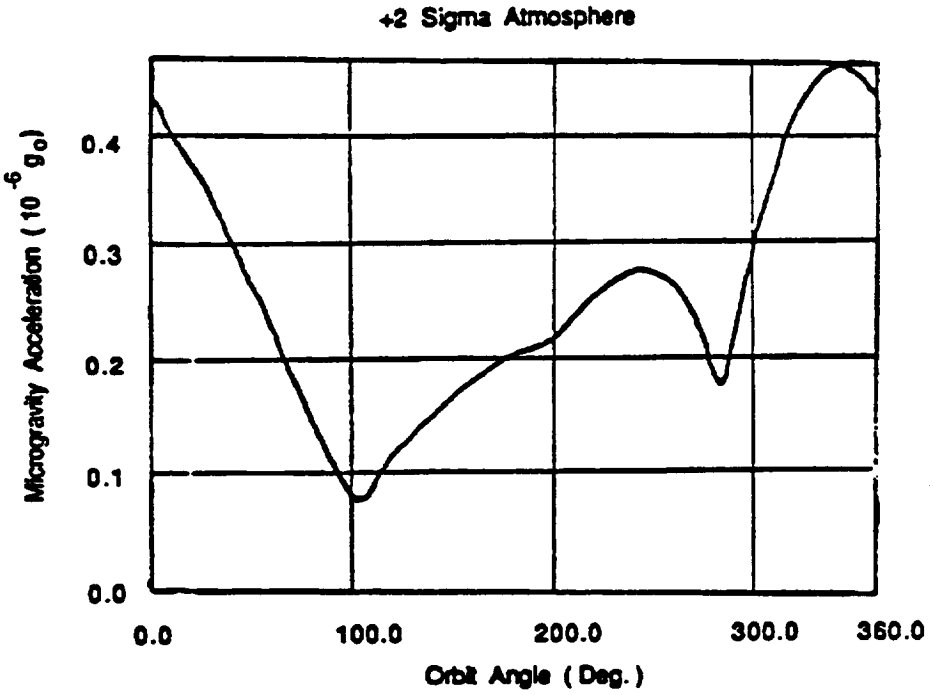

FIGURE 8. Deceleration of Space Station Freedom due to atmospheric drag in OF-2 configuration at torque equilibrium attitude (after Space Station Program Report, 1988)

it is not a single-frequency harmonic oscillation. In fact, there are some rather severe gradients which are apparent in the vicinity of roughly 100° and 290°, representing the transition from day to night and vice versa, which occur over the course of minutes rather than ten's of minutes. There may also be other disturbances generated by the large variation in solar insolation in the transition from day to night, such as thermal expansion and compression stresses which could generate strong structural oscillations. The fluid response to a given disturbance is related, among other things, to the time necessary for diffusion of momentum, heat and species relative to the characteristic time of the disturbance. Varia-

tion of the residual acceleration on the order of minutes may be significant in the determination of the viability of a particular materials process.

Atmospheric drag represents a significant, but probably not overwhelming, contribution to the overall acceleration field. However, the transition period from the heated day side of the earth to the colder night side exhibits some rather severe gradients. Especially if these variations are accompanied by other behavior such as structural oscillations from thermal expansion and compression stresses, these portions of the cycle could require careful attention. The magnitude of this acceleration source might decrease with a scaled-down version of SSF if its projected area-to-mass ratio is minimized.

2.2.1.3 Euler accelerations

Euler accelerations arise from the variation of angular velocity such as might occur from, e.g., an elliptical orbit, rather than a circular one. If the osculating eccentricity of the orbit is less than 10^{-6}, this is much smaller than the contributions from the preceding quasisteady forces (Alexander and Lundquist, 1988).

2.2.1.4 Coriolis accelerations

Coriolis accelerations occur whenever there is translation along a rotating path. These accelerations are ignored here but might be important if particles are moving in a vacuum or in a low-viscosity fluid (Alexander and Lundquist, 1988). Processes such as low-pressure physical vapor transport may therefore need to consider Coriolis accelerations in appropriately characterizing the acceleration environment.

2.2.1.5 Solar radiation pressure

The transfer in photon momentum induces a small but finite pressure variation directed away from the sun. Estimates by Hamacher et al. (1987) are 3.8×10^{-9} g_0 for the Shuttle or 1.1×10^{-8} g_0 for SSF.

2.2.2 Oscillatory disturbances

Oscillatory components of the residual acceleration are categorized as those which can be described by a sinusoidal modulation. The most problematic acceleration sources in this category are crew activity (potentially "large" in magnitude in a sensitive frequency range) and structural vibration (for SSF, in a critical frequency range). Other disturbances include equipment operation and environmental control.

2.2.2.1 Structural vibration

Every transient disturbance will excite the flexibility modes of the spacecraft itself as well as the structure and walls of the laboratory. The response due to a transient should damp out given enough time, but structural resonance may be significant for small time intervals. The excitation will be manifested at the eigenfrequencies (and at their higher harmonics, albeit at continuously decreasing acceleration levels). The response depends on the location at which the stimulus is applied as well as its duration and magnitude. The Shuttle clearly exhibits a multifrequency response to various disturbances at 5, 7-8, 11 and 17 Hz. Internal disturbances such as crew activity cause the spacelab (SL) racks to vibrate at 5 Hz; see, e.g., Hamacher et al. (1986a-c, 1987) regarding the hop-and-drop experiment and latch openings near the fluid experiments system; this frequency was also seen in SL3 data by Rogers and Alexander (1991a, b). In addition, there is another characteristic SL excitation frequency at 7-8 Hz which Hamacher et al. (1987) identifies as the eigenfrequency of spacelab row racks. Cooke et al. (1986) calculate Orbiter structural response at 5.2 Hz (the fuselage first normal bending mode) and at 7.4 Hz (the fuselage first lateral bending mode). External disturbances, e.g., thruster firings, cause a concomitant 11 Hz excitation. Finally, the KU band tracking antenna of the Shuttle operates with a duty cycle of 17 Hz (hard-wired into the system) which is responsible for body force levels on the order of 10^{-2} g_0 at that frequency, when in operation. These active frequency ranges were identified in the analysis of Spacelab 3 acceleration measurements by Rogers and Alexander (1991a), a sample of which is shown in figure 9.

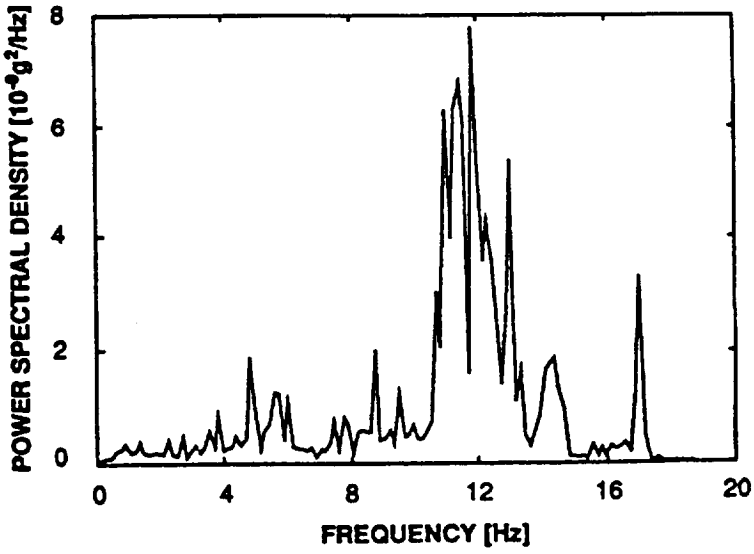

FIGURE 9. Power spectral density of representative time window aboard Spacelab 3 (after Rogers and Alexander, 1991a)

The large magnitude of the tracking antenna contribution could cause significant impact on the SSF acceleration environment. If the array of antennae on SSF operate similarly, the duty cycle must be optimized for minimized effect on the residual acceleration environment. Flexibility in the operating frequency would be useful, as would consideration of other options such as "frictionless" antennae, which by including countermoving mass, minimize accelerations transmitted to the structure.

For SSF, the fundamental structural vibration mode of the trusses (the first of 107 significant modes below 3 Hz) was found to occur at about 0.17 Hz in NASTRAN calculations (Sullivan, 1990), substantially below the eigenfrequencies of the more compact Shuttle. Undoubtedly, other structural components will vibrate at other characteristic frequencies. For example, the frequency of the solar arrays is expected to be about 0.1 Hz (Karchmer, 1990). Even if the final design for SSF is modified somewhat, these frequency values are useful to typify the structural resonance regime of large-scale space structures; the conclusions reached in section 3 are meant to be general over a broad range of frequency.

Structural vibration of the Orbiter is seen in the frequency range of 1 to 10 Hz, while SSF structural response is anticipated at lower frequency, on the order of 0.1 to 1 Hz. The lower-frequency modes of SSF, or any large-scale space structure for that matter, will likely be in a sensitive frequency range for many materials processes, so we should view these structural vibrations with extreme concern. In addition, the multifrequency nature of structural vibration leads to additional complications in analysis (see section 3.1.2.2 and appendix B).

Since Space Station Freedom will undoubtedly have a complex and intricate array of antennae, flexibility in choosing an appropriate frequency for the duty cycle should be stressed. Furthermore, attention should be given to the design of "frictionless" antennae.

2.2.2.2 Crew activity

Although many of the disturbances attributable to the crew will be impulsive in nature (see section 2.2.3.2), repetitive crew activity such as exercise will induce cyclic modulation of the acceleration environment. For the treadmill, Thornton (1989) determined that a force was generated of up to three times the body weight at 1-5 Hz, which falls within the range reported aboard the Orbiter (Chassay and Schwaniger, 1986, 10^{-3} g_0; Dunbar and Thomas, 1990 and Schoess, 1990, about $10^{-2}g_0$ at 3 Hz; see also Dunbar et al., 1991a, b). Figure 10 is a composite of six five-second histories of HISA accelerometer data which was recorded during 41 minutes of actual treadmill activity on STS-32. The accelerometer

was mounted on the front of the Fluids Experiment Apparatus on the Orbiter middeck.

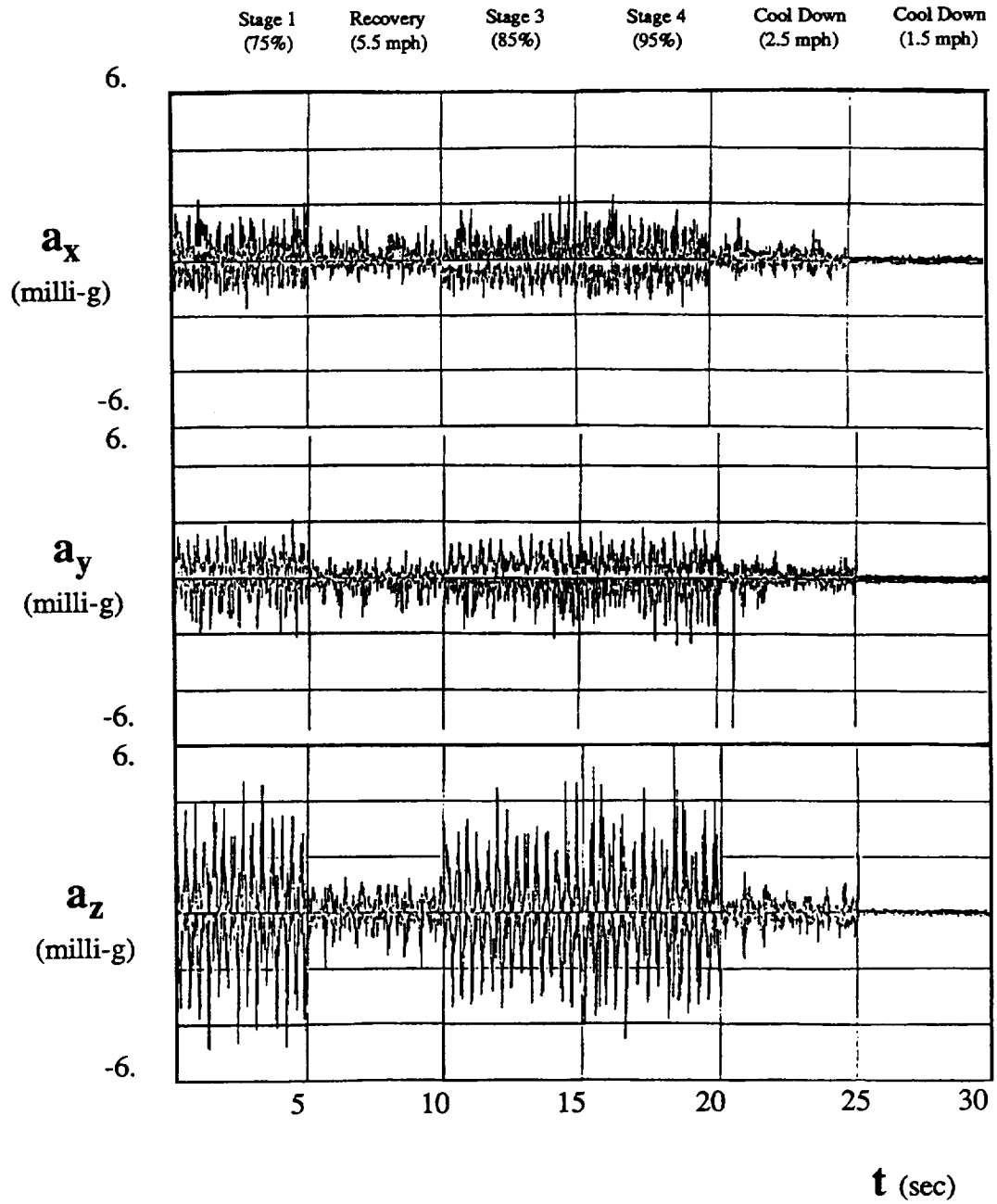

FIGURE 10. Accelerometer data at the Fluids Experiment Apparatus during six typical five-second intervals occurring during 41 minutes of treadmill use on STS-32 (after Dunbar and Thomas, 1990)

The effects of the five different running speeds on varying body-force level is immediately apparent. Appreciable *g*-levels were generated in all three primary directions by this periodic disturbance of up to $9.2 \times 10^{-3} g_0$ (off the scale in this figure). These accelerations

were also transmitted very effectively from the middeck to the payload bay (Thomas, 1990).

Eventually, eight astronauts are expected to live on SSF, each being allowed an hour per day of exercise. Early conceptual studies of the effects of a traditional treadmill on the SSF acceleration environment indicated that this vibration source could be substantial, causing acceleration levels orders of magnitude greater than that allowed by specifications (see, e.g., Space Station Freedom Microgravity Environment Definition, 1988). Even an isolated treadmill jog was found to create a severe disturbance in numerical simulation, as shown in figure 11. This clearly indicated the need for using effective vibration isolation

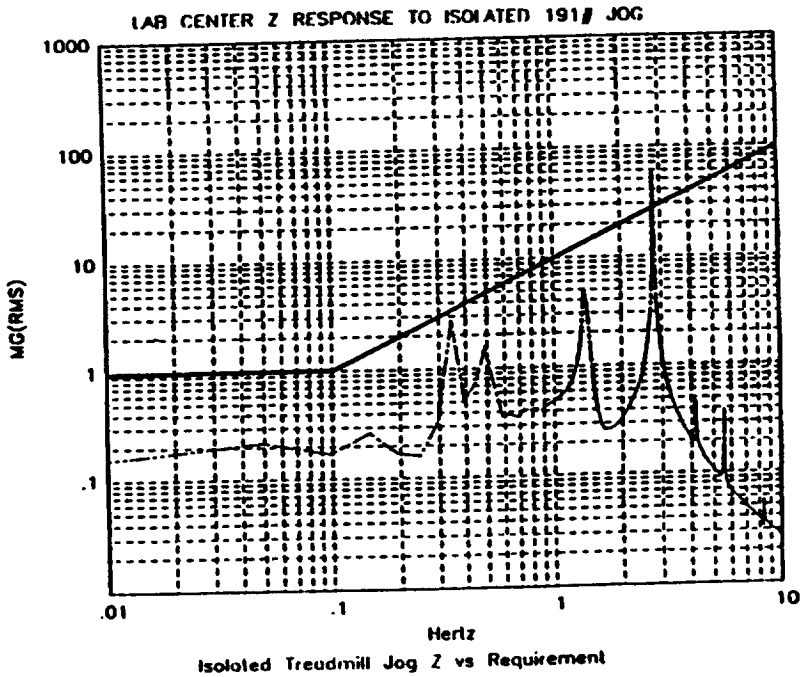

FIGURE 11. Calculation of SSF environment in laboratory module in response to an isolated treadmill jog (after Lindenmoyer, 1989)

or for an alternative type of exercise equipment.

The treadmill on STS-32 was seen to generate periodic modulation of the acceleration environment in the vicinity of the fluids experiment apparatus in all three primary directions with magnitude in the z-axis approaching 10^{-2} g_0. The significant length of time during which exercise equipment will be used and the large magnitude of the disturbances caused by such crew exercise require the use of effective vibration isolation to meet existing SSF specifications.

2.2.2.3 Operation of machinery

The experiments themselves may introduce some noise through fans, pumps, and other mechanical means, primarily in the high-frequency domain, in addition to the machinery necessary for maintenance of the space platform. A ground-based test at Marshall Space Flight Center suspended an experiment from a crane and recorded the accelerations experienced by the experiment, finding considerable high-frequency accelerations (Chassay and Schwaniger, 1986), which, as will be shown later, are of less pertinence to materials processing.

One exception may be the life sciences centrifuge, which is required to provide steady values of gravitational acceleration for its laboratory spaces in the range of 0.01 to 2.0 g_0. The 2.5 m version to be located in an SSF node is expected to operate at about 0.1 Hz (corresponding to rotational speeds on the order of 45 rpm). Final decisions regarding size and type of vibration isolation cannot be considered definitive until SSF design is finalized (at least), but the minimization of this source of residual acceleration must be considered with care. Searby's (1986) calculations showed an early version of the centrifuge to be a significant acceleration source over a broad range of frequency even though the results indicated that the disturbance of the centrifuge would not by itself exceed SSF specifications. Another analysis of a different version of the centrifuge was shown in figure 3(a) of section 2.1. Both analyses are similar in that centrifuge operation generated a wide band of large-amplitude acceleration levels with appreciable components in the frequency range of 0.1 - 10 Hz. Consequently, accelerations will be produced by both structural resonance and the centrifuge in a frequency range which is a sensitive area for most materials processes of interest. The additive effects of these frequency-dependent components must be considered very carefully by designers and users of the low-*g* environment. Care must therefore be taken in isolating the centrifuge in order to allow a quality low-gravity environment.

Fortunately, the frequency band produced by most machinery is typically too high (on the order of 10^2-10^3 Hz) to affect typical materials experiments greatly. The exception in this category is the centrifuge which is apt to be a significant contributor to the residual acceleration environment, especially since it will produce frequency components in the same range as structural oscillation. Furthermore, this frequency range will likely be a sensitive regime for most materials processes of interest. Caution must be exercised by providing effective vibration isolation to allow a quality low-g environment on SSF suitable for materials processing.

2.2.2.4 *Gas and fluid dumps and fluid control loops*

The contribution of gas and fluid dumps and control loops to the overall residual acceleration environment is estimated for the Shuttle to be about 10^{-5} g_0 (Carruthers and Testardi, 1983).

2.2.3 Transient disturbances

All other sorts of time-dependent disturbances fall into this category. The largest in magnitude are likely to be caused by thruster firings, Shuttle dockings or berthings, and mass translations. It may be possible to schedule the most disruptive disturbances to accommodate users of the low-gravity environment, such as thruster firings and Shuttle dockings or berthings. Other impulsive disturbances will be nearly impossible to schedule for this purpose, e.g., the routine crew activity of the astronauts who will live, eat, breathe and move about in this environment.

Externally applied impacts, such as extra-vehicular activities, or thruster burns can result in an uncompensated pulse or pulse train. Motions internal to the vehicle, e.g., moving about the hab or an internal hab soar, will result in no net change in momentum of the space platform, because the vehicle will respond with an equal and opposite acceleration. Unfortunately, there is no corollary zero net fluid transport within an experiment in response to such a disturbance. One effect of such "compensating" pulses may include net transport due to the varying diffusivities of momentum, heat and mass (see section 3.1.3.2). It should also be borne in mind that these transient disturbances will also excite structural resonance modes (section 2.2.2.1), which are likely to cause a significant contribution to the acceleration environment.

Although large transient accelerations of up to 2.5×10^{-2} g_0 were seen by Rogers and Alexander (1991b) in SL3 data, their appearance was limited to a fraction of a second. If the duration of the disturbance is short in comparison to characteristic diffusion times of the fluid, the response to transient disturbances has been found to be a function of the integrated acceleration over time, which is related to the momentum input to the system. The simplification afforded by this finding is that the shape of the acceleration disturbance (square pulse, sawtooth, or other) does not dictate the fluid behavior (see sections 3.1.3.1, 3.1.3.2 and 3.1.3.5), which is instead a function of the integrated g-level with respect to time and characteristic diffusivities.

2.2.3.1 Space vehicle maneuvers

Attitude corrections to maintain a gravity-gradient mode will be required for Space Station Freedom, as they are for the Shuttle; periodic reboosts and collision avoidance maneuvers to avoid space debris will also be necessary. (SSF will also have a control moment gyro in continuous operation for momentum management.) Of these, the thruster firings will undoubtedly cause the largest-magnitude disturbance to the acceleration environment. On the Shuttle, Chassay and Schwaniger (1986) found thruster firings to be on the order of 3×10^{-2} g_0. One example of recorded accelerometer data aboard Spacelab1 which included that particular disturbance was shown in figure 1. Appreciable accelerations in all three primary directions were apparent. Structural resonance modes are also be excited by these large-scale disturbances (see sections 2.1, 2.2.2.1). It also may be important to note for certain experiments that there will be spatial variation in the induced local acceleration so that the net acceleration environment may vary throughout the experimental chamber.

Current predictions for SSF are that the thrusters will only need to be fired for reboost five times per year. The estimated number of collision-avoidance maneuvers which will be required of SSF range from about 4 to 20 (Hackler, 1990), which may have a major impact on the duration of the low-*g* periods available for materials processing (see section 2.5).

If the disturbance is very short in comparison with characteristic fluid response times, recent results by Alexander et al. (1991) indicate that the solutal field response may be more sensitive to the other, more long-lived, components of the acceleration environment for certain processes (see section 3.1.3.6).

The largest contribution to the acceleration environment due to space vehicle maneuvers will likely be due to thruster firings. If thrusters only have to be fired five times per year as currently predicted, it should be possible to schedule this disturbance around the relatively quiet times allotted to low-gravity materials science.

2.2.3.2 Crew motions

Even relatively innocuous crew motions will cause appreciable residual accelerations in the vicinity of the motion such as the impulsive startup of the treadmill (Thornton, 1989). Accelerometer data of measured body force peaks can be correlated to pushoff from walls on the order of 10^{-3} g_0 (Chassay and Schwaniger, 1986) or more (see figure 3(b)); cough tests (10^{-3} to 10^{-4} g_0; Chassay and Schwaniger, 1986, or see table 2). Figure 12 shows the triaxial acceleration measurements during the opening and closing of the container doors of the fluids physics module on spacelab during D1 with peaks exceeding the full scale of

10^{-2} g_0 (Hamacher et al., 1986a-c, 1987). The same references report on the hop-and-drop experiment, also aboard D1, which recorded acceleration peaks of 10^{-2} g_0. Routine crew

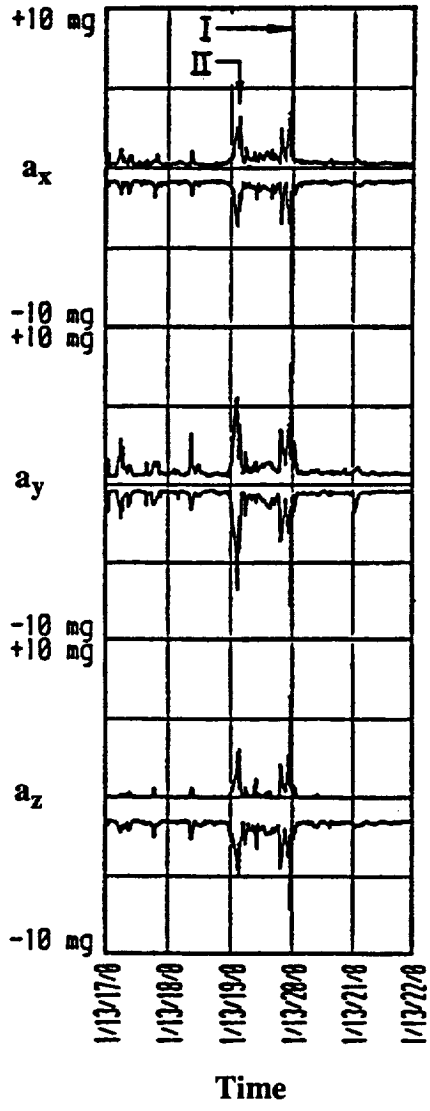

FIGURE 12. Crew disturbances due to opening and closing of container door of Fluid Physics Module (FPM) during D-1 mission (after Hamacher et al., 1987). "I" represents the closing of the container door in Spacelab's ceiling, while "II" is related to astronaut activities on the FPM

activities should be anticipated to cause disturbance levels of up to at least 10^{-3} g_0.

Other transient activities of concern for Space Station Freedom include intra-vehicular maneuvers (IVA's, i.e., hab soars) and extra-vehicular maneuvers (EVA's), which can cause acceleration levels which are significantly greater than that allowed by specifications (see figure 3(b)). These disturbances will also excite the flexibility modes of the space vehicle. One conclusion of the Space Station Freedom Microgravity Environment

Definition (1988) was that these crew activities "cannot be isolated and are the critical disturbances which define the microgravity environment that can be expected on [an inhabited] space station." It must be noted that if the disturbances are short in comparison to characteristic fluid response times, they could be considered separately to estimate impact on the fluid system. For example, it would be useful to consider the relatively brief disturbance in terms of momentum input to the system (see sections 3.1.3).

Ignoring the schedulable disturbances of thruster firings, mass translations, satellite launch and Shuttle dockings or berthings, the response to crew activity could well dominate the acceleration environment. In particular, both intra- and extra-vehicular maneuvers will introduce significant accelerations. The duration of these transients are important because the response of the velocity, thermal and concentration fields to a given (short) transient disturbance are functions of the integrated acceleration over time which is input to the system and of the characteristic diffusion times. This will be discussed further in section 3.1.3.

2.3 *Orientation of residual acceleration*

The forces of atmospheric drag a_d and tidal acceleration a_t comprise the most significant quasisteady body forces. Consequently, some thought has been given to orienting the axis of the experiment not about the local vertical (say, radial from the earth for the gravity-gradient attitude) but rather in the direction of average body force produced by these two residual-gravity components, as shown conceptually in figure 13. This can be an appreciable variation; for Space Station Freedom, this is estimated to be as much as 17° (Sullivan, 1990), depending on location.

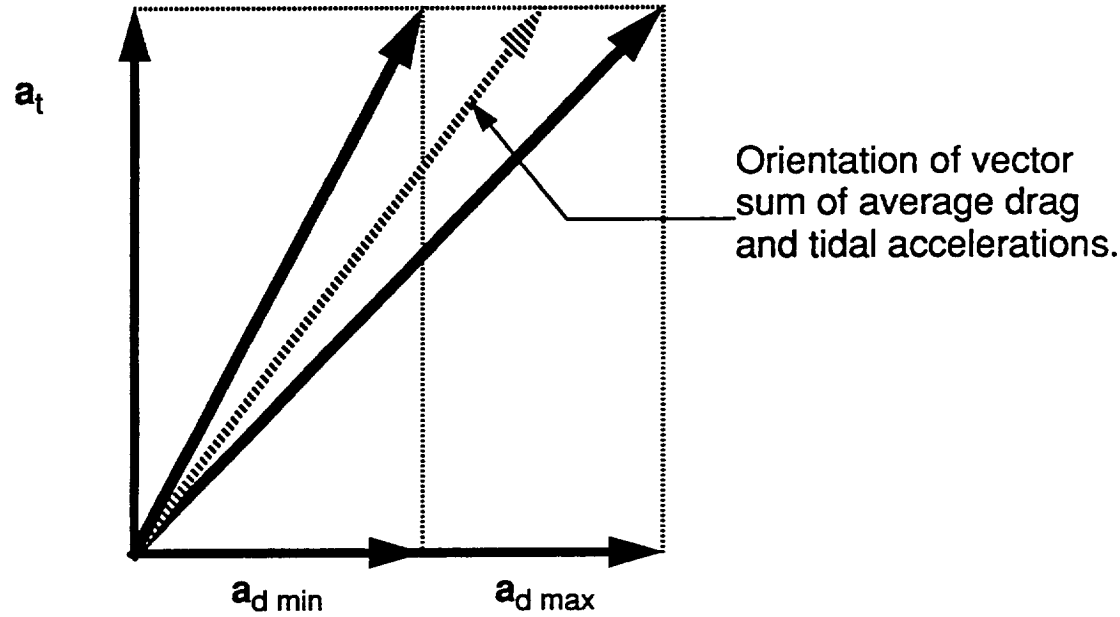

FIGURE 13. Primary quasisteady forces of tidal acceleration a_t and atmospheric drag a_d, the latter of which varies over an orbit from $a_{d\ min}$ to $a_{d\ max}$ (magnitudes are not quantitative)

There are two considerations which undermine the logic of this suggestion. During flight, atmospheric drag will induce some tilt of SSF relative to its initial local vertical/local horizontal attitude. This orientation, called the torque equilibrium attitude (TEA), can be maintained with the minimum energy consumption. The TEA may be appreciable in magnitude. Some estimates place TEA at 5± 0.5°, although other predictions range to much larger values. For any given configuration of SSF, the TEA is a constant value, but during different stages of development of SSF, the TEA will be modified accordingly. This means that precise alignment of an experiment in any particular direction will require repositioning with each change in TEA. Furthermore, this alignment can still vary by the aforementioned tolerance. The allowable fluctuation of ± 0.5° relative to TEA may be enough to cause substantial modification of fluid behavior (see section 3.1.1.2).

Furthermore, the large amount of jitter which is superimposed on these quasisteady components renders this analysis superfluous, at least for the Shuttle. The orientation of *g* was found to vary dramatically in all three dimensions in the analysis of SL3 data by Rogers and Alexander (1991b). Figure 14 shows that the direction cosine for one of the principal axes as measured by a HISA accelerometer during a typical time period varied between approximately ± 90°. The other axes' direction cosines also were found to vary similarly

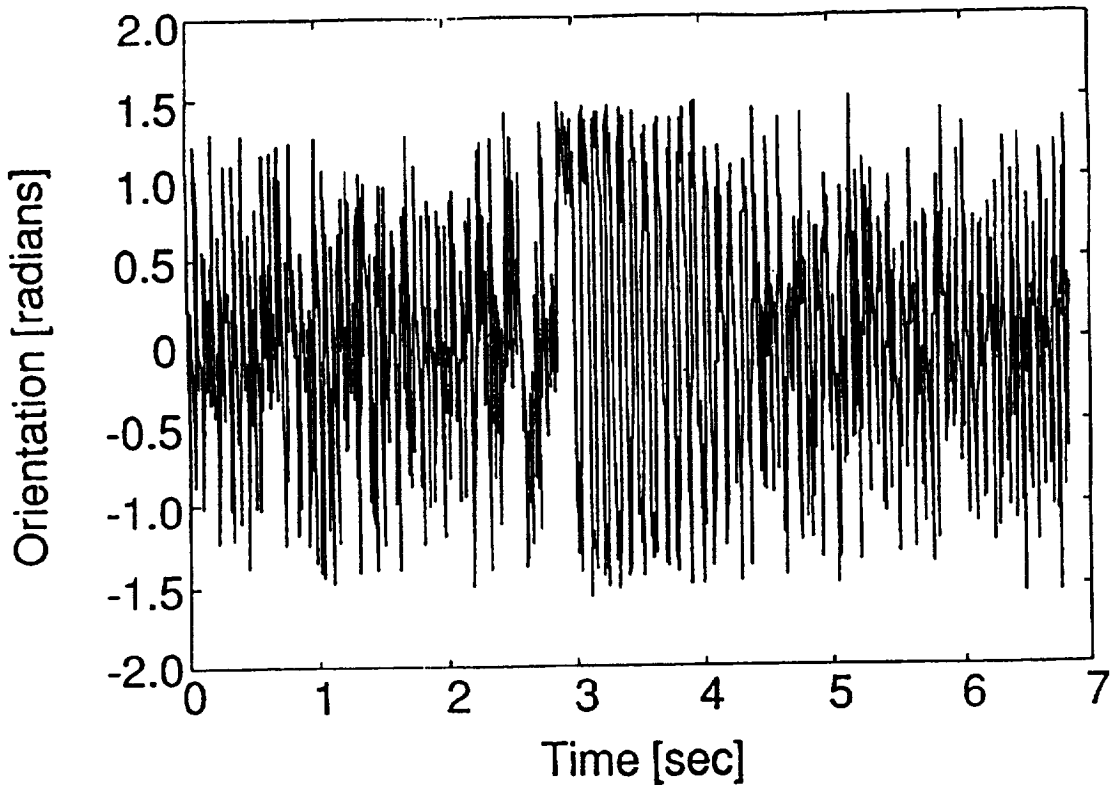

FIGURE 12. Direction cosine for one of the principal axes as measured on Spacelab 3 (after Rogers and Alexander, 1991b)

between the positive and negative directions. Particular disturbances acting in a particular direction (e.g., thruster firings) did cause a preferred direction to appear in the accelerometer data momentarily. However, in general, no preferred orientation was otherwise found to exist for the direction of the residual acceleration.

It is somewhat sobering to realize that not only does g-jitter dominate the acceleration environment, but its orientation is, for all practical purposes, completely unpredictable.

2.4 Minimization of disturbance levels

It will be mandatory to carefully isolate some large-magnitude acceleration sources from the rest of the Space Station Freedom acceleration environment to meet the desired low gravity levels, a conclusion reached in the Space Station Freedom Microgravity Environment Definition (1988). These sources should include the induced accelerations caused by crew exercise (see section 2.2.2.2) and the centrifuge (see section 2.2.2.3). The above study also concluded that isolation of crew exercise equipment would decrease its impact on the acceleration environment, but another layer of complexity, specifically, the isolation of the experiments, would still be necessary to meet existing SSF low-gravity environment specifications.

It is not as easy to isolate the experiment itself from the acceleration environment. It is more costly, takes up space, can consume power, and adds weight to an already fully loaded SSF. It also requires specialized hardware because different experiments will likely be most vulnerable to disturbances of differing frequency range. Nevertheless, vibration isolation for experiments will probably be a prerequisite for many, if not most, materials processes. High-frequency disturbances can be damped out passively using simple methods such as placing the experiment on a foam pad. On the other hand, lower frequencies are more problematic due to the large-amplitude motion involved in long-period accelerations and will probably require active isolation which is not easily implemented. Unfortunately, the lower-frequency disturbances are of most import to materials processing.

A great deal of work is ongoing in this area. Active and passive vibration isolation are discussed in the references found in appendix C.

Active vibration isolation is more costly, both in terms of production and in terms of weight; it puts additional demands on SSF due to the increased volume, power and complexity. However, it will be imperative to have such isolation for both major disturbance sources and for at least some of the experimental facilities to maintain adequately low acceleration levels for materials processing.

2.5 *Duration of low-g environment*

Current specifications call for six or more periods per year of minimum 30-day duration in which the abovedescribed acceleration environment will be maintained. These are reasonable time spans in which to accommodate the materials science user community. From a designer's point of view, these specifications are very restrictive and simply will not tolerate large-scale disturbances, such as that caused by thruster firings and Shuttle dockings and departures. The intent is that these large-scale disturbances can be scheduled around the low-*g* periods. If reboost thruster firings are only necessary five times per year, for example, and other disturbances are similarly sparse and easily schedulable, this may be feasible. We should however be aware that there are a number of unknowns which will influence the viability of this assumption. SSF will be required to perform collision-avoidance maneuvers to avoid damage from space debris, for example. Hackler (1990) indicated that between 4 to 20 such unschedulable maneuvers per year are expected, but the exact number at this point can only be an estimate. She concluded that if the number of collision-avoidance maneuvers moves toward the high end, there may not be *any* complete 30-day periods of low gravity available.

It is important to note that recent work by Alexander et al. (1991) indicates that the more long-lived components of the acceleration may be of more consequence in setting the solutal response than short-duration impulsive transients for certain systems (see section 3.1.3.5).

A minimum of six 30-day periods is anticipated during which the earlier described low-g environment is maintained. It should be remembered, however, that even with careful design, there are still some unknowns which may make this requirement difficult to meet, such as the required number of unschedulable collision-avoidance maneuvers.

2.6 *Recording of the acceleration environment*

Although we have had some experience with using the low-gravity environment, the characteristics of the residual acceleration field in the (relatively) familiar Shuttle environment have not been unequivocally resolved. The tradeoff between having an absolutely complete and comprehensive set of accelerometer data conflicts with the difficulty of acquiring, storing and processing vast quantities of information. How do we decide what are the relevant frequency ranges and threshold sensitivities? When do we sample and how much do we store? Our understanding of these questions has been evolving as we gain experience in the extra-terrestrial environment. The logistics of such sensitive data acquisition,

the low signal-to-noise ratio, and the often tricky correlation of mission events to the accelerometer signal also serve to increase the complexity of this problem.

As an example of the evolutionary process of learning how to quantify the residual acceleration environment, one notes that there is little available in the literature today in the way of useful middeck accelerometer measurements. Although the microgravity acceleration measurement system (M-GAMS) with two-axis capability was flown on STS-3, some ambiguity existed in the resulting data since the background electronic noise of one bit, corresponding to $\pm 10^{-4}$ g_0, effectively masked the signal of lower-level accelerations. Moreover, as shown in section 2.3, we now know that it is not possible to adequately characterize the Shuttle residual acceleration environment without resorting to full three-dimensional characterization.

Recent work in the microgravity disturbances experiment on STS-32 presents three-dimensional acceleration data from an HISA accelerometer in the middeck and corresponding acceleration information from the payload bay, provides correlation to mission events, and documents the effects of particular disturbances on the float-zone crystal growth of indium (see figure 10; Dunbar and Thomas, 1990; Schoess, 1990; see also Dunbar et al., 1991a, b). This full characterization of the surrounding acceleration field is absolutely vital in reproducing experimental results. It is also essential to monitor the integrity of the process, to correlate *g*-jitter effects to specific experimental results, to accurately model low-gravity materials processes, and to possibly tailor experiments to the environment (rather than vice versa). See, for example, section 3.

The routine use of sophisticated and adaptable accelerometers will play a critical role in documenting the conditions under which materials processes are performed. The Space Acceleration Measurement System (SAMS) is one such device. It includes up to three triaxial sensor heads which can be independently set to a choice of six low-pass frequency bands, ranging from 2.5 to 100 Hz. The SAMS unit can incorporate two different sensor types with sensitivities of 10^{-6} and 10^{-8} g_0. Some of the accelerometers which are currently available for use on the Orbiter are briefly outlined in appendix D.

Since the accelerometers which will accompany low-gravity materials experiments will be custom fit to a frequency range and threshold sensitivity for a given experiment, they are not a substitute for an overall acceleration field mapping strategy of Space Station Freedom. Relying on users' accelerometers alone would also be difficult for characterizing the all-around SSF environment because the transmission of vibrations between any two locations is extremely complex in character.

Accurate characterization and monitoring of the acceleration environment should not be minimized. We would like to be able to perform repeatable materials experiments, and perhaps the most critical parameter is the maintenance of a controlled (or at least documented) environment, including the residual acceleration field. Routine and liberal use of sophisticated accelerometers is therefore essential to the maintenance of a low-gravity facility for useful materials processing.

Accelerometers with capabilities appropriate to the measurement of the low-gravity environment are beginning to be incorporated as part the philosophy of experiment design with increasing awareness of the potentially profound implications of g-jitter. The characterization of the Shuttle environment and correlation of its effects to specific experiments must be a top priority. This information can be used to monitor processes, to explain experimental results, to numerically model and assess g-jitter effects on various classes of materials processes, and perhaps in some instances to tailor a particular experiment for a particular environment.

2.7 Data analysis and reduction

The analysis of the huge amount of accelerometer data is as important as its initial recording. The volume of information is so large that sifting through raw data is a completely impractical option (Thomas, 1990). Relatively simple processing can give researchers essential information in an understandable format.

The peak detection method involves the choice of some threshold value, e.g., the maximum tolerable acceleration magnitude for a process of interest. Simple sifting of the data to detect any peaks which exceed this value may then be performed, and more detailed analysis of these time periods undertaken. If orientation information is of interest, analysis of direction cosines is also a simple data-reduction technique. See Rogers and Alexander (1991a, b) for a good discussion of SL3 data.

Obtaining frequency data from the raw accelerometer output is somewhat more tricky since it depends in a very critical way on the total temporal length of the record as well as the discrete time interval between sampling. Choosing too large a time window may mean smearing out some of the higher-frequency or impulsive information, while a minuscule time window will rule out the possibility of obtaining low-frequency data. The choice of a standard time window or set of windows should be coordinated with SSF designers. In addition, the multifrequency data will typically be comprised of components of very different orders of magnitude. It must be noted that a multitude of other clever ways of reducing

raw acceleration data to manageable size have been developed, ranging from simple linear interpolation between peaks to sophisticated spectral data compression and pattern recognition techniques.

As pointed out by Rogers and Alexander, the monumental task of correlating acceleration information to specific events is immensely facilitated by the relatively simple task of keeping a detailed timeline on the space vehicle.

The analysis and reduction of accelerometer data is an area of importance if the acceleration information is to have any meaning. We have the techniques for this data analysis readily available, but must standardize formats, time windows, etc. for routine use.

3. Effect of the acceleration environment on materials processing

There may be unique advantages to performing materials science in the space environment. Beneficial effects of low gravity include reduced natural convection, lower settling rates, and larger sample size for containerless processing, among others. Additionally, solids at elevated temperature and reduced gravity will be less likely to deform and form dislocations under their own weight due to creep. Containerless processing eliminates container contamination effects in molten materials, and in low gravity requires only weak positioning and manipulating fields. Already some of the potential of implementing materials processes in space has been realized, for example, in the polymerization of uniformly spherical latex droplets and in protein crystal growth. For an overall perspective on space processing, see Chait (1990); Naumann (1988a, b, 1979); Chassay and Carswell (1987); and Carruthers and Testardi (1983).

Section 3 deals with the effects of g-jitter on specific materials processes. The first subsection (3.1) is concerned with bulk phenomena. G-jitter enters this discussion primarily through the modification of the process of natural convection. The second subsection (3.2) considers g-jitter effects on the surfaces of fluids. The most important considerations relevant to this topic are the effects of g-jitter on the stability of interfaces, and the increased importance of surface-tension driven convection, or Marangoni flow. A brief overview immediately follows.

Although buoyancy-driven convection will certainly be reduced in an extraterrestrial environment, there are a number of complicating factors which must be considered. With reduced natural convection, other, more subtle, forces which are normally masked on earth by gravity-driven convection may come into direct competition or even play a dominating role. For example, surface-tension driven convection becomes dominant in establishing the velocity field in liquid bridges, and, therefore, in setting the convective heat, momentum and mass transport. Also, radiative heat transfer may assume a more important role relative to conductive and convective heat transfer. This is significant because our current numerical radiation models can consume a great deal of CPU time, require significant memory storage allocation, and are nonetheless often woefully inadequate if too simplified (see, e.g., Kassemi and Duval, 1989, 1990).

It is not possible to understand the effects of g-jitter on the materials process of interest without understanding the effects of steady g upon them. This is too broad of a topic to address adequately here; these areas have been the focus of ongoing research for decades

and entire books in varying fields have been written about these subjects. Some of the general areas of interest for space processing and good general sources of information (although not intended to be a complete bibliography) follow.

- on natural convection, see, e.g., Jaluria (1980);
- on natural convection in the low-gravity environment, see Ostrach (1982); and Grodzka and Bannister (1974);
- on convective instability in natural convection, see Olson and Rosenberger (1979a, b);
- on interfacial phenomena, see Batchelor (1967); Drazin and Reid (1981); Zeren and Reynolds (1972); Jacqmin (1990); Jacqmin and Duval (1988);
- on general melt growth, see Hurle (1983);
- on directional solidification, see the review by Brown (1988);
- on crystal growth for substances which are soluble in aqueous solution, e.g., proteins, electronic and electro-optical materials, see Wilcox (1983);
- on the growth of crystals from the vapor phase in the processes of physical vapor transport or chemical vapor deposition, see Westphal (1983); and Zappoli (1986);
- on interfacial transport in crystal growth, see Rosenberger and Müller (1983);
- for containerless processing in general, see Barmatz (1982); and Carruthers and Testardi (1983);
- for float zone or the related purely fluid mechanical problem of liquid bridges, see Hurle (1983);
- on the stability of time-dependent flows, see Davis (1976).

For a discussion of the nondimensional quantities of interest to space processing, see appendix A and the pages which follow; also see Legros et al. (1987).

The temporal and spatial variation of the gravitational force may play a decisive role in several direct ways:

- Different flow modes may be excited:
  - in natural convection in an enclosure, see Ramachandran (1990a) and Duh (1989);
  - in directional solidification, see Arnold et al. (1990, 1991);
  - in crystal growth from solution, see Nadarajah et al. (1990);
- The stability limits and the path to instability of a given process may be affected:
  - in thermally driven natural convection, see Gresho and Sani (1970); and Biringen and Peltier (1990); also Wadih et al. (1990); Wadih and Roux (1987); Smutek et al. (1985); Goldhirsch et al. (1989);
  - in directional solidification by McFadden and Coriell (1988); Coriell et al. (1989); Murray et al. (1990);
  - in liquid bridges by Langbein (1987); and Martinez (1987).

Most of the understanding of the effects of *g*-jitter on materials processing is the result of numerical analysis, because the explicit correlation of the local acceleration environment to physical experiments is limited at this time. Consequently, it is noted that the bulk of the discussion which follows is based on computational analysis. Before turning to detailed discussion of the various phenomena and processing, it is worthwhile to briefly describe the relative merits and simplifications involved in each of the classes of analyses used in the following studies. Broadly speaking, we can classify these into either experimental or theoretical in nature. Theoretical studies are further classified in the context of this report as either based on order-of-magnitude analysis or a full numerical simulation.

- Ultimately, the most reliable gauge of whether or not a materials process is viable in a given space laboratory would be *direct experimental observation.* Experimental analysis of space processes is enormously costly in terms of human time, effort, and resources, in addition to money. We can all agree that materials processing in the space environment is vastly different from that in a materials laboratory on earth. In space, however, we do not have the luxury of doing exhaustive multiparametric or iterative studies due to prohibitive costs and limited time. Additionally, a direct observation leading to a concrete piece of knowledge on *g*-jitter effects necessitates both good *in situ* acceleration data recording capabilities *and* an adequate numerical or other model of the experiment.
- *Order-of-magnitude analysis* [O(M)] is a simplified analytical approach which can yield general qualitative understanding by selecting characteristic scales to simplify the governing equations. However, the validity of the quantitative predictions of such an analysis will depend upon how faithfully the scales chosen represent the transport mechanisms in the problem. The choice of appropriate scales may not be immediately obvious due to the inherently multiparametric nature of these problems; indeed, it may not be possible to quantify one set of representative scales which adequately characterize any of these complicated processes. Different regions of the physical domain may have different characteristic scales, as in phase change problems, or the relevant criteria for choosing the scales may change over the course of an experiment, as in onset-of-convection problems. Therefore, quantitative reliance on order-of-magnitude analysis alone is unwarranted for this class of problems. In the absence of any more quantitative analyses (e.g. numerical analyses), [O(M)] specifications can provide qualitative understanding, but these should be supplemented by other means.
- *Numerical analysis* has the potential of being the least costly practical approach to understanding *g*-jitter effects. However, we are not at a sufficiently mature stage of development to accurately model much better than fairly idealized systems. The inherent three-dimensionality of the acceleration environment complicates analysis, for example. Furthermore, many of the relevant transport mechanisms are not apparent in a terrestrial laboratory in which natural convection is of dominating influence. Consequently, incomplete physical understanding may lead to deficient models. The numerical approach represents a practical first step to understanding the new and funda-

mentally different physical phenomena which appear in space-based materials processing. Nevertheless, numerical analysis efforts are sparse and presently not well coordinated, so their results cannot yet be directly extrapolated to an environment such as on Space Station Freedom in the form of absolute specifications.

Further discussion of these different analysis techniques and accompanying assumptions can be found in appendix B.

A first estimate of the sensitivity of materials processes to *g*-jitter may be deduced from order-of-magnitude analysis, as shown in the work by Demel (1986) in figure 15. This graph shows the theoretical response of a number of materials processes to a *single-frequency g-jitter disturbance.* However, the ordinate in this figure should *not* be read as an

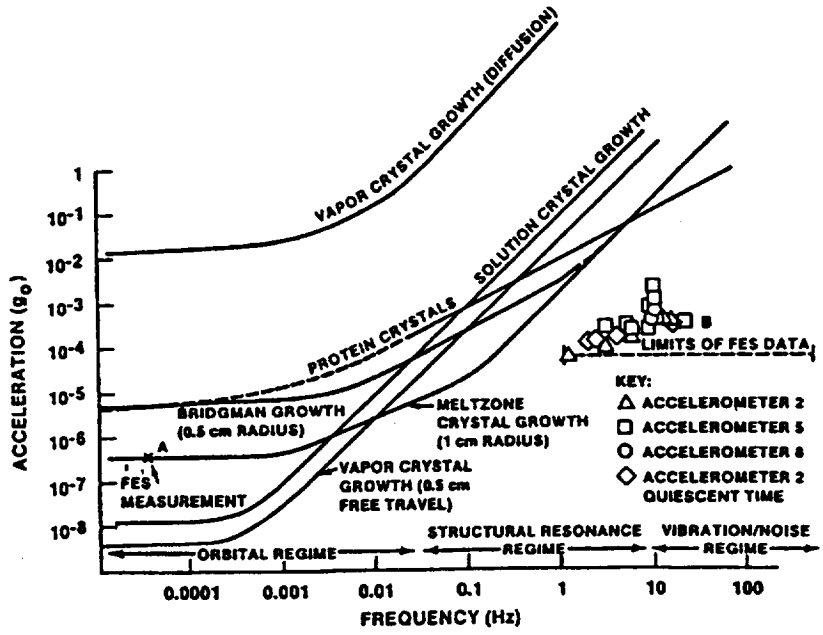

FIGURE 15. Tolerable *g*-levels as a function of frequency for a variety of materials science experiments *as predicted by order-of-magnitude analysis for a single-frequency disturbance* (after Demel, 1986)

absolute quantitative requirement of allowable *g*-levels due to the serious oversimplifications made by the analysis (see appendix B). These curves are also subject to variability for different geometries and material properties. It is more appropriate to utilize this chart to predict general trends in a qualitative way and permit some comparison of various processes. Seen in this light, one may presume that diffusion-dominated crystal growth from the vapor phase is less sensitive to *g*-jitter than Bridgman growth. Below a critical frequency (which is dependent on the specifics of the process), the tolerance level to a single-

component harmonic modulation is essentially independent of frequency. Sensitivity to sinusoidal disturbances decreases as the frequency increases (however, see the discussion of subharmonic response in section 3.1.2.1 and on multiple-frequency disturbances in 3.1.2.2). There should at least be cause for concern about the levels of residual acceleration which accompany the structural resonance regime (for SSF, on the order 10^{-1} to 10^{0} Hz) due to the relatively low tolerance levels predicted, even with this simplified analysis.

It is difficult to make broad generalizations as to the effect of g-jitter on a class of materials processes due to its multiparametric nature. The processes are dependent on the thermal environment, growth rate, and material properties as well as the geometry and the specific character of the forcing provided by the residual acceleration field. Transport processes are significantly altered in a space laboratory, and the full impact of these changes is not completely understood at present, requiring us to approach the physics of processes from a very fundamental perspective; that which is routinely of marginal importance and therefore neglected in earthbound processing may become a dominating feature in the space environment. This underscores the need to view order-of-magnitude analysis as purely qualitative; no acceleration specifications for any spacebound vehicle should be made on order-of-magnitude analysis alone, however, in the absence of other methods, it could provide qualitative information not otherwise available (see appendix B.1.1).

3.1 Buoyancy-driven convection

In general, a steady body force such as gravity acts in concert with density variation in a fluid to drive natural convection. Fluids whose properties vary with temperature and concentration, e.g., binary alloy melts, can acquire density gradients through: (1) thermal gradients, primarily by external heat addition (or extraction) or by latent heat release upon a phase change; and/or (2) concentration gradients which arise from, for example, rejection or incorporation of solute at the solidification interface. Significant density gradients can arise due to the disparity in the molecular weights of the constituent materials. In either case, the gradient is destabilizing if the fluid density decreases in the direction of gravitational acceleration. In practical situations, both thermal and concentration gradients will be present in fluids to varying degrees, and these gradients may be either stabilizing, destabilizing or in competition with each other. In the case of a temporally varying body force, the situation becomes much more complex. In fact, even for the case of a constant-density fluid, g-jitter can theoretically modify stability limits (Jacqmin, 1990).

The fluid velocity, temperature and concentration fields interact in manners commonly described through the equations for conservation of mass, momentum, energy and species:

$$\frac{\partial \rho}{\partial t} + \nabla \bullet (\rho \underset{\sim}{v}) = 0 \tag{2}$$

$$\rho \frac{\partial \underset{\sim}{v}}{\partial t} + \rho \underset{\sim}{v} \bullet \nabla \underset{\sim}{v} = -\nabla p + \nabla \bullet [\mu (\nabla \underset{\sim}{v} + \nabla \underset{\sim}{v}^T)] + \rho \underset{\sim}{b} \tag{3}$$

$$\rho C_p \left(\frac{\partial T}{\partial t} + \underset{\sim}{v} \bullet \nabla T \right) = \nabla \bullet (\kappa \nabla T) + Q + other \tag{4}$$

$$\frac{\partial c}{\partial t} + \underset{\sim}{v} \bullet \nabla c = \nabla \bullet (D \nabla c) + Q_c + other \tag{5}$$

where ρ is the density, $\underset{\sim}{v}$ is the velocity vector, p represents pressure, μ the absolute viscosity, C_p the heat capacity, T the temperature, κ the thermal diffusivity, Q the heat transfer, c the species concentration, D the species diffusivity and Q_c a species source term. These equations are general, although other higher-order terms may be included. There are also a varying set of process-specific initial and boundary conditions for any given problem. In the above equations, the body force is $\underset{\sim}{b}$ and includes the gravitational acceleration and electromagnetic forces, among others. With decreasing levels of steady gravitational acceleration, the vigor of the resultant buoyancy-driven convection decreases since the forcing provided by $\rho \underset{\sim}{b}$ also decreases. For crystal growth, this is desirable because the diffusion-dominated growth regime produces radially and axially uniform solute fields near the (flat) growth interface. The conditions in the neighborhood of the crystal interface can determine the chemical homogeneity of the crystal. Since the molecular diffusion in the solidified crystal is small, the local concentration field in the melt near the interface will determine the solute (or dopant) distribution in the crystal.

An open issue remains as to the method of quantifying the undesirable effects of *g*-jitter while retaining most of the relevant physics. For example, it is reasonable to correlate solute distribution at the interface with final crystal chemical homogeneity. Alexander et al. (1989) use the (relatively arbitrary) criterion of 10% variation in radial species concentration at the growth interface. Other studies compare solute distribution relative to purely diffusion-dominated conditions, e.g., Coriell et al. (1989). Nadarajah et al. (1990) note that crystals grown from solution are notoriously sensitive to small but sudden changes in the growth conditions[1] and consequently use variation in growth rate as the sensitivity parameter. Convection levels in terms of maximum values of the stream function or velocity

1. Nadarajah et al. cite the work of Brooks et al. (1968) which notes that, for protein crystal growth, even a 0.03° C step change can lead to occlusions in the crystal.

are convenient to obtain in numerical simulation of transport by thermally driven natural convection, and correlate, although not necessary directly, to the interfacial composition. Therefore, comparison of convection levels induced from specific time-dependent forcing relative to that caused by low levels of steady residual acceleration may provide another tolerance criterion.

The residual acceleration acts in concert with density gradients to drive natural convection. Minimization of the overall steady gravitational level decreases the vigor of the resultant natural convection. In typical crystal growth processes, density gradients can be acquired through temperature or concentration gradients, or both. G-jitter serves to complicate the analysis of these problems.

Ideally, the tolerance criterion for a given materials process should be directly related to the quality of the final product. Barring the availability of such a quantitative measure, useful trends can be obtained from all of the foregoing, since all of the above phenomena are related. Bear in mind, however, that this may not fully predict the success (or lack thereof) of final crystal quality, since the response of momentum, thermal and solutal fields vary in a related but indirect fashion[1]*. Moreover, the numerical simulation of crystal growth is routinely carried only to solidification, whereas the final quality may be determined by solid-state effects, e.g., dislocation generation during cooldown.*

3.1.1 Quasisteady gravitational acceleration

The effect of very low-frequency disturbances on materials processes is an area of current interest. One might expect that if the relatively small momentum diffusion time scales are vastly removed from the longer period of orbital variation (about 90 minutes), the fluid would not experience any net effect at all, a conclusion reached by Nadarajah et al. (1990) for a purely sinusoidal disturbance of low frequency in a protein crystal growth simulation (recall that this low-frequency representation may not be an accurate description of atmospheric drag, as was shown in figure 8, section 2.2.1.2). While sinusoidal disturbances will be discussed further in section 3.1.2, the discussion which follows considers *purely steady* residual accelerations.

1. The behavior of the momentum and solute and/or thermal fields to time-dependent forcing levels are very different due to vastly disparate characteristic diffusion time scales. See the discussion on the role of diffusivity in sections 3.1.3.1-3.1.3.2.

3.1.1.1 Magnitude of residual acceleration

Although it is somewhat inappropriate to generically lump all varieties of g-jitter as a perturbation on top of a steady g-level (since in many cases, g-jitter *dominates* the acceleration field), it is an instructive first step.

One of the most important nondimensional parameters of interest to space processing relates the characteristic rates of heat transfer by convection and conduction, i.e., the Rayleigh number:

$$Ra = \frac{g\beta\Delta T L^3}{\nu\kappa} \tag{6}$$

where β is the coefficient of thermal expansion; ΔT is the relevant thermal variation; L is a characteristic length scale; ν is the kinematic viscosity; and κ is the thermal diffusivity.

In directional solidification, a segregation coefficient as a function of Rayleigh number is shown in Brown (1988), reproduced in figure 16[1]. The worst case for radial segregation

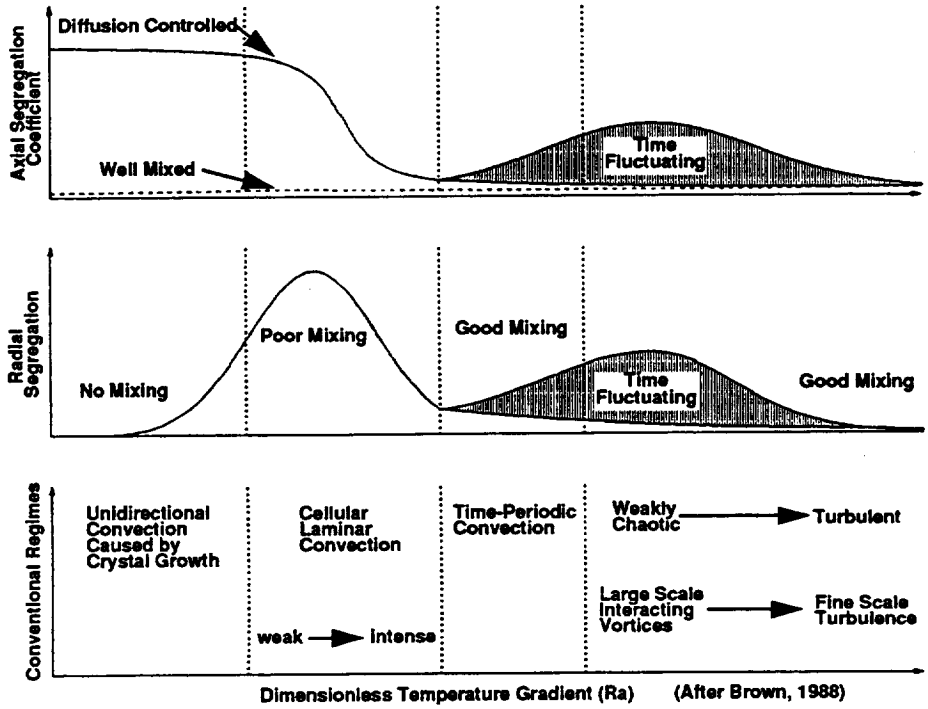

FIGURE 16. Rayleigh-number dependence of segregation and convection regimes for directional solidification (after Brown, 1988)

1. For this figure, the axial segregation coefficient k_{eff} is not the traditionally used k, i.e., the ratio of solid-to-liquid equilibrium concentration for a given mixture, but rather is given by $k_{eff} = (k\langle\langle\tilde{c}\rangle\rangle)/\langle\tilde{c}\rangle$. For this case, $\langle\langle c\rangle\rangle$ is the volume-averaged concentration of solute in the melt and $\langle\tilde{c}\rangle$ is the ratio of the maximum difference in concentration across the crystal to the average concentration across the crystal. Consequently, a k_{eff} of 1 indicates purely diffusion-controlled conditions.

ensues when the convective and diffusive velocity scales are of the same order (within the cellular laminar convection regime on figure 16). Alexander et al. (1989) confirms that maximum lateral solute nonuniformity occurs when convective and diffusive velocities are of the same order. In space, we would hope to find ourselves in the purely diffusion-dominated regime due to the relatively lower g (i.e., low Ra), but may instead be on the borderline between convection and diffusion-dominated growth, which is the worst possible situation. Thus, although there is a gravitational level below which convection does not play an appreciable role, there may be drastic changes in crystal quality associated with rather small variation in the steady background acceleration level. Coriell et al. (1989) found that even very small flow velocities on the order of 4 μm/sec can cause a twofold variation in solute distribution at the crystal/melt interface (relative to the pure diffusion case) in PbSn alloys. (See also Polezhaev, 1979.) It would, however, be simplistic to presume that diffusion-dominated transport alone will automatically guarantee crystal chemical uniformity. In the crystal growth of triglycine sulphate, Nadarajah et al. (1990) point out that other complicating factors must be considered, such as nonuniform temperature distribution across the crystal (due to the crystal's finite thermal conductivity) and interface kinetics.

The effect of decreased buoyant convection in a (steady) low-g environment has been examined by, e.g., Gokoglu et al. (1989) in chemical vapor deposition of silicon, and by Ménnétrier and Duval (1990) for the case of physical vapor transport.

For a given materials process, we expect to find a steady g level below which the fluid is not dominated by buoyancy-driven convection, e.g. in directional solidification, when low body-force levels allow diffusion-dominated growth. This can lead to more uniform chemical composition in the final product. However, we must remember that very deleterious regimes may exist near the desired diffusion-controlled growth regime. Therefore, we must be careful in specifying the steady acceleration level, especially in view of the next section.

3.1.1.2 Orientation of residual acceleration

The numerous sources of g-jitter will undoubtedly give rise to directional variation in the body force acting on a given experiment (see section 2.3). Neglecting temporal variation in g-jitter for a moment, we know that the orientation and magnitude of the steady gravitational field determines the flow regime and pattern for many processes of interest. Off-axis alignment of the body force (relative to the ampoule centerline in directional solidification) may excite completely different convective flow modes from those driven by a

well-aligned body force. The new convective flow patterns would in turn be expected to modify the concentration field in the vicinity of the solidification interface, thereby affecting the chemical homogeneity of the crystal. Polezhaev et al. (1980) was the first to show that the orientation of gravity during growth affects the compositional uniformity of the crystal.

For the Bridgman directional solidification of GaAs in a complete numerical simulation of the GTE space flight experiment, Arnold et al. (1990, 1991) showed that very slight misalignment of gravity with the growth axis profoundly affects the fluid behavior in thermally driven convection at steady values of 10^{-5} g_0. The recognizable result (from an earthbound standpoint) of a small axisymmetric toroidal cell just above the solidification interface was recovered in a three-dimensional simulation when the residual acceleration was oriented exactly parallel to the growth axis (figure 17(a)). However, when the gravitational acceleration was oriented perpendicular to the growth axis, the stronger large-celled shallow-cavity mode dominated as shown in figure 17(b). Tilting the ampoule relative to gravity at an angle θ by as little as 0.05° induced a competition of the axisymmetric mode with the shallow-cavity flow mode. This is seen in figure 17(c) through the ratio of maximum velocity to the maximum velocity in a purely axisymmetric mode (i.e., gravity perfectly aligned with the centerline). In fact, the shallow-cavity mode completely dominated the flowfield at a 0.5° tilt, as shown in figure 17(c). This initially startling result is easily explained by the large driving force of the longitudinal thermal gradient, which quickly becomes dominant over the much smaller radial gradient. This result is qualitatively valid for all directional solidification experiments and is of particular concern in light of current SSF specifications, which call for holding Space Station Freedom to the torque equilibrium attitude ±0.5° (see section 2.3).

Similar conclusions were reached by Alexander et al. (1989) in an investigation of the effects of steady residual accelerations on an idealized Bridgman crystal growth for GeGa. Three cases of gravitational orientation were studied: gravity aligned perfectly with the growth axis (analogous to the axisymmetric flow above), perpendicular to the growth axis (i.e., the shallow-cavity mode discussed above), and at 45° to the growth axis. They concluded that strong asymmetries can occur if gravity is not aligned to the growth axis, and in addition that gravitational orientation and compositional nonuniformity are related nonlinearly. Even the low steady g-level of 10^{-6} g_0 was found to cause unacceptable consequences for lateral solute nonuniformity if the residual acceleration was oriented parallel to the growth axis. The tolerance level decreased by an order of magnitude if the acceleration was perpendicular to the growth axis.

FIGURE 17. Sensitivity of directional solidification of GaAs to orientation of gravitational acceleration (steady g of 10^{-5} g_0): (a) gravity exactly parallel to growth axis; (b) gravity normal to growth axis; (c) fluid velocity response as a function of graviational acceleration orientation (after Arnold et al., 1991)

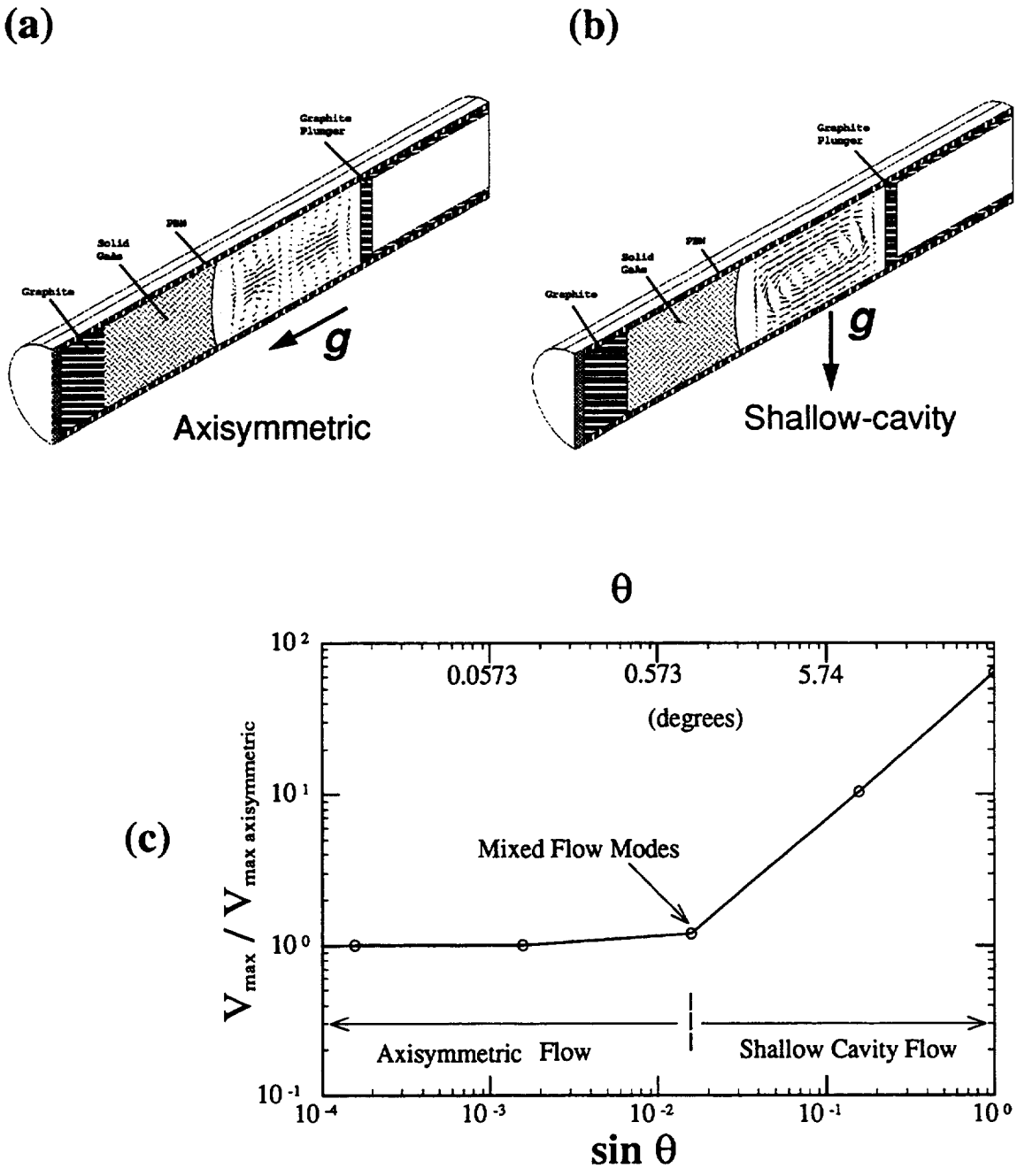

In Rayleigh-Benard natural convection in an enclosure, the bottom wall is heated relative to the top wall, and the sidewalls either insulated or perfectly conducting. The destabilizing effect of the (thermally induced) density gradient sets up cellular convection when critical Rayleigh number is reached. Rayleigh-Benard convection has been extensively studied in the classical fluid mechanics literature, experimentally, numerically, and theoretically. The convection patterns are known to be extremely sensitive to variation of the boundary conditions, the initial conditions and/or orientation with respect to the gravitational vector. For example, in a two-dimensional numerical study of thermal convection in an enclosure, Duh (1989) elucidated some facets of the complex flow phenomena which occur in the change from unicellular to multicellular oscillating flow under a body force steady in magnitude but varying in orientation. In particular, the critical Rayleigh number was found to depend on the orientation of the gravitational acceleration.

Orientation of g also modifies the time of the onset of convection. The effects of a steady background gravity level at varying orientation was studied for crystal growth from solution by Nadarajah et al. (1990). At 10^{-6} g_0, convective contributions to the overall fluid behavior became important after about three and five hours for orientation of the residual acceleration parallel and perpendicular to the top face of the crystal, respectively.

The orientation of the residual acceleration is absolutely critical to the fluid behavior and subsequent solute lateral uniformity. It affects the onset of convection as well as the flow pattern. This sensitivity is exacerbated in Bridgman crystal growth (and other melt growth processes) due to the inherently large axial thermal gradients, for which off-axis orientation of less than 1° in typical experiments can have profound consequences. This sensitivity to orientation may be a critical determinant of the viability of a particular process for SSF.

3.1.2 Oscillatory residual gravity

The great bulk of the numerical and analytical work done to date has been on sinusoidal variation of the residual gravitation. The importance of structural oscillations and other periodic disturbances in the g-jitter spectrum makes this a particularly important area. As pointed out by Rogers and Alexander (1991b), although the character of particular transient disturbances arising from, e.g., crew activity may be considered somewhat random, the structural response to these disturbances at a given location aboard the space vehicle will mostly be sinusoidal and deterministic.

The subject of the stability of time-periodic flows has been reviewed by Davis (1976). Other references follow in the text.

3.1.2.1 Single-frequency sinusoidal modulation

There are several interesting phenomena resulting from single-frequency sinusoidal disturbances and which are germane to materials processing on Space Station Freedom. In general, the observation that tolerable body-force modulation increases with its frequency (for single-frequency forcing) holds true for broad classes of problems and for a variety of different tolerance criteria, e.g., Alexander (1990); Monti et al. (1987, 1990); Ostrach (1982); Schneider and Straub (1989); Wadih and Roux (1988); Griffin and Motakef (1989a, 1989b); Murray et al. (1990); Coriell et al. (1989); McFadden and Coriell (1988); Polezhaev et al. (1984). This is due to the finite fluid response time: simply speaking, if the forcing is at a high enough frequency, the fluid does not have enough time to react due to its own inertia. Kamotani et al. (1981) pointed out that viscosity allows phase shifts in the velocity oscillations in the fluid relative to the modulation of the body force. Similarly there may be a phase shift between the fluid velocity field and the solute or thermal field, depending on the value of the Schmidt number or the Prandtl number, respectively. The Prandtl number compares the rate of diffusion of momentum and heat, i.e.:

$$Pr = \frac{\nu}{\kappa} \tag{7}$$

where ν is the dynamic viscosity and κ is the thermal diffusivity. Typical ranges of Prandtl number are shown in table 4:

TABLE 4. Typical material properties of physical liquids (after Wadih et al., 1990)

	$\nu\ (cm^2 \cdot s^{-1})$	$\kappa\ (cm^2 \cdot s^{-1})$	Pr
Gases	10^{-1}	10^{-1}	1
Liquid Metals	10^{-3}-10^{-1}	10^{-2}-10^{0}	10^{-3}-10^{-1}
Organic Liquids	10^{-3}-10^{-2}	10^{-4}-10^{-3}	10^{-3}-10^{-1}
Molten glasses	10^{2}	10^{-2}	10^{3}-10^{4}
Molten salts	10^{-3}-10^{-2}	10^{-3}	10^{0}-10^{1}
Silicone oils	10^{-2}-10^{1}	10^{-4}	10^{1}-10^{4}
Water	10^{-2}	10^{-3}	10^{1}

The Schmidt number similarly compares diffusivities of momentum and species:

$$Sc = \frac{\nu}{D} \tag{8}$$

where D is the species diffusivity. The difference in characteristic transport rates also may lead to another interesting phenomenon: increased values of response parameters such as lateral solute nonuniformity may be more severe in the first couple of periods following startup of a sinusoidal forcing. The effects of these disparate diffusivities will be discussed further in sections 3.1.3.

The first case discussed here is the rotation of the gravitational acceleration (i.e., the magnitude of the residual acceleration is fixed, but the orientation rotates through 360° at a constant rate). Schneider and Straub (1989) find that for natural (thermal) convection in a differentially heated long cylinder of air at $Ra = 2000$ and 5000 and for water at $Ra = 5000$, the most important frequency range is 10^{-1} to 10 Hz. Beyond some critical frequency $f^*=fL/\kappa$ (where f is the dimensional frequency, L is the cylinder diameter, and κ is the thermal diffusivity), the fluid response decreases with increasing frequency, as shown in figure 18. The frequency at which the dropoff occurs was found to be lower for air ($Pr =$

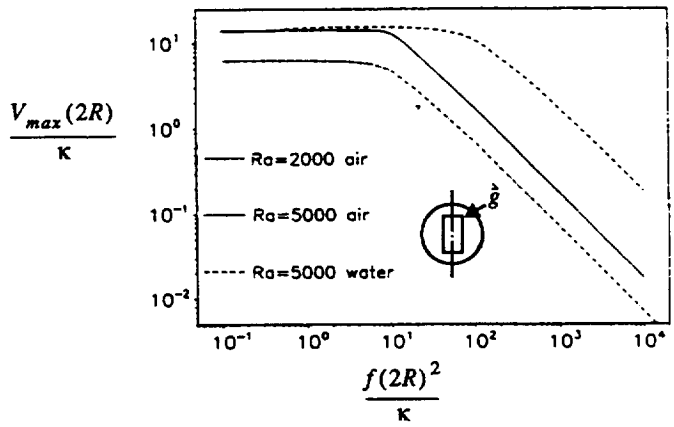

FIGURE 18. Dependence of fluid response on nondimensional frequency of rotating gravitational acceleration for thermal convection in a cylinder (after Schneider and Straub, 1989)

0.71) than for water ($Pr = 7$). Note that the maximum velocity attained (normalized by κ) increased with increasing forcing levels. In their study of solutally driven convection, McFadden and Coriell (1988) found that compositional nonuniformity increased with increasing angular rate of rotation, as shown in figure 19[1]. Some ground-based experimental

1. The ordinate $\Delta c/c_\infty$ is the ratio of the concentration variation at the melt/solid interface to the concentration far from the interface.

work on using low-frequency vibration to control the interface shape and position has been performed by Liu et al. (1987) on $CsCdCl_3$ and Lu et al. (1990) on CdTe.

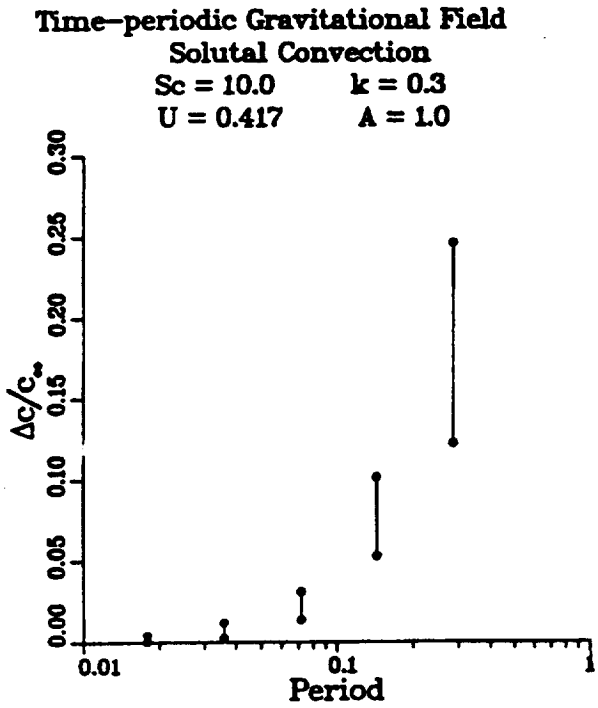

FIGURE 19. Dependence of solute nonuniformity on period of rotating gravitational acceleration for solutal convection in a cylinder (after McFadden and Coriell, 1988)

The trend of decreasing sensitivity above a critical frequency is also observed for the case of a constant orientation of g, but a sinusoidally varying magnitude: Griffin and Motakef (1989) found that the response of convection levels to a sinusoidal disturbance with a background g-level of 10^{-6} g_0 was a function of the reciprocal of the momentum diffusive time scale (i.e., L^2/ν, where ν is the kinematic viscosity). This trend (with comparable quantitative values for similar cases) was also found by Schneider and Straub (1989). Polezhaev et al. (1984) found that the lateral solute distribution in response to sinusoidal g-jitter was greatest for lower-frequency g-jitter. Alexander et al. (1991) confirm this finding during the numerical simulation of the Bridgman growth of dilute GeGa, concluding that the largest compositional nonuniformities occurred when the forcing was below 10^{-2} Hz and of amplitude 10^{-6} g_0 or greater. They also showed that in multiple-frequency simulations, the flowfield was still most sensitive to the lower-frequency components after an initial transient phase.

Another widely observed result is that, at any given frequency, there is a threshold amplitude above which the sensitivity increases nonlinearly. This is due to the nonlinear terms

in the governing equations starting to affect the transport of momentum and heat. This trend is seen, e.g., for thermal convection in a square enclosure subject to wall-temperature oscillations by Xia and Yang (1990). Large changes in the growth rate of TGS crystals grown from solution (0.4 - 238%) with increasing body-force amplitude at a fixed frequency were calculated by Nadarajah et al. (1990), indicating that above a critical residual acceleration level, the growth rate was markedly increased. However, when the period of modulation exceeded the viscous time scale L^2/ν (here, 100 seconds), the threshold amplitude was independent of the frequency and would presumably be governed by the sensitivity to a steady residual acceleration. They concluded that a purely harmonic single-frequency disturbance at or below 10^{-2} Hz and of magnitude less than 10^{-3} g_0 would probably not significantly affect this process.

Different flow patterns emerge with the application of sinusoidal forcing. Ramachandran (1990a) found that, for natural convection in a square enclosure with a steady background gravitational acceleration of 10^{-4} g_0, multicellular (rather than unicellular) flow patterns appeared in the range of 10^{-2} to 10 Hz and amplitude 10^{-3} to 10^{-2} g_0. The lowest frequency studied caused the most significant effects. A modification of the flow pattern in response to harmonic forcing was also seen in the related case of modulated wall temperature in Benard convection by Roppo et al. (1984). Application of harmonic forcing can set up convection cells of opposing rotational sense; see Alexander et al. (1991) for a good discussion of the velocity response and accompanying behavior of the solutal field in Bridgman growth.

Amin (1988) analyzed the heat transfer for a spherical body in a fluid undergoing sinusoidal gravity modulation, and found that even though the mean forcing value was zero, the Reynolds stresses accompanying the fluid modulation caused steady streaming, resulting in significant modification of the heat transport relative to the case of purely conducting heat flow. This would also be expected to modify the mass transport as well. The presence of steady streaming in systems undergoing sinusoidal modulation has also been discussed by Kamotani et al. (1981) and Alexander et al. (1991). For the Benard problem, Gresho and Sani (1970) showed that some modulated flows transport less heat than corresponding unmodulated flows. Variation in the heat transport relative to the steady-state case was found to be a function of Pr by Ramachandran (1985).

Biringen and Peltier (1990) studied Benard convection in a three-dimensional transient fully nonlinear Navier-Stokes analysis with the Boussinesq approximation. Different Prandtl-number fluids (air at $Pr = 0.71$ and water at $Pr = 7$) and a wide Rayleigh number range were examined for mean background gravitational levels of both zero g and 1 g_0 on

which was superimposed some body force variation. Confirming the results of Gresho and Sani (1970), they found that at low to moderate frequencies, the fluid response was synchronous with the acceleration forcing; however, at higher frequencies, a subharmonic behavior was found (i.e., periodic variation in the flowfield twice per the forcing period).

Murray et al. (1990) systematically investigated the coupling of morphological and convective instabilities in an idealized Bridgman growth undergoing a harmonic, axially directed body force for a range of Schmidt number from 1 to 81. The response to such forcing was complex and exhibited both synchronous and subharmonic instabilities, depending on the forcing frequency and amplitude. They found that, under certain conditions in which the base state was convectively unstable, the gravitational modulation actually served to stabilize the process. This last observation is an interesting result from a fundamental standpoint and serves to underscore the intricacies of the problems associated with *g*-jitter. See also Coriell et al. (1989); McFadden and Coriell (1988).

Steady streaming and the associated modification of heat transport have been noted for harmonic modulation of the body force about a zero mean. The response of a fluid to sinusoidal forcing of a particular frequency is related to the characteristic diffusion times.

From the standpoint of predicting the behavior of specific materials processes, the understanding of single-frequency g-jitter is an important step, but may not be directly translated into quantitative tolerable g-levels in the multifrequency and impulsive environment of SSF and the Shuttle; for that case, it is necessary to consider the combined effects of multifrequency and impulsive disturbances. Presuming that the response to multifrequency forcing is linear, the single-frequency analysis can be a very practical intermediate step. See, e.g., sections 3.1.2.2 and 3.1.3.

3.1.2.2 Multiple-frequency disturbances

The relatively low levels of forcing provided by the residual acceleration in the space environment allow us to consider the fluid systems as linear (except perhaps near resonance conditions). In this case, the response to several disturbances, for example, that of multiple-frequency body-force modulation, should be simply additive. There is evidence to support this contention both in numerical analysis and in space experimentation. In the DMOS experiment which flew on STS-61-B (Radcliffe et al., 1987), the mass transfer by mixing of organic liquids was shown to exhibit an additive response to the multifrequency and impulsive Shuttle environment.

A recent numerical investigation by Alexander et al. (1991) showed that the response of the solutal field in Bridgman growth of a dilute two-component system also exhibits an additive response to a multifrequency disturbance. Nevertheless, the same trend of decreasing sensitivity to higher frequency forcing, discussed in the previous section, was still found to hold. A tricomponent acceleration field oscillating parallel to the crystal/melt interface was applied to a two-dimensional setup. The frequency components were 10^{-2}, 10^{-1}, and 1 Hz of amplitude 10^{-5}, 10^{-4}, and 10^{-3} g_0, respectively with zero background gravitational levels. Figure 20 shows the velocity at a point within the flowfield as a func-

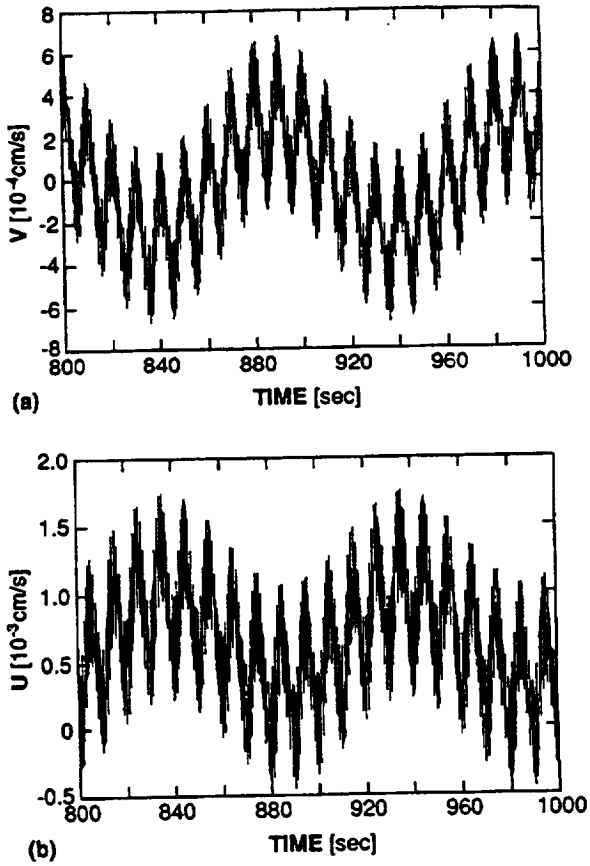

FIGURE 20. Velocities at a point in the flowfield after periodicity of the velocity field has been attained for a tricomponent gravitational disturbance with components of frequency 10^{-2}, 10^{-1}, and 1 Hz of amplitude 10^{-5}, 10^{-4}, and 10^{-3} g_0 respectively (after Alexander et al., 1991)

tion of time after an initial transient period, on the order of 100 seconds. Although the multiple-frequency nature of the response is readily distinguishable, at this point the largest-magnitude fluctuations in the velocity field modulate at about 10^{-2} Hz, corresponding to the lowest-frequency body-force component (which was also the lowest-amplitude forcing component). The behavior of the solute field was somewhat different from the velocity response. It was characterized by a longer transient period (on the order of 3000

seconds) with a maximum lateral nonuniformity, ξ, of 6%. Following this adjustment period, the solute field periodically fluctuated between 0.18% and 0.55% over a period of 50 seconds, as shown in figure 21. The solute field responded most strongly at long times to

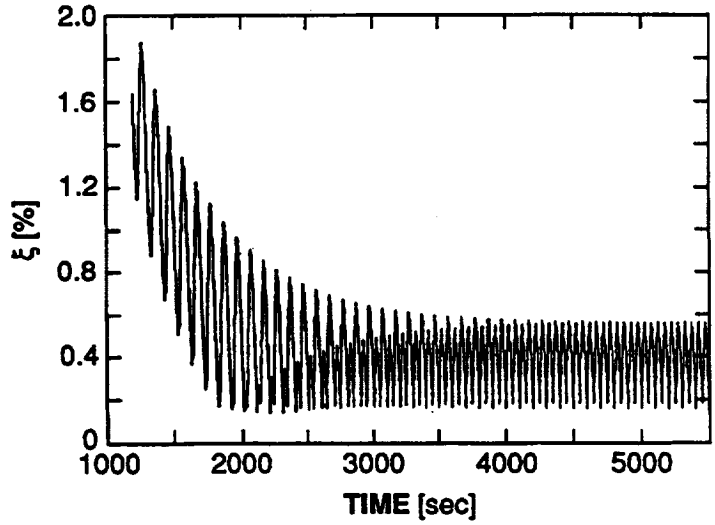

FIGURE 21. Solute field response at the end of the transient period: solute nonuniformity ξ in response to tricomponent acceleration field with components of frequency 10^{-2}, 10^{-1}, and 1 Hz of amplitude 10^{-5}, 10^{-4}, and 10^{-3} g_0 respectively (after Alexander et al., 1991)

the lowest frequency disturbance (10^{-2} Hz) with a maximum lateral nonuniformity occurring twice per forcing period, reflecting the complete flow reversal during each forcing cycle. Further discussion will be made of the effects of multiple-frequency disturbances on the velocity and solutal fields in section 3.1.3.5, which will include startup transient effects as well.

It is encouraging that some evidence exists that under typical conditions, fluid systems behave linearly to body-force modulation (except perhaps near resonance conditions). Provided that this assumption holds and that the actual multifrequency acceleration environment is well-characterized, it may be possible to analyze the effects of harmonic disturbances by the relatively simple linear superposition of the body force components. One should recall however that even simple addition may result in a very complex response due to phase and period relationships.

The additive behavior of fluid systems to multifrequency forcing is of great concern for assessing the adequacy of SSF specifications. Since the tolerance curves for allowable residual acceleration in figures 2 and 14 were based on the response predicted by an order-of-magnitude analysis to a single-frequency disturbance, that analysis may provide overly

generous tolerance levels. Much more research in this area is a prerequisite for adequate forecasting of process viability on SSF.

3.1.3 Transient disturbances

Transient disturbances may consist of a single impulsive transient or a pulse train, so-called "compensated" double pulses, or arise from startup/ending transients from equipment operation. See section 2.2.3.

3.1.3.1 Single pulses

Single pulses in the residual acceleration field can result from externally applied forces on the space vehicle or platform, e.g., impacts such as extra-vehicular activities or thruster firings. Both the duration as well as the magnitude of an impulse will affect the response of a particular experiment. It must be pointed out that the two cases which immediately follow are for very particular cases of materials, geometries, and unique simplifications, subjected to particular impulsive driving forces. However, the background acceleration field and the magnitudes of the disturbances are very reasonable and well within the range of what can be expected on the Shuttle and SSF.

Recovery of the solute field from a pulse can take a long time, on the order of thousands of seconds, as shown by Alexander et al. (1989). Figure 22 shows the solute field for an idealized Bridgman-Stockbarger crystal growth of dilute GeGa. The steady background residual acceleration was set to $1x10^{-6}$ g_0 oriented precisely along the growth axis (perpendicular to the crystal/melt interface, which is the bottom of the rectangular domain in the figure). The solute nonuniformity at the interface due to the steady background acceleration was already appreciable at 11.3%. A one-second pulse of magnitude $5x10^{-3}$ g_0 oriented parallel to the crystal interface (worst orientation) was applied to the system. One second later (figure 21(a)), the solute field's response is clearly seen near the sidewalls. The solute nonuniformity ξ initially decreases, then reaches a maximum of 40% at 250 seconds. Although the velocity field reverted back to steady-state conditions by 300-400 seconds, the consequences of such an impulse to the solute field are longer-lasting; 2000 seconds must pass before the solute field approaches its original distribution.

In contrast to the semiconductor crystal-growth simulations, at similar conditions (10^{-3} g_0 for one second on a steady background level of 10^{-6} g_0) for the TGS crystal growth of Nadarajah et al. (1990), the sharp peak of velocity which followed the impulse died out fairly rapidly, and they concluded that such an impulse would probably not be overly damaging.

On the other hand, 10^{-2} g_0 was expected to produce unacceptable results; this level is likely within the acceleration domain aboard SSF.

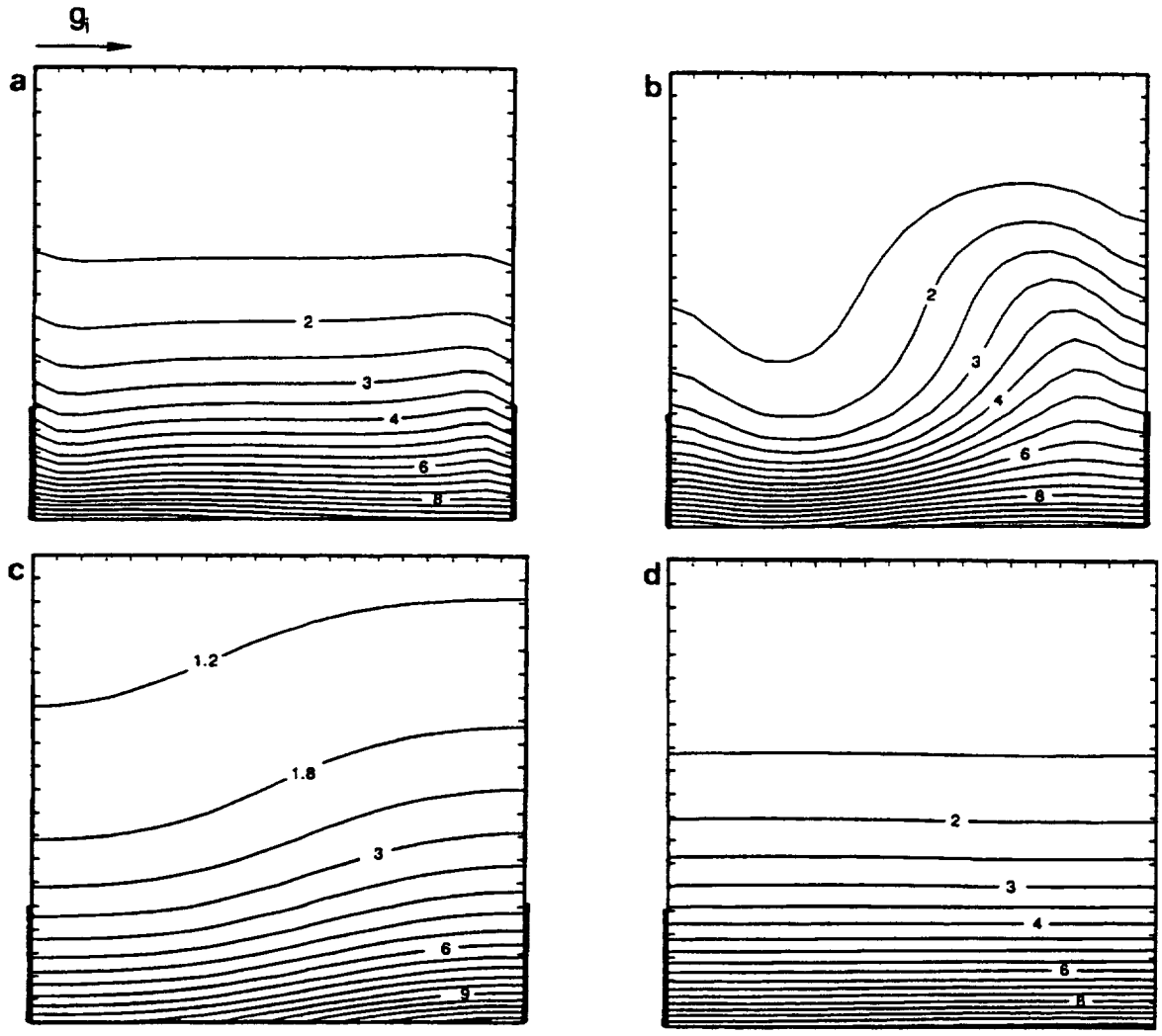

FIGURE 22. Solute field development in directional solidification of Ge:Ga subjected to a one-second $5x10^{-3}$ g_0 pulse against a steady background acceleration of 10^{-6} g_0: Time elapsed is (a) 1 sec (ξ=11.3%); (b) 30 sec (ξ=0.67%); (c) 250 sec (ξ=40%); and (d) 1250 sec (ξ=3.4%). (After Alexander et al., 1989)

Shorter pulses are similarly damaging, but to a much lesser degree. A comparison of two cases in which the duration of the pulse was varied (0.1 sec vs. 1 sec) for the same magnitude pulse ($3x10^{-3}$ g_0) and steady background g-level of $\sqrt{2}x10^{-6}$ g_0 (with accompanying solute nonuniformity for the steady-state at 21.5%) was also made by Alexander et al. (1989). While the higher-magnitude pulse caused large variation in ξ (from a minimum of 0 to a maximum of 26%), the lower-magnitude pulse caused much smaller variation (minimum of 17% to a maximum of 22%). The length of time for both solute fields to fully recover to steady-state conditions was still on the order of a thousand seconds, unlike the

velocity field which recovered quickly (300-400 seconds and 50 seconds respectively). Later calculations (Alexander et al., 1991) incorporated the measured acceleration levels on SL3 to the same numerical setup. Although the velocity field responded quickly and dramatically to a thruster firing sequence, the compositional nonuniformity was more sensitive to the more long-lasting residual acceleration components, due to the larger characteristic diffusivity for the solute field.

The "energy input" to a system by a pulse (more correctly, the "momentum input") can be characterized by the area under the curve of residual acceleration as a function of time. If the disturbance is short in comparison to the characteristic diffusion time, the response of a system to a given pulse follows predictable trends. Monti (1990) studied the response of a system driven by thermal convection to transient disturbances. The short-term behavior for response to square pulses of varying amplitude and duration (but equal area) varied in different but predictable ways. In addition, the long-time behavior was the same for the three following cases:

Table 5. Pulse statistics for three cases of thermally driven flow (after Monti, 1990)

	g/g_0	Gr	Δt (s)	$G_1=\Delta t\, g_p/g_0$ (s)	$G_2=Gr\Delta t$ (s)
I	5×10^{-4}	40,000	4	2×10^{-3}	160,000
II	1×10^{-3}	80,000	2	2×10^{-3}	160,000
III	2×10^{-3}	160,000	1	2×10^{-3}	160,000

The second column gives the magnitude of the pulse, g_p, followed by the corresponding Grashof number, Gr, the duration of the pulse and the integrated momentum input G expressed both in terms of g and Gr. The Grashof number is defined as:

$$Gr = \frac{g\beta\Delta TL^3}{\nu^2} \tag{9}$$

The Rayleigh number given in (6) above is easily seen to be related to the Grashof number. They are linked together through the Prandtl number which compares the rate of diffusion of momentum and heat, so that $Gr = Ra / Pr$. For all cases, the short-time behavior of the velocity field indicated that the maximum velocity reached was the *same* for all cases, as shown in figure 23, and was *proportional to the momentum input.* Furthermore, the maximum velocity increased linearly throughout the duration of the pulse with a slope that was proportional to the magnitude of the pulse. Other test cases were run in which pulses of different shape but equal area were studied, including triangular spike profiles. For all

cases, the velocity maximum was defined by the integrated value of residual acceleration with respect to time.

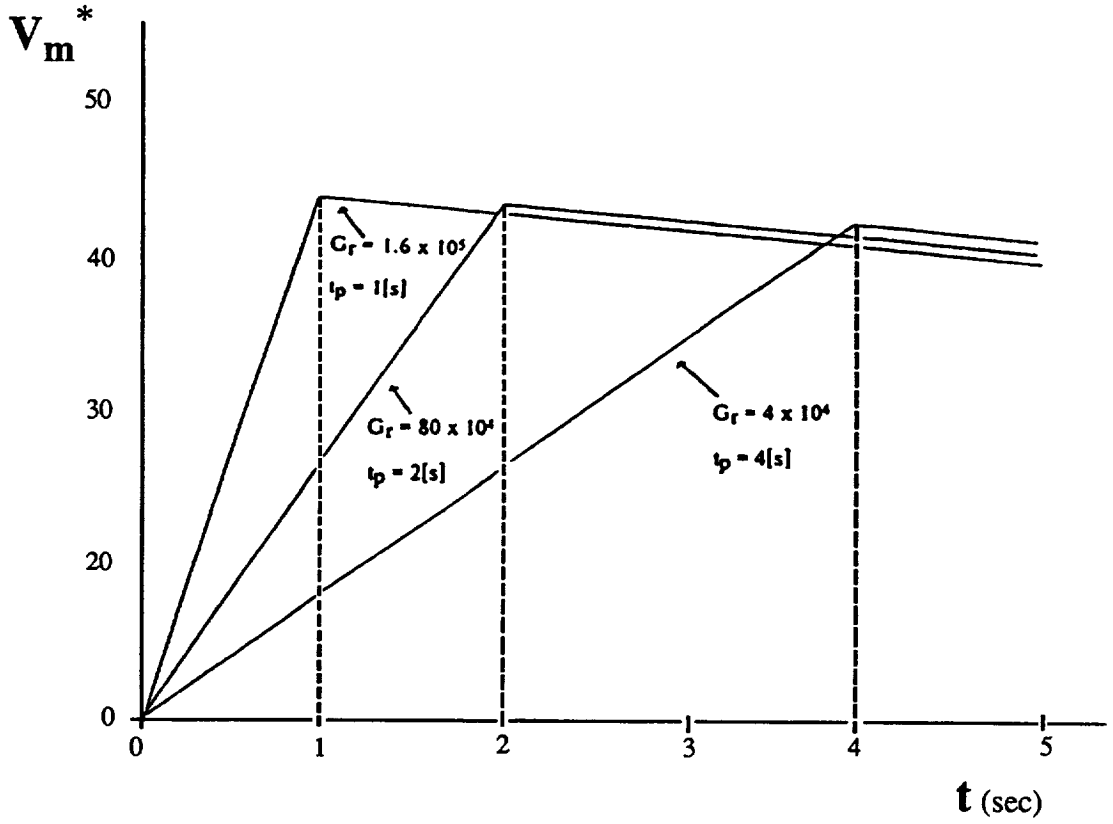

FIGURE 23. Velocity response (nondimensional) to square gravitational pulses of different duration and magnitude but equal momentum input (after Monti, 1990)

A relaxation phase follows the forcing phase. Figure 24 shows the long-time behavior of the system for all three cases of table 5, above. The velocity response, expressed in terms of a local maximum V_m, as well as the maximum value of the stream function ψ_m, reaches a peak at the end of the pulse and decays exponentially.

On the other hand, the thermal field behaves very differently. The thermal disturbance is here expressed in terms of a variation from the steady-state (purely diffusive) conditions: The magnitude of the difference between the local nondimensional temperature at a given time and the local nondimensional temperature at steady state is computed over the entire computational domain. The local disturbance D_m is the maximum value of this quantity over the flowfield at a given time. The overall temperature distortion is given by D_T, which is the sum of (the magnitudes of) these local disturbances over the flowfield at a given time.

The first point to note is that the long-term behavior of the system to three different pulses of equal momentum input is indistinguishable, which lends additional credence to the contention that the initial shape of the pulse is unimportant in comparison with the level of forcing integrated over time. The second is that the velocity field and the thermal field behave very differently. The momentum input, represented by the integrated *G* defined in ta-

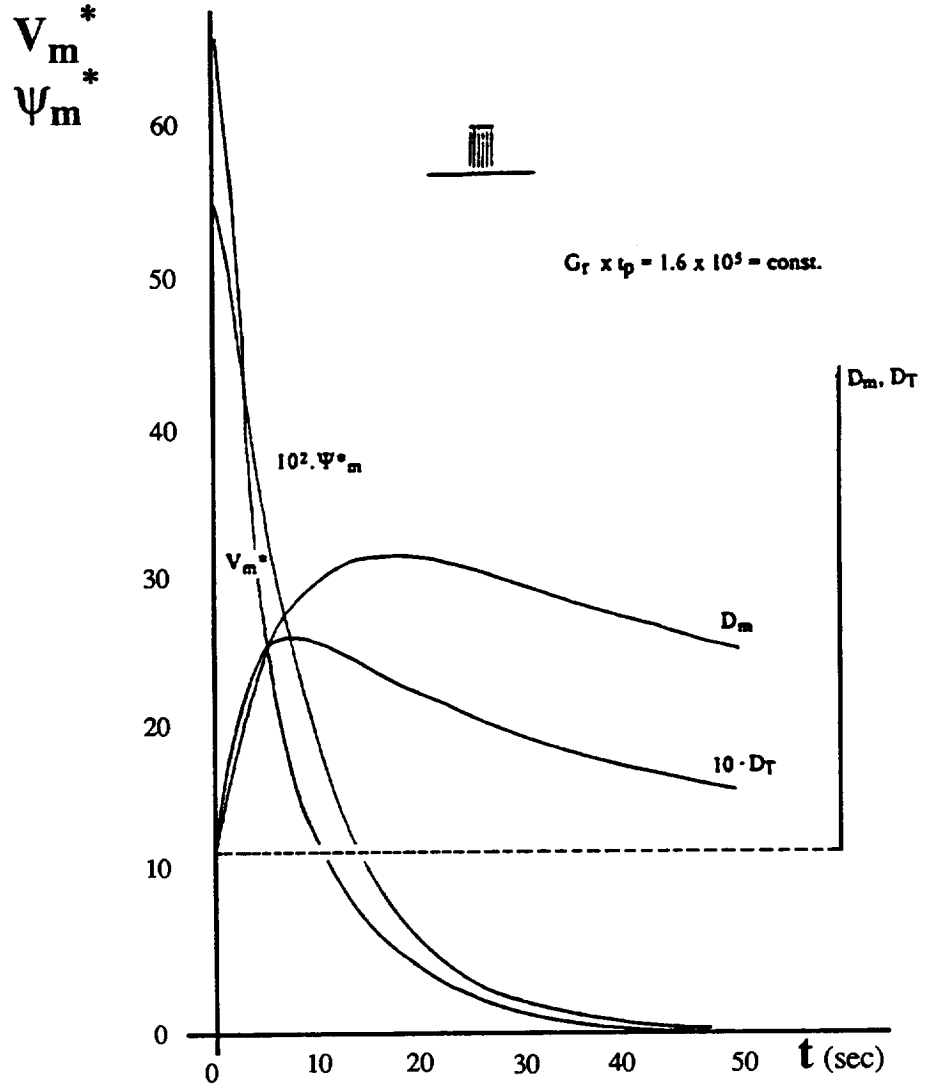

FIGURE 24. Response of velocity and thermal fields to acceleration pulses with momentum input of 2000 g_0 sec (see table 5 above) showing relaxation behavior (after Monti, 1990)

ble 5 above, caused a velocity disturbance to develop which was proportional to its magnitude. Following the pulse, the velocity field was seen to undergo exponential decay. However, the thermal field in Monti's computation (and the solute field in Alexander's simulation) was still reacting to this velocity disturbance which in turn had lasted much

longer than the original acceleration pulse. The response of the scalar field continued to grow after the velocity response peaked. The amount of time required for the growth of the thermal disturbance to peak and to decay was found to be a function of the Prandtl number by Monti. The Schmidt number relates momentum to species' diffusivity just as the Prandtl number relates momentum to thermal diffusivity. We would therefore expect the Schmidt number to play an important role in the distortion to the solute field, just as the Prandtl number defined the time to reach the peak thermal distortion and decay time in Monti's case. They are direct multipliers (more precisely, included in the thermal and solutal Rayleigh numbers) of the convective terms (i.e., the coupling between the velocity and thermal or solutal fields). The long-term relaxation behavior can then be understood in the comparison of the momentum diffusivity to that of heat (or mass). The relaxation time for solute fields may be very long due to their characteristically small diffusivities. Finally, it is noted that, in principle, knowledge of the impulse response may be sufficient to determine the frequency response to single-frequency sinusoidal excitation (and vice versa). This follows from basic linear system theory, and has the potential of significantly reducing the necessary number of numerical or experimental tests, but has yet to be proven or used in practice.

Pulse magnitude and duration are of critical importance in determining its net effect on a materials process. It should be possible to generalize the effects of pulses as long as the duration of the pulse is short relative to the characteristic diffusion time. In this case, the shape of the pulse is not as important as the momentum input, characterized by the integrated sum of the curve of acceleration with respect to time. This parameter determines the momentum response for a given system; other fluid parameters govern the relaxation phase. While these results should not be read quantitatively without additional (and preferably experimental) verification, we should certainly be concerned about the effects of the impulsive disturbances generated unknowingly by a crew going about its business of living and working in a space vehicle. More work in this area is required.

3.1.3.2 Multiple pulses

Mass dislocations which are internal to the space vehicle or platform result in "compensated" double pulses. The net momentum change to the platform is zero, and thus the pulses are compensatory in terms of momentum, but this does *not* necessarily hold true for the net transport due to the role of diffusivity. Other scenarios of multiple gravitational pulses with the same orientation can easily be envisioned. For both of these cases, in addition to the criteria of momentum input and fluid properties described above in section 3.1.3.1, the fluid response to multiple pulses is dictated by the time delay between pulses.

Monti's (1990) study (also described in the preceding section) related thermal and velocity distortion for multiple pulses. Again the process must be understood in light of the momentum diffusivity. If two or more pulses are applied "close" together in comparison to the diffusive time scale, the thermal or solute field does not have a chance to dissipate the momentum input of the first pulse before it must absorb the succeeding one[1]. This is readily seen in figures 25 and 26 which shows the velocity and thermal response to com-

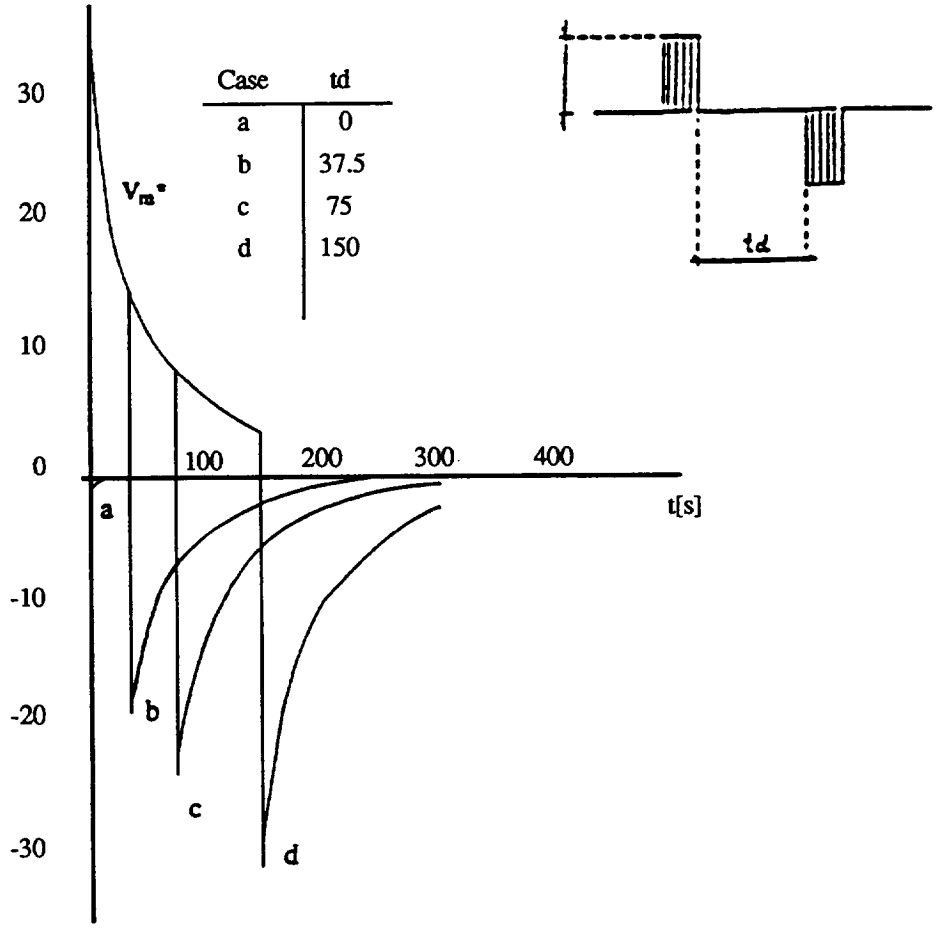

FIGURE 25. Temporal response of velocity field to "compensating" double pulses with varying time delay (after Monti, 1990)

pensated pulses with varying time delay between pulses. In all cases, the velocity responds quickly to the second pulse and decays exponentially. The response of the thermal field is more complex. If the second negative pulse occurs after a short time, distortion of the thermal field is minimized (curves a and b) both in terms of magnitude and in relaxation time to steady state. On the other hand, if the second pulse occurs after the time when the max-

1. Recall the discussion in the previous section regarding the integrated effect of the acceleration with respect to time if the pulse duration is small relative to the diffusion time.

imum thermal distortion has developed, the "damage" to the thermal field has already been done, and the maximum overall disturbance can be very close to that observed for the single-pulse case. Alexander et al. (1989) and Dressler (1981) also observed residual effects in both the velocity and scalar fields following two pulses of opposite sign.

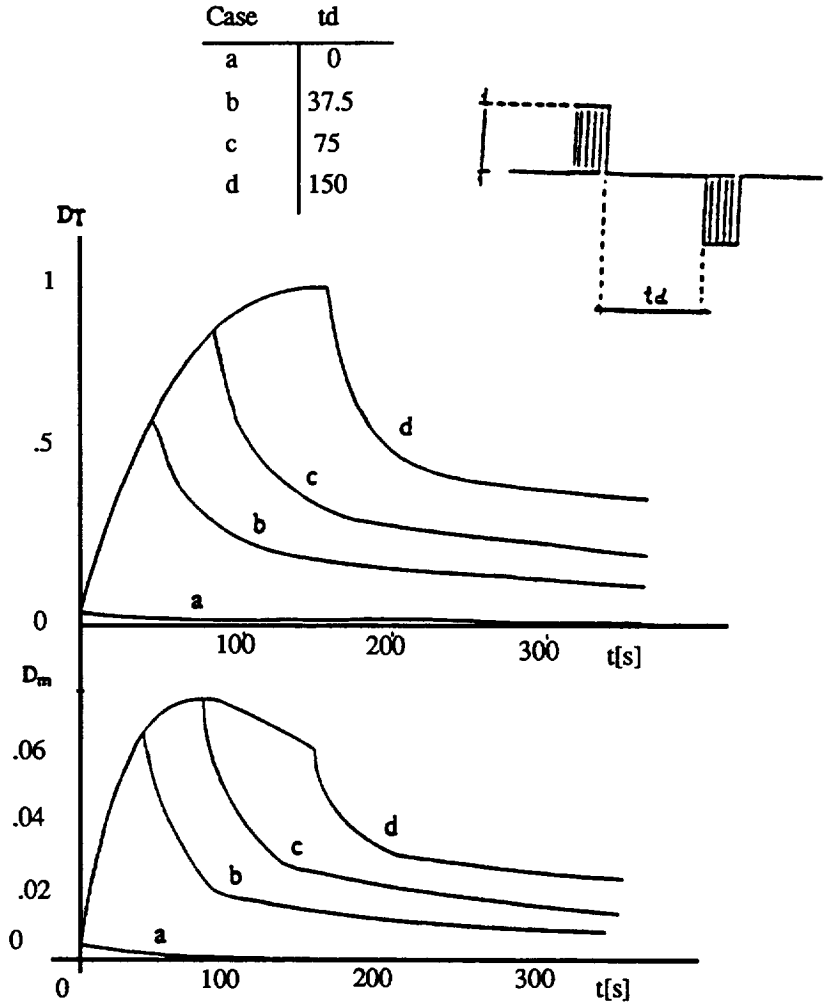

FIGURE 26. Temporal response of the thermal field to "compensating" acceleration pulses with varying time delay (after Monti, 1990)

For the Bridgman growth described above in section 3.1.3.1 (Alexander et al., 1989), two one-second pulses of magnitude $3x10^{-3}$ g_0 and the same orientation separated by one second were superimposed on a steady background g-level of $\sqrt{2}x10^{-6}$ g_0. They were found to have drastic consequences on the solute nonuniformity, with a maximum value of 76%, or almost *double* the amount of nonuniformity which each single pulse alone would cause. This supports the argument that the momentum input to the system (discussed in section 3.1.3.1 above) is more important than the shape of the accelerative forcing with respect to

time when the disturbance is "short" relative to characteristic diffusion times. These conclusions are confirmed for an even longer time delay by Monti (1990). In their case, with a time delay of 150 seconds between pulses ($g_p = 1x10^{-3}$ g_0 for one second), the velocity field had time to dissipate nearly completely before the application of the second pulse. Thus the velocity distortion parameter exhibited two successive peaks with magnitudes comparable to that of a single pulse. On the other hand, the thermal field did not have time to dissipate the momentum input and exhibited nearly double the distortion levels that a single pulse alone would cause, as shown in figure 27.

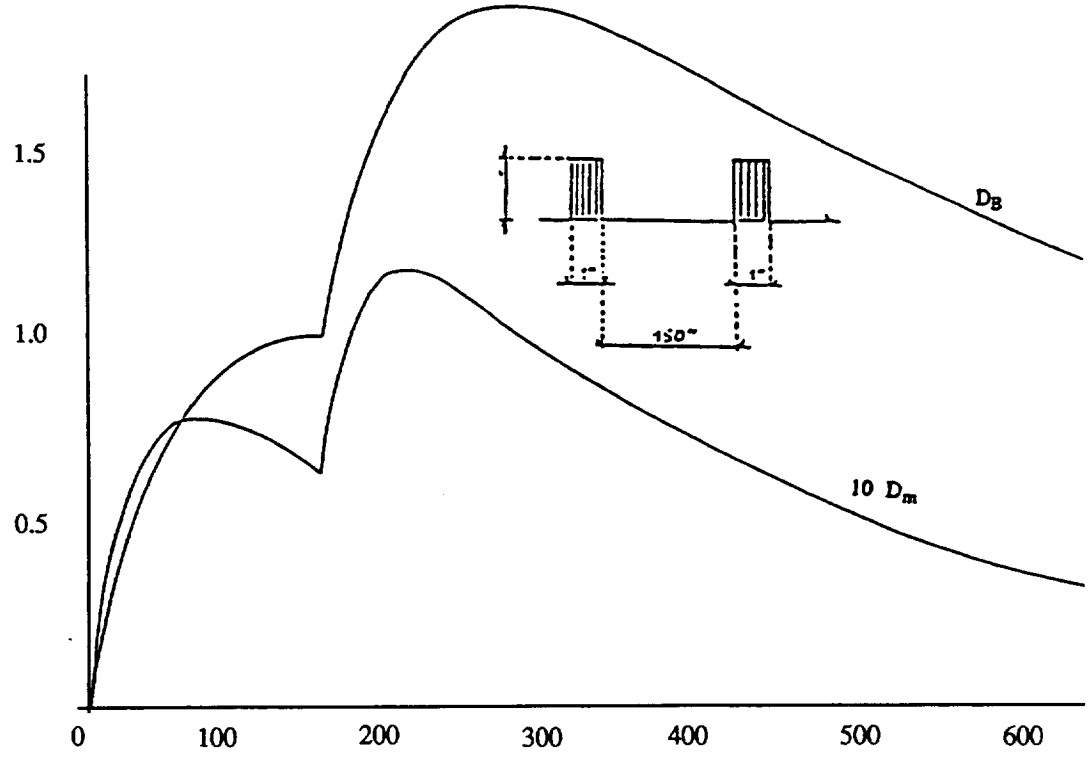

FIGURE 27. Thermal field distortion resulting from two successive acceleration pulses with a time delay of 150 seconds (after Monti, 1990)

The time delay between the pulses is dominating factor in determination of the degree of distortion to the thermal or solute fields for a particular system. As for the single-pulse case, the velocity disturbance was seen to dissipate rapidly, while the solute and thermal fields grew and decayed more slowly, with mass transport relaxation times being very long due to the characteristically long diffusion times. Therefore, if the thermal (or solute) field is allowed to reach appreciable distortion levels before the second pulse is applied, the consequences are much more severe than for pulses which follow in rapid succession (provided they have the same momentum input). For pulses of opposing sign, the thermal

field could be distorted as much as for the single-pulse case. For pulses of the same sign, the solute and thermal fields could be distorted by almost double the value attained for single-pulse forcing. More work in this area is needed.

3.1.3.3 Step changes in gravity

For single step changes in the body force, recovery time to the steady-state conditions was found to be dependent primarily on momentum diffusion for $Pr = 0.01$ in the Bridgman directional solidification of semiconductors by Griffin and Motakef (1989) for a Rayleigh number range of 0 - 1.5×10^5. This agrees with the low-*Pr* number results of Schneider and Straub (1989) who studied thermally driven natural convection in a cylinder over a range of Prandtl number ($Pr = 0.023$ (silicon) - 134.9 (glycerin); $Ra^* = 200$ - 5000). The latter study also found that for high-*Pr* fluids ($Pr > 1$), the thermal diffusivity (and not momentum diffusivity) was found to be the dominating factor for recovery time. The fluid response to body-force variation is governed by a diffusion process after the growth phase. For low-*Pr* fluids, momentum transport is less efficient than the transport of heat; consequently the overall time to steady state is governed by momentum diffusion. The reverse holds true for high-*Pr* fluids. The important point to note again is that, typically, the thermal, velocity (and, for that matter, species) fields each respond to forcing at different rates because the diffusivities for heat and momentum (and mass) are, in general, different.

Both studies found that when a step increase in g was applied of up to some critical step magnitude, the disturbance died out exponentially at a rate independent of Rayleigh number. This is shown in figures 28(a) and (b) from Griffin and Motakef, which shows a response time τ^1 as a function of *Ra*. In figure 28(b), the time to recover from a step

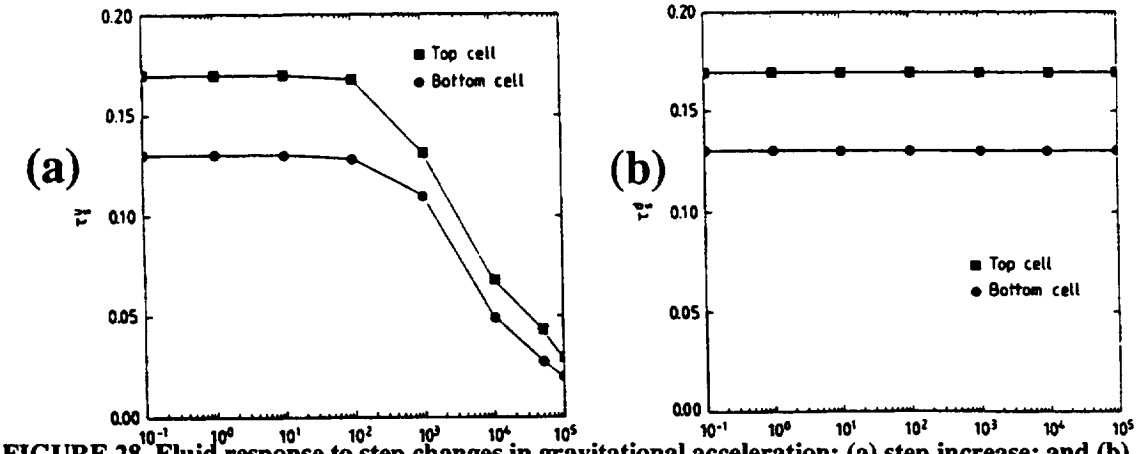

FIGURE 28. Fluid response to step changes in gravitational acceleration: (a) step increase; and (b) step decrease (after Griffin and Motakef, 1989)

1. τ is the nondimensional response time, i.e., the time required to reach 99% of steady-state conditions after application of the step divided by the momentum diffusion time scale (R^2/ν).

decrease to a zero acceleration level was independent of Rayleigh number; this represented the diffusion of fluid momentum by friction at the walls. Although the characteristic times were the same for the step increase in gravitational acceleration at low Rayleigh number (figure 28(a)), a dropoff in characteristic time above a Rayleigh number of about 100 is apparent, which is due to the increasing role of the nonlinear convective terms.

Chait and Arnold (1988) reached similar conclusions studying directional solidification with a step decrease in gravity for various low-g vehicles. By comparing their results to those of Griffin and Motakef, they produced a fairly universal "sensitivity" graph (figure 29) for directional solidification experiments, strictly applicable to gravitational orienta-

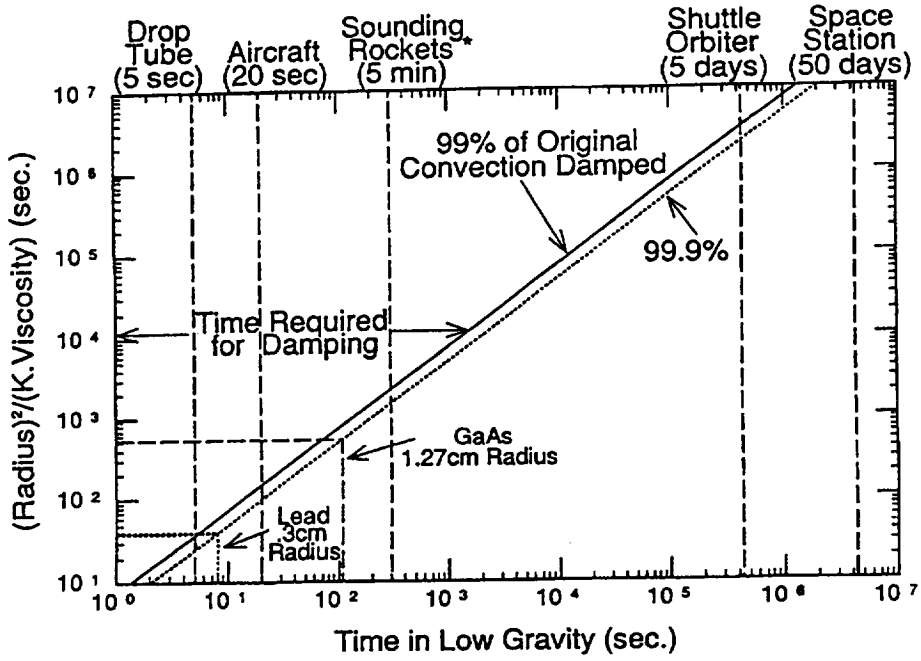

FIGURE 29. Required time for damping out of convection levels induced by a step decrease in gravitational acceleration for directional solidification experiments (after Chait and Arnold, 1988)

tion parallel to the growth axis. The lines provide the required amount of time for an initial convection level to damp out to within an arbitrary level (here 99% and 99.9%).

Another source of buoyancy is that due to the density difference between interfaces of two fluids. Dewandre and Roesgen (1988a, b) studied the behavior of drops and bubbles in response to harmonic modulation and Heaviside variation of the gravitational acceleration. The sensitivity criterion which was used was that the displacement of the drop be less than 10% of the drop's radius. They found that drops are less sensitive to g-jitter than bubbles (due to the smaller density variation between the fluids). In addition, at early times which

are dominated by fluid inertia, smaller drops were found to be less sensitive to step changes in the body force than larger drops (displacement/R varies as $1/R$), while at longer times, the reverse holds true (displacement/R varies as R; this can be easily understood in light of the discussion above, as the appropriate viscous diffusion time scale is R^2/ν).

There are short-time and long-time behaviors associated with step changes in gravity, too. Recovery to overall steady-state conditions is seen to be a function of viscous diffusivity for low Prandtl-number fluids, and a function of thermal diffusivity at high Prandtl number.

3.1.3.4 Random disturbances

Biringen and Peltier (1990) argue that random disturbances would better represent the space acceleration environment, and offer the interesting conclusion that random disturbances (whether they are random in magnitude *or* orientation) are more dangerous than sinusoidal oscillation for certain fluid systems. For both conditions of zero background gravity and in the case of 1 g_0, random disturbances caused instability in Rayleigh-Benard convection which were stable under the same sets of conditions for sinusoidally varying disturbances. As they point out, it is intuitively obvious (and reinforced by the easier path to instability found for this case), that metastable states which can be observed on earth will be unlikely to occur in space due to the broad-band nature of the spatial and temporal acceleration variation.

For Rayleigh-Benard convection (i.e., a zero velocity base state which is linearly unstable when a certain critical Rayleigh number is reached), the fluid was more sensitive to random excitation (either in magnitude or orientation) than to sinusoidal modulation of the residual acceleration.

3.1.3.5 Startup transients associated with sinusoidal disturbances.

The fluid response to the startup of a sinusoidal disturbance can also be characterized as a transient disturbance, exhibiting short-time behaviors which can be more severe than that evidenced by the steady periodic conditions which prevail at a later time. Alexander et al. (1991) found that the short-time response of a solute field (i.e., much less than the characteristic time scale for solutal diffusion, $t = L^2/D$) to either single- or multiple-frequency disturbances could be up to ten times higher than at subsequent times and was qualitatively independent of the type of disturbance. This can be understood in light of the momentum input considerations and variable rates of diffusivity discussed above in sections 3.1.3.1 and 3.1.3.2, above. Figure 29 shows the response of the velocity field during the

first 200 seconds after application of a multiple-frequency body-force modulation, composed of frequencies of 10^{-2}, 10^{-1} and 1 Hz of magnitudes 10^{-4}, 10^{-3}, and 10^{-2} g_0, respectively (with zero background acceleration level). After an initial transient phase, the fluid

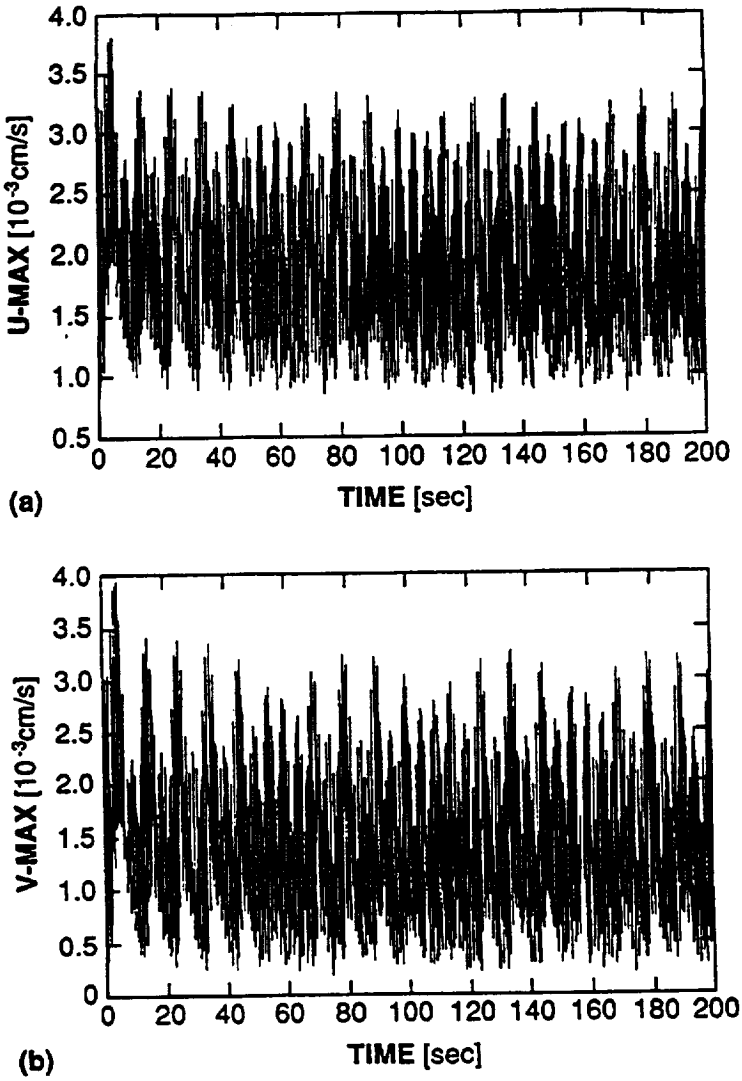

FIGURE 29. Temporal record of maximum velocities resulting from the startup of a tricomponent sinusoidal acceleration with frequency components 10^{-2}, 10^{-1}, and 1 Hz at amplitudes of 10^{-5}, 10^{-4}, and 10^{-3} g_0 respectively (after Alexander et al., 1991)

behavior became essentially periodic in character. However, the behavior of the solute field was very different from that of the velocity field, as in the case of pulses and harmonic disturbances discussed in the preceding sections. Specifically, the smaller characteristic diffusivity for the solute field caused the lateral nonuniformity, ξ, to grow at a slower rate than the velocity field (figure 30). The influence of the lowest-frequency component became apparent after about 80 seconds and was responsible for the most significant fluctu-

ations, although this corresponded to the lowest-amplitude forcing. Solute nonuniformity peaked at a maximum of about 6% at about 250 seconds, followed by a slow decay process until it fluctuated about a mean of 0.4% after several thousand seconds. (See also the

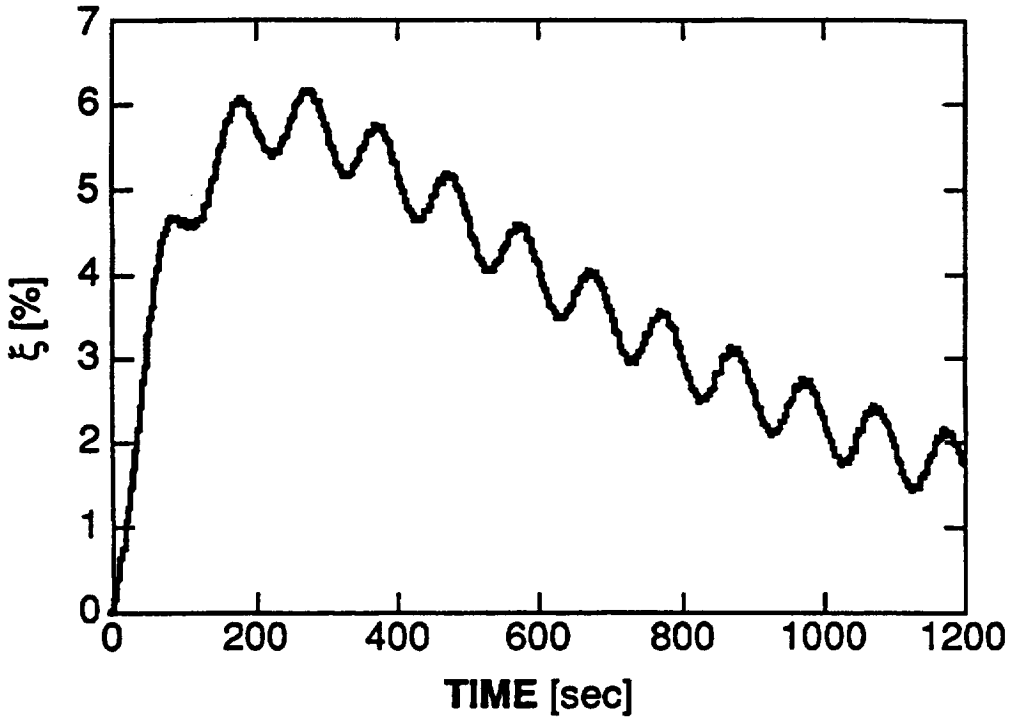

FIGURE 30. Temporal record of lateral solute nonuniformity resulting from the startup of a tricomponent sinusoidal acceleration with frequency components 10^{-2}, 10^{-1}, and 1 Hz at amplitudes of 10^{-5}, 10^{-4}, and 10^{-3} g_0 respectively (after Alexander et al., 1991)

behavior closer to achievement of fully periodic conditions in figure 21 of section 3.1.2.2.) The response to startup transients engendered during application of sinusoidal disturbances is also discussed by Monti (1990).

The short-time response of the solutal field (i.e., much less than the characteristic diffusion time) to the startup of a single- or multiple-frequency modulation of the body force may be significantly greater than the levels attained once fully periodic conditions are attained.

3.1.3.6 Actual space environment

To achieve diffusion-dominated Bridgman growth, we may require a quieter environment than can be provided on the Shuttle or Space Station Freedom. Numerical simulation of an idealized system by Alexander et al. (1989) for their particular case indicates that even steady background levels of 10^{-6} to 10^{-7} g_0 may cause unacceptable effects in terms of radial segregation due to convective effects on the solutal distribution, depending on the ori-

entation. At the very least, this conclusion should give us cause for concern for the broad variety of materials and geometric and thermal environments which would conceivably be candidates for space experiments. At the most recent COSPAR conference, Tatarchenko (1990) goes so far as to say that in *all* of the wealth of accumulated experimentation by the Soviets in crystal growth from the liquid phase, which encompasses on the order of 500 experiments, *not a single one* could prove conclusively that the space environment produced better-quality crystals. Admittedly, it is plausible to assume that equipment problems, etc., could be the dominating factors in these results; however, it is equally plausible to assume that the quality of the low-gravity environment aboard space vehicles may be responsible for some of these experiences. Furthermore, their expectations concerning the heat transfer in the space environment were not directly translatable from their ground-based experimentation, and he suggested that, for example, our understanding of radiative heat transfer in the space environment is inadequate at this point.

A simulation by Alexander et al. (1991) utilizing SL3 acceleration data for body-force input found that the solute field response was less affected by the impulsive transient of a short thruster firing sequence than by the broadband multifrequency environment[1]. The raw acceleration data of a characteristic quiet time was decomposed into a Fourier spectrum of 46 components with frequency components in the range of 3 - 10 Hz, shown in figure 31. (Note that this decomposition precludes the steady-state and very low-frequen-

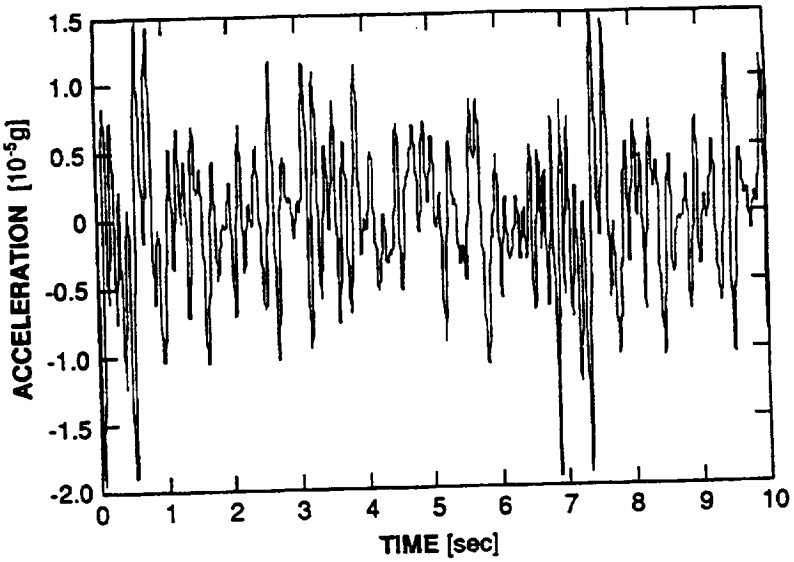

FIGURE 31. Acceleration profile of quiet time during SL3 derived from 46 Fourier spectral components in the frequency range 3-10 Hz (after Alexander et al., 1991)

1. In contrast, the behavior of the velocity field was very dramatically responsive to the thruster firing; see the discussion on the role of diffusivity in sections 3.1.3.1-3.1.3.2.

cy components to which prior simulations showed great sensitivity.) A second profile which included a thruster firing was similarly decomposed, with 27 components in the range of 0.03 to 1 Hz (shown in the inset of figure 32). The two sequences were then com-

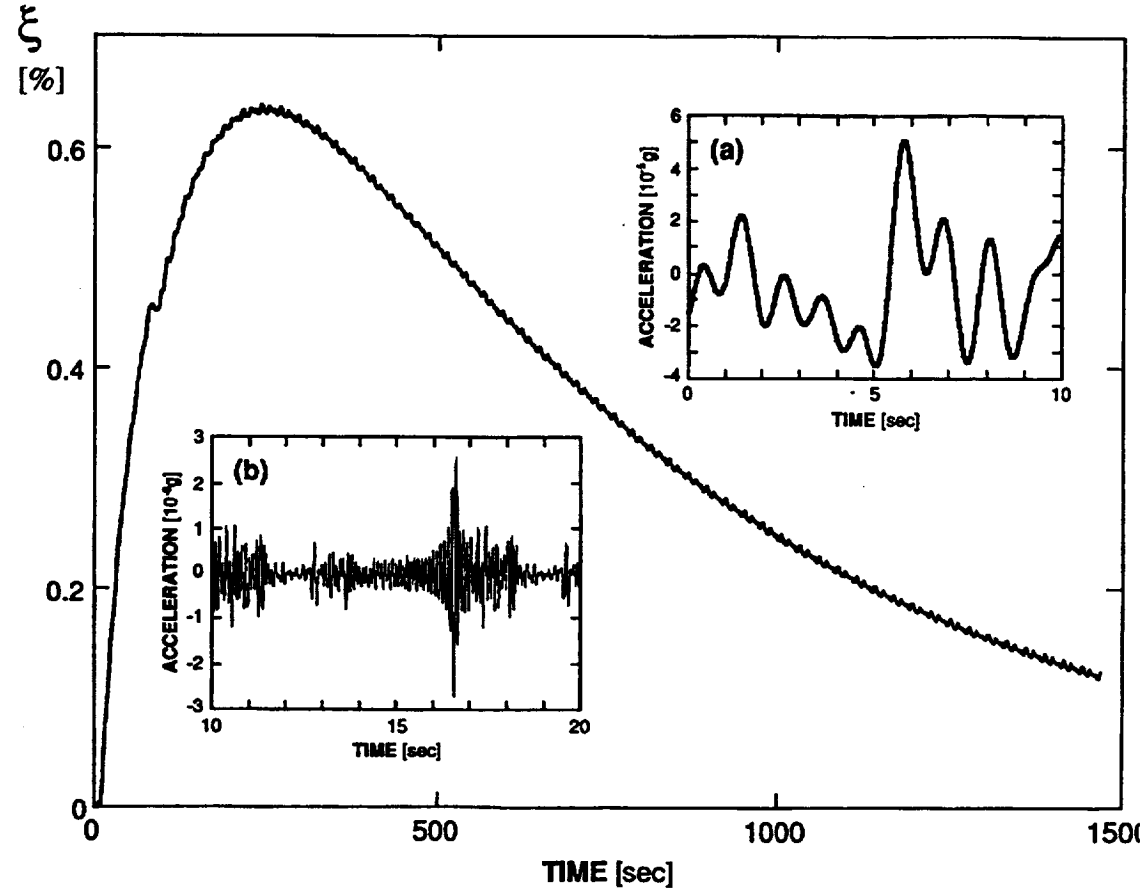

FIGURE 32. Temporal record of lateral nonuniformity ξ in response to a sequence of two thruster firings synthesized from Fourier spectra of SL3 acceleration data (after Alexander et al., 1991)

bined to form body-forcing inputs. The former quiet-time forcing was applied at 0-10 seconds, 20-80 seconds, and from 90 seconds to the end of the simulation, and the latter applied at 10-20 seconds and 80-90 seconds to simulate two successive thruster firing sequences. The maximum value of solute nonuniformity ξ_{max} was 0.6%, attained after 200 seconds (figure 32). However, a similar value of ξ_{max} was reached at a comparable time with another simulation using simply the first-mentioned quiet-time forcing levels *alone*. Thus, the response parameter was more sensitive to the long-lived acceleration components comprised of the quiet-time forcing than to the short-duration thruster firings, even though the frequency components of the thruster firings were in a sensitive range for this process (see sections 3.1.2.1 to 3.1.2.2). If the momentum input to the system is relatively small *and* if the disturbance is of short duration relative to the characteristic diffusion

times, the effects on the solute field may be minimal *provided* that the other components of the residual acceleration environment are conducive to crystal growth.

Some success by both the Soviets (Tatarchenko, 1990) and by the U.S. has been had in the areas of solutal and vapor crystal growth, which should suffer less from g-jitter effects due to the decreased role of buoyancy in less dense media. Van den Berg grew "crystallographically perfect" crystals of HgI_2 on Spacelab 3 (see, e.g., Kaldis et al., p. 396, 1987) which have not so far been reproduced or explained. Yoo et al. (1988) with accompanying modeling by Nadarajah et al. (1990) also obtained interesting but inconclusive results on Spacelab 3 on the growth of triglycine sulphate (TGS) crystals. This experiment will be reflown.

Palosz and Wiedemeier (1988) find a much larger mass flux in the low-g environment of Skylab relative to the earth environment for the chemically reacting system of GeSe-GeI_4, but no such dramatic variation in mass flux in space relative to earth for the nonreacting system of Ge-Se in the buffer gas Xe. This is to date not fully explained.

Recent numerical evidence on Bridgman crystal growth suggests that the solute field may not be as sensitive to disturbances as large as thruster firings, ***provided that*** *the momentum input to the system is small, the disturbance is of short duration relative to characteristic diffusion times,* ***and*** *if the other components of the residual acceleration environment are conducive to crystal growth. However, recall that the same system was shown to be sensitive to relatively low levels of steady residual acceleration, on the order of* $10^{-6}\ g_0$ *if the residual acceleration was parallel to the growth axis, and on the order of* $10^{-7}\ g_0$ *is the residual acceleration was perpendicular to the growth axis (section 3.1.1.2).*

Some success has been made in the areas of solutal and vapor crystal growth in a low-gravity environment, but additional analysis is necessary.

There is much to be learned in the space materials laboratory which results from replacing a strong steady background acceleration with a lower-level but highly variable one. We will require either a very long time in iterating on specific types of processes, or require a well-coordinated experimental/numerical/analytical effort to sort out the complex phenomena which are simultaneously occurring. Central to this effort will be the full characterization of the environment. Further basic fluid physics experiments must be performed with appropriate diagnostics in the space environment and adequate numerical models to elucidate the underlying phenomena.

3.2 *Surface phenomena*

This section is concerned with the effects of g-jitter on interfaces between phase boundaries (primarily liquid/liquid or liquid/gas interfaces). For background:

- on the classical theory of interfacial phenomena, see, e.g., Batchelor (1967);
- on the stability of interfaces, see, e.g., Drazin and Reid (1981);
- on (steady) gravity-related effects on float zones, see Clark and Wilcox (1980).

Here we choose to focus on float zones and liquid bridges, but for other low-gravity studies:

- on wetting and sloshing, see Bauer and Eidel (1990); Peterson et al. (1989); Langbein et al. (1990);
- on drop and bubble deformation, see Siekmann and Schilling (1989); Lundgren and Mansour (1988).

Although all of the complexities of buoyancy-driven convection which have been explored previously may still play an important role in space processing of float-zone experiments, additional complications arise due to the nature of the free surface. Of primary interest to this discussion are: (1) the severe sensitivity of interfaces to disturbances at the characteristic resonating frequency due to the low damping associated with free surfaces; and (2) the increased role of surface-tension driven (Marangoni, or thermocapillary) convection which accompanies the decreased importance of buoyancy-driven convection.

In a typical float-zone process, an energy source, e.g., a heater, laser or electron beam, is translated along the axis of a cylindrical feed rod, establishing a molten zone suspended between two solid crystals, as shown in figure 34. Contamination from the crucible and

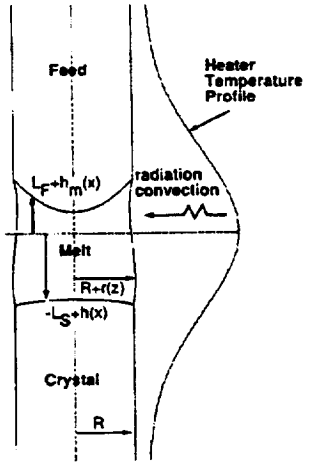

FIGURE 34. Schematic of the float-zone process (after Young and Chait, 1989)

the stresses associated with expansion or contraction of the charge within the crucible are avoided by this means of containerless processing. The effects of the deformable liquid/ gas free surface and surface tension must be accounted for, along with the heat transfer between the heater, ambient and solid and liquid phases, the fluid behavior of the melt, and he distribution of solute for determining the shape and stability of the zone.

Different aspects of the process may be isolated by simplifying this complex problem. The related case of a liquid bridge suspended between two cylindrical disks either at uniform temperature or at unequal temperatures give information about the behavior of stable zone shapes and important features of the fluid mechanics and heat transfer, but ignore the non-planar interfaces. Most of the work to date has focused on purely axial harmonic accelerations.

3.2.1 Quasisteady g

Martinez et al. (1987) have calculated stable zone shapes for isothermal liquid bridges under steady gravitational acceleration acting in the axial direction as a function of the static Bond number, which relates the relative magnitudes of gravitational to surface-tension forces:

$$Bo = \frac{\rho g L^2}{\sigma} \tag{10}$$

where σ is the surface tension and the radius R is the characteristic length, as shown in figure 35. The hydrostatic pressure (which increases with fluid depth) is balanced by the sur-

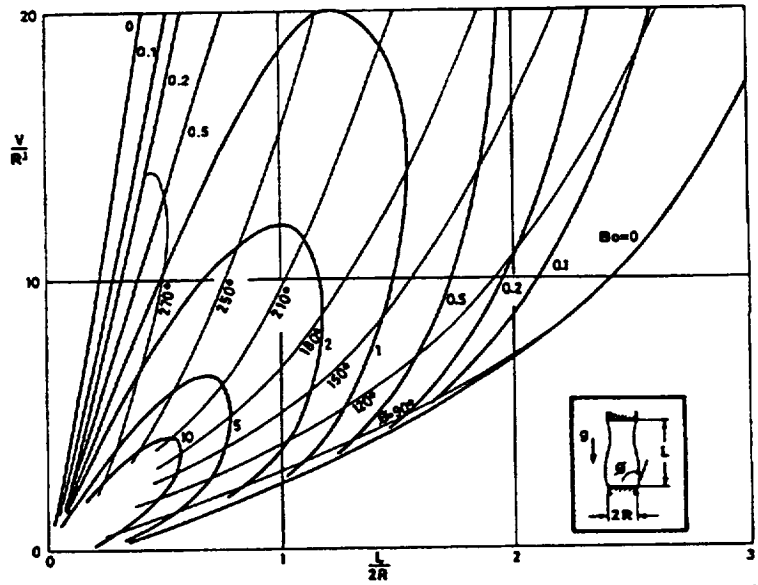

FIGURE 35. Stability limits for a liquid bridge of volume V and length L subjected to axially directed acceleration (after Martinez et al., 1987)

face energy in the geometrically curved free surface, acting through surface tension. The allowable length of the liquid zone is a function of its volume, the contact angle and the static Bond number. With decreasing levels of gravitational acceleration, the allowable length prior to zone breakage tends to increase. The theoretical maximum length that a liquid bridge can attain (the Rayleigh limit) is reached in a null gravitational field (Bo=0) with volume equivalent to $\pi R^2 L$ and a contact angle of 90°; this value is $2\pi R$. The classical Rayleigh (capillary) instability of liquid bridges is still a mechanism for zone failure in the space environment. However, another type of instability, the Heywang (dewetting) instability (see, e.g., Carruthers and Grasso, 1972), which would cause failure on earth for a silicone liquid bridge at R/L greater than unity, does not seem to appear in the low-gravity environment (see Langbein, 1986). The effect of eccentricity upon a bridge in the absence of gravity was studied by Perales et al. (1990).

For nonisothermal liquid zones between two inert solids, the analysis of Sekerka and Coriell (1979) indicates that, at earthbound gravity levels, the zone shape is dominated primarily by the capillary effect due to the large Bond number, while in low-g environments, the temperature gradient at the free surface will determine the zone shape. Alexander (1990) adds that g-jitter effects will require consideration also of dynamic distortion and of the dynamic Bond number and surface tension Reynolds number.

Intriguing results from space experiments on liquid bridges indicates that the low-gravity environment may have a profound effect on zone stability. Much more work in this area is necessary, particularly in numerically exploring the more realistic case of a three-dimensional body force (rather than a purely axially directed one).

3.2.2 Oscillatory g

Langbein (1986) and Zhang and Alexander (1990a) have shown that liquid columns are notoriously unstable to sinusoidal single-frequency g-jitter near their resonance frequency, with the tolerable acceleration levels dropping by up to two orders of magnitude. This is due to the low damping provided by the fluid in the absence of a solid wall. Figure 36 presents Langbein's results for a number of slenderness ratios for his one-dimensional linear oscillator model. In all cases, sharp drops in the tolerable acceleration (i.e., zone failure) are apparent corresponding to the Rayleigh instability. For typical bridges, the sensitive ranges are from 10^{-3} to 10^{-1} Hz and with tolerable magnitudes ranging from 10^{-4} g_0 to as low as 10^{-7} g_0. At higher frequency, instabilities of other mode shapes can also cause zone

failure. Zhang and Alexander further find, with their one-dimensional nonlinear model, that increasing viscosity serves to increase the tolerable acceleration at all frequencies.

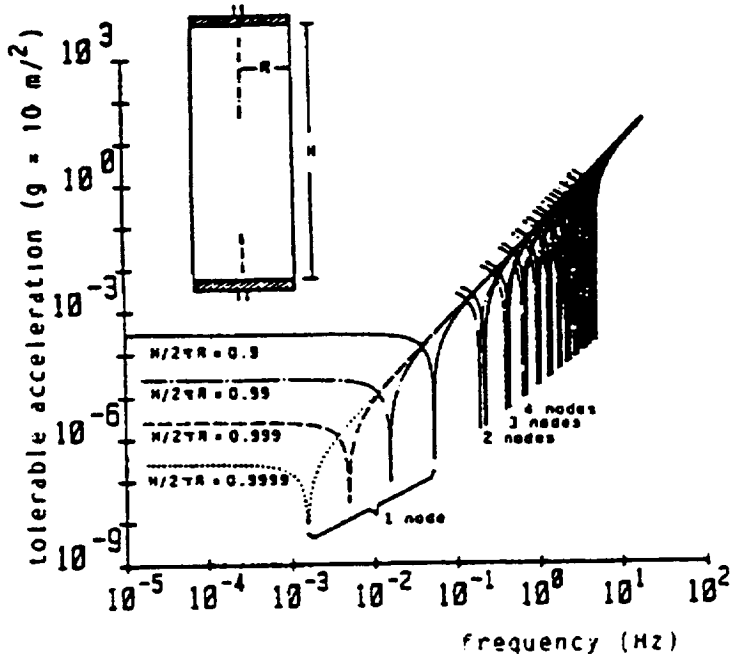

FIGURE 35. Tolerance of liquid bridges to sinusoidal axially directed residual accelerations (after Langbein, 1987)

Zhang and Alexander (1990b) found that, for nonisothermal bridges, the weaker buoyancy-driven flow and the surface-tension driven convection cells can interact to modify the thermal field. In a later work, Alexander and Zhang (1991) calculated the response of an axisymmetric nonisothermal liquid bridge with the properties of molten indium. The bridge was subjected to a purely axial harmonic acceleration with a frequency of 0.5 Hz. They found that surface-tension driven flow predominated over the buoyancy-driven flow. Varying the steady background levels from 10^{-4} g_0 to zero (again acting in the axial direction) indicated that the system was more sensitive to the effects of the free surface motion than to the internal buoyancy. A tolerability diagram for the liquid indium is presented in figure 36. and an assumed linearized variation in surface tension with temperature. The upper curve denotes tolerable g-level prior to zone breakage, and the lower curve represents a 10% shape change criterion. Note that, as was typical of the response for water and silicone oil liquid bridges discussed above, the tolerable acceleration drops dramatically near resonance frequencies, but the sensitive frequency range is higher, on the order of 1 to 10 Hz.

Other relevant work includes that of Meseguer (1988), who calculated the dynamic response of long inviscid liquid bridges between unequal discs in an axially aligned but

time-dependent low-gravity field. See also Meseguer et al. (1990). Planar interfaces be-

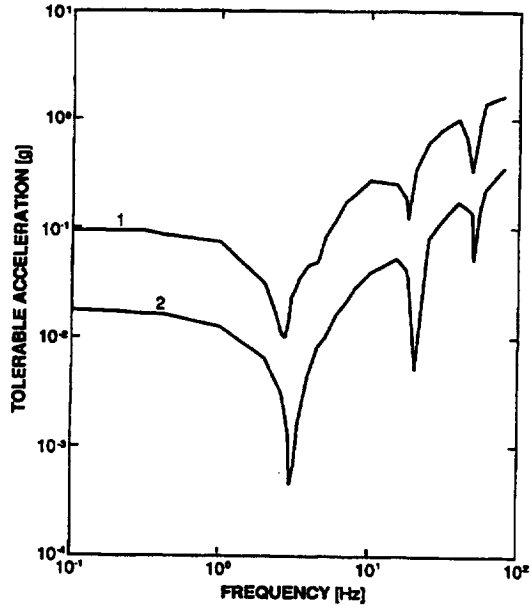

FIGURE 37. Tolerance of a liquid bridge with the properties of liquid indium to axially directed harmonic acceleration modulation (after Zhang and Alexander, 1990b)

tween two liquids also exhibit instability due to a resonance phenomenon (Jacqmin and Duval, 1988).

There is not a plethora of information on time-varying effects of the residual acceleration field on the float-zone process, but more is becoming available in the simpler case of liquid bridges, both isothermal and nonisothermal. The nature of the free surface is such that near resonant frequencies, the tolerable levels of residual acceleration drops dramatically by several orders of magnitude. Increasingly viscous flows are found to be less sensitive to g-jitter.

3.2.3 Transient g

Martinez (1987) found that residual acceleration had a significant effect on a liquid silicone bridge experiment. The maximum recorded acceleration was 10^{-4} g_0, which is certainly large enough to have an impact on the basis of the foregoing results. They tried to excite one type of instability near the Rayleigh limit, but found instead that a different one resulted. Langbein (1986) suggested that axial vibration actually enhances Rayleigh-limit stability. See also Martinez and Meseguer (1986); Carruthers (1974).

Extrapolation from liquid bridges to float zones is not straightforward. The surface of the hot melt almost inevitably absorbs contaminants from the surrounding medium, which can

greatly alter the surface tension. In addition, the high-*Pr* fluids used for typical liquid bridges exhibit a very different response to *g*-jitter than the low-*Pr* semiconductors typically grown with this method (Ramachandran and Winter, 1990).

The first experiment to explicitly correlate the effects of the space acceleration environment to *any* materials process was the float-zone growth of an indium crystal by Dunbar on STS-32 in January 1990 (see Dunbar and Thomas, 1990; also Dunbar et al., 1991a, b). Dramatic video footage which recorded the sinuous pulsation of the liquid zone in response to various disturbances such as treadmill operation, a thruster burn, and the relatively small disturbance of a cough, were all seen to exhibit substantial impacts on the zone shape. The ability of the melt to gracefully absorb large accelerations (with correspondingly large-amplitude deformations) indicates that there is still much to be understood in the float-zone process. The post-flight characterization of the samples are not yet available, at the time of the publication of this work.

It should be noted that several upcoming space experiments will attempt to quantify these effects as part of their experimental program.

The space environment was seen to alter stability limits and the path to instability for liquid bridges. The extrapolation from liquid bridges to the float-zone process is not straightforward due in part to the large variation in Prandtl number between typical fluids used for these respective processes. The only space experiment to date known by this author to directly correlate the acceleration environment to a materials process showed that disturbances as noisy as a thruster burn and as gentle as a cough caused significant modification to the shape of the free surface in the float-zone growth of indium. Although it greatly complicates the problem, numerical analysis should address the three-dimensionality of the body force. More research is necessary on both liquid bridges and float zone.

4. Conclusions

4.1 Space Station acceleration environment

Providing for the high-quality low-gravity environment currently envisioned for Space Station Freedom presents severe engineering challenges. Furthermore, there are inevitable unknowns associated with building any large space structure, for example, the behavior of joints in space and the effects of thermal cycling. If our space experience to date is any guide, we should expect *g*-jitter to *dominate* the acceleration environment due to the high-magnitude disturbances of crew activities, aerodynamic and aeromechanical forces and facility operations. Also of concern will be the contribution of the crew exercise equipment and life sciences centrifuge if they are not adequately isolated from the SSF residual acceleration environment. Learning from our experience in the design of the Orbiter, one may recall that the design expectation for the residual acceleration of the Shuttle was a steady-state 10^{-5} g_0; what was actually delivered was a multifrequency and impulsive acceleration environment more on the order of 10^{-3} g_0. This was not because the engineering judgment was poor, but simply because we have insufficient experience in designing a high-quality microgravity laboratory, especially on board an inhabited space vehicle. We have learned from building the Orbiter, but constructing large space structures presents a whole new set of engineering intricacies. We would be rather shortsighted and unimaginative if we do not expect to receive some surprises on SSF.

We must expect that, by its very nature, the residual acceleration environment will be highly three-dimensional and be comprised of both multiple-frequency and impulsive components. Variation will exist with translation and addition of masses on Space Station Freedom as well as from point to point within SSF. Some of the unavoidable contributions to the acceleration environment will occur at frequencies in the structural resonance, centrifuge operation and crew-activity regimes of 10^{-1} to 10 Hz. Unfortunately, it appears that some materials processes will be most sensitive to frequencies in the range of the fundamental structural response and lower. Vibration isolation will obviously be a critical prerequisite for both large sources of disturbance, e.g., the centrifuge and the exercise equipment, as well as for the experiments themselves for quality materials research and processing. Still, the isolation of very low-frequency structural vibrations is, in principle, an exceedingly difficult subject to address.

These comments are general for any SSF design, and not necessarily simply for the baseline configuration, because they are qualitative in nature. All large space structures will be subject to low-frequency structural oscillation and to orbital variation in residual accelera-

tion contributions from atmospheric drag. Inhabited structures will experience additional accelerations. Scaledown of SSF could be advantageous for the acceleration environment if it creates a higher-frequency structural resonance regime, decreases the overall atmospheric drag on the vehicle, and minimizes tidal accelerations by placing the laboratory spaces closer to the center of mass. All these effects should be beneficial from the standpoint of minimizing deleterious g-jitter effects on particular materials processes.

It is known that the orientation of g affects the fluid flow in any materials process. Current expectations are for SSF attitude to be controlled to within 0.5° of the torque equilibrium attitude, which will itself vary with each developmental configuration of SSF. Other uncertainties in the instantaneous local orientation of the residual acceleration will be introduced through contributions from structural oscillation, some equipment operation and crew activity. Very small misalignment (less than one degree) of the residual acceleration with the growth axis was shown to cause substantial modification of flow behavior in Bridgman growth. The (probably substantial) variation in the instantaneous direction of g and the high sensitivity of flows dominated by buoyant convection to the orientation of g both tend to indicate the following conclusion: from a materials processing standpoint, the tight control of SSF attitude is of less importance than the minimization of the overall steady and transient gravitational levels.

The specifications as written (tolerable g-level as a function of frequency) are of limited value in assessing the repercussions of SSF's acceleration environment on fluid behavior. They were created on the basis of a severely reduced set of physical laws through order-of-magnitude analysis, restricting their applicability to *single-frequency* disturbances and simplified systems. They simply do not address the realistic space environment or the complex fluid response, particularly the potentially disastrous effects of multifrequency summation and of impulsive transients. We must expect that the appearance and overall time domain response will surely be different from the single-frequency responses which are the basis for the specifications. To provide adequate specifications for future space platforms we should, in the near term, develop and apply sophisticated numerical models and correlate them with specifically planned experiments. Acceptable levels of performance criteria of each experiment could then be determined, and the allowable *combined* inputs could be identified and/or their frequency spectra. These spectra would have to be decomposed and backed out to allowable spectra for each individual source of vibration, while considering all other sources operating at the same time. As for transient disturbances, if their duration is significantly shorter than the appropriate diffusion times for the experiment, they could be classified as a group, regardless of their shapes or origins, and

specifications developed which would be general enough for many transient acceleration sources. Longer transients could be decomposed and analyzed using Fourier transform techniques and their effects deduced from the allowable experiment-specific frequency specifications. Admittedly, this procedure requires a high degree of coordination among the designers of various apparatus and their carrier platforms, together with the concerted numerical effort outlined above, but it is *feasible, timely and may provide practical and useful answers* at relatively low cost. Such a procedure may provide a much more sound alternative than the present specifications and their interpretation.

The accurate characterization of the low-gravity space environment and correlation to particular disturbances and specific materials processes therefore assume an immediate and vital importance. We need well-resolved three-dimensional experimental acceleration data from the apparatus vicinity for correlating the effects of the environment on the process. These acceleration data could be effectively used by experimenters, e.g., in concurrent monitoring of the integrity of a process, and in later interpretation of results. Reduction of the well-resolved acceleration data must become standardized and routinely employed to simplify these analyses. However, interpretation of g-jitter effects on actual experimental data is difficult, if not impossible, without resorting to a numerical model, based on the governing physical laws of the experiment as a whole. Such *explicitly designed* integrated experiments/models provide the only sensible means of systematically documenting g-jitter effects and interpretation of the experimental results. These data could also possibly be used to *tailor an experiment to the environment*, rather than vice versa, at least in some cases, as suggested by Alexander et al. (1991).

4.2 Implications of this environment for materials processes

General qualitative trends regarding the effects of g-jitter on materials processes have been documented too extensively to be altogether dismissed. This author feels that it is not sufficient to dismiss the current knowledge as too sparse and subjective and to simply wait until SSF is built for the real data. A summary of the effects of single-frequency g-jitter on several materials processes may be seen by referring to figure 38, which is reprinted from Alexander's (1990) review. The tolerance curves of Nadarajah et al. (1990) and SSF specifications have been added by this author for easy reference. It must be emphasized that these tolerance curves were calculated on the basis of *single*-frequency disturbances which were directed in a particular orientation; they do, however, provide some important qualitative conclusions. The results on directional solidification for an idealized Bridgman crystal growth indicate that there is some cause for concern, even at steady background levels of residual acceleration. This is particularly sobering in light of the extreme sensi-

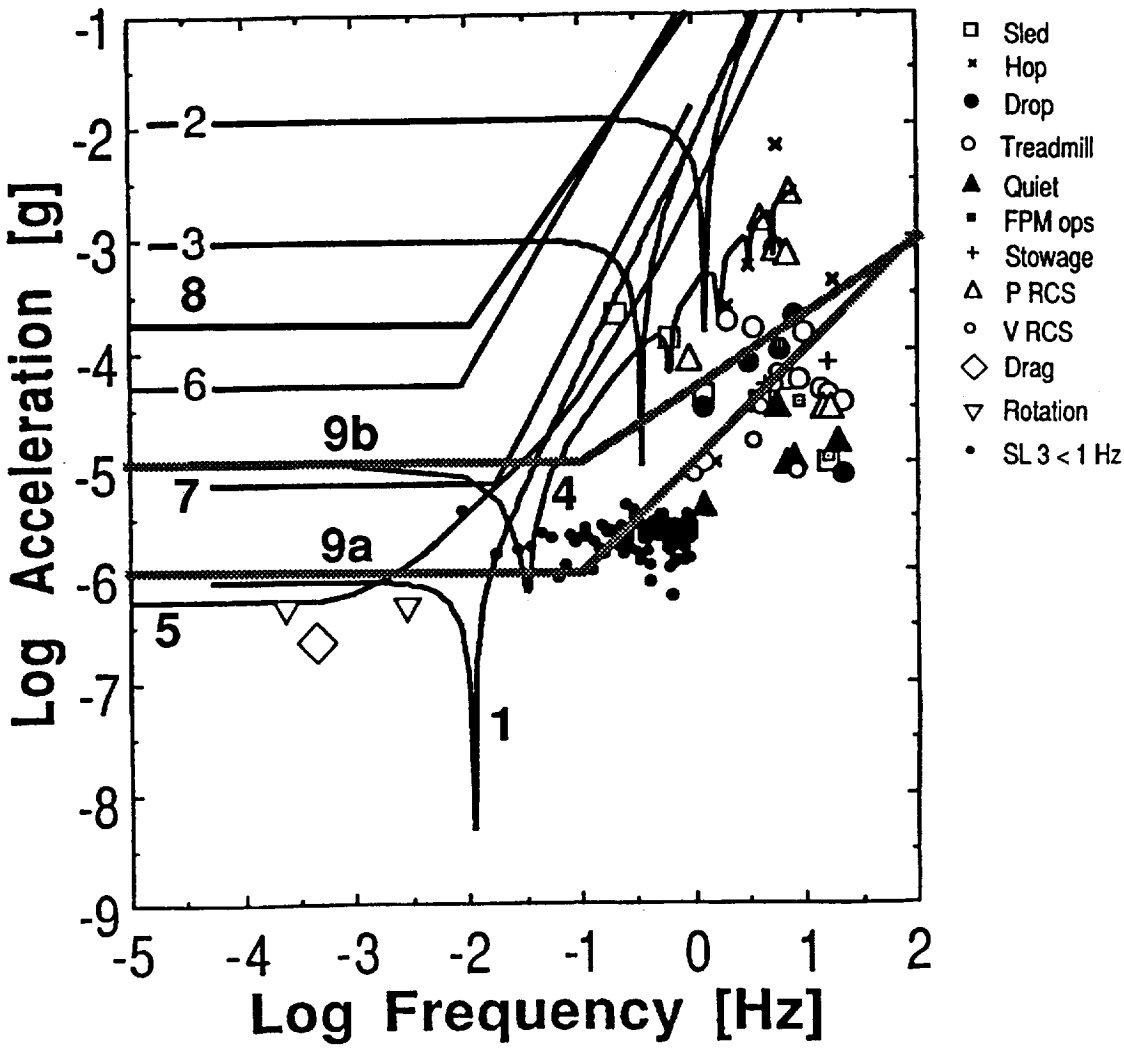

(1) Liquid column; n=1; $\Lambda = 0.9999$

(2) Liquid column; n=1; $\Lambda = 0.9$

(3) Liquid column; n=2; $\Lambda = 0.9999$

(4) Liquid column; Bo=0.002; $g=1.42 \times 10^{-5} g_o$

(5) Semiconductor melt growth

(6) Metal melt growth

(7) Thermodiffusion expt (Monti et al.)

(8) TGS solution crystal growth (Nadarajah et al.)

(9a), (9b) SSF requirements

FIGURE 38. Tolerable g-levels calculated for single-frequency harmonic forcing and experimentally measured acceleration peaks (after Alexander, 1990) with Space Station Freedom design specifications superimposed

tivity of melt growth processes to very slight misalignment of the body-force vector. The importance of this materials process dictates additional, carefully characterized research. Float-zone melting, another potentially important crystal-growth process in the low-gravity environment, involves a self-supported liquid bridge. Analogous physical sciences experiments have shown liquid bridges to be extremely intolerant of accelerations at their resonance frequencies. Solution and vapor crystal growth are less sensitive to the effects of buoyancy-driven flow than crystal growth from the melt. However, at present we lack the solid experimental/numerical database and the detailed fundamental understanding to be certain about the viability of *specific* materials or processes on SSF. Nevertheless, in general terms, it is likely that some materials processes will not be compatible with the residual acceleration environment associated with a large inhabited space structure. Although all of the problems associated with g-jitter are not solved by utilizing a free flyer, the concept may be a viable alternative platform for performing certain experiments which would be overly sensitive to the SSF environment. The option of using a free flyer is one which has been examined before, and this author feels that it ought to be incorporated into new SSF design and future utilization strategies.

The behavior of fluid systems sensitive to buoyancy-driven convection in response to a time-dependent body force is inextricably linked to characteristic diffusion time scales, a theme which is echoed over and over: for example, in the role of the viscous time scale in decreasing sensitivity of fluid motion to higher-frequency sinusoidal g-jitter. Since this behavior is by now well documented, indications that fluid behavior displays additive effects to multifrequency forcing (except perhaps near resonance conditions) are encouraging and can simplify numerical analysis greatly. The growth and decay of disturbances of the solutal fields in particular is typically very different from that of the momentum field due to vastly disparate characteristic diffusivities. If the duration of the disturbance is much shorter than the characteristic fluid diffusion time, the analysis of impulsive disturbances may be greatly simplified. In this case, the short-time fluid velocity response can be predicted based on the momentum input to the system by the transient disturbance alone, and not on the shape of the impulse (g as a function of time). The long-time behavior was shown to be dependent on solutal and thermal diffusivities as well as the initial momentum input. This insight makes the effects of multiple pulses and other transients more understandable and explains the critical nature of the time delay between pulses in a pulse train.

However, there are other complexities associated with the fundamental modification of transport in the space environment. Even if buoyancy-induced convection is reduced, we

cannot ignore the fact that other physical phenomena which are routinely neglected on earth (and, in general, rightly so), may become of competing or even dominating importance, e.g., Marangoni convection or radiative heat transfer. Since these phenomena are less well known from the standpoint of the familiar terrestrial laboratory, we must be expected to require some remedial education in the form of fundamental science research. In particular, high-temperature materials experiments which are exhaustively optimized by ground studies on the flight apparatus duplicates may behave unexpectedly when the unfamiliar action-at-a-distance effects of radiation compete with conduction due to the reduction of convection in space. Other components of materials processing have been left undiscussed here, such as electromagnetic damping, which may prove of practical importance in space processing of semiconductor melts, in particular, in providing simple solutions to *g*-jitter uncertainties.

There are profoundly fundamental differences in designing and utilizing a materials science laboratory in space; on that we can all agree. We would shortchange ourselves by locking into specific materials, processes or types of analysis at this point. Although we have made substantial strides in understanding the phenomena relevant to space processing, we will probably not fully know how to effectively utilize the space environment until our experience base is much more extensive and sound.

Acknowledgments

This work was supported by RTOP's 674-24-05, 674-21-05 and 412-00-00 under the Microgravity Science and Applications Division of NASA Headquarters. There are a great number of people who are responsible for providing information and encouragement in the process of writing this paper (although they are not responsible for my conclusions and opinions). A special thanks to: D. Thomas, G. Martin, F. Kohl, J. Sullivan, P. Bogert, W. Bastedo, J. Lubomski, R. Delombard and M. Horkachuk. In addition, the author appreciates the patience and care taken in the review of this manuscript in its unpolished form by M. Kassemi, T. Glasgow, A. Chait, and J.I.D. Alexander, and the invaluable contributions in its preparation by M. Oziomek. Also, thanks to C. Ménnétrier, for support in making presentations presentable and impossible tasks possible.

Bibliography

_____. "Measurement and characterization of the acceleration environment on board the Space Station." Workshop proceedings. Guntersville, AL. NASA/Marshall Space Flight Center and Teledyne Brown Engineering (August 11-14, 1986).

_____. "Spacecraft Dynamics as related to laboratory experiments in space". Workshop proceedings. NASA Marshall Space Flight Center (May 1-2, 1979). Also **NASA Conf Pub 2199** (1981).

Alexander, J.I.D. "Low-gravity experiment sensitivity to residual acceleration: a review". **Microgravity Sci and Tech 3**:52-68 (1990).

Alexander, J.I.D. and Lundquist, C.A. "Motion in fluids caused by microgravitational acceleration and their modification by relative rotation". **AIAA J 26**:34-39 (1988).

Alexander, J.I.D., Amiroudine, S., Ouazzani, J. and Rosenberger, F. "A numerical analysis of the sensitivity of Bridgman-Stockbarger solidification to steady and time-dependent residual acceleration". Submitted to **IUTAM Symposium on Microgravity Fluid Mechanics**. Bremen (1991).

Alexander, J.I.D., Ouazzani, J. and Rosenberger, F. "Analysis of the low gravity tolerance of Bridgman-Stockbarger crystal growth: Part II. Transient and periodic accelerations". **J Crystal Growth 113**:21-38 (1991).

Alexander, J.I.D., Ouazzani, J. and Rosenberger, F. "Analysis of the low gravity tolerance of Bridgman-Stockbarger crystal growth: Part I. Steady and impulse accelerations". **J Crystal Growth 97**:285-302 (1989).

Alexander, J.I.D., Ouazzani, J. and Rosenberger, F. "Analysis of low-gravity tolerance of model experiments for Space Station: Bridgman technique". **NASA Contract NAG8-684. First Semi-Annual Progress Report** (April 14, 1988).

Alexander, J.I.D. and Zhang, Y. "The sensitivity of a non-isothermal liquid bridge to residual acceleration". Submitted to **IUTAM Symposium on Microgravity Fluid Mechanics**. Bremen (1991).

Amin, N. "The effect of *g*-jitter on heat transfer". **Proc Roy Soc London A 419**:151 (1988).

Arnold, W., Jacqmin, D., Gaug, R. and Chait, A. "Convection phenomena in low-gravity processing: the GTE GaAs experiment". **AIAA 90-0409**. Presented at the 28th AIAA Aerospace Sciences Meeting, Reno, NV (1990).

Arnold, W., Jacqmin, D., Gaug, R. and Chait, A. "Three-dimensional flow transport modes in directional solidification during space processing". **J Spacecraft and Rockets 28**:238-243 (1991).

Barmatz, M. "Overview of containerless processing technologies". In G.E. Rindone, ed. (1982).

Batchelor, G.K. **An introduction to fluid dynamics**. Cambridge University Press (1967).

Bauer, H.F. "Natural frequencies and stability of circular cylindrical immiscible liquid systems". **Appl microgravity tech II**:27-44 (1989).

Bauer, H.F. and Eidel, W. "Linear liquid oscillations in a cylindrical container under zero-gravity". **Appl microgravity tech II**:212-220 (1990).

Biringen, S. and Peltier, L.J. "Computational study of 3-D Benard convection with gravitational modulation". **Phys Fluids A 2**:754-764 (1990). Also **AIAA Paper** 89-0068.

Brooks, R., Horton, A.T. and Torgesen, J.L. "Occlusion of mother liquor in solution-grown crystals." **J Crystal Growth 2**:279-283 (1968).

Brown, R.A. "Theory of transport processes in single crystal growth from the melt". **AIChE J 34**:881-911 (1988).

Camel, D. and Favier, J.J. "Scaling analysis of convective solute transport and segregation in Bridgman crystal growth from the doped melt". **J de Physique 47**:1001-1014 (1986).

Carruthers, J.R. and Grasso, M. "Studies of floating liquid zones in simulated zero gravity". **J Appl Phys 43**:436-445 (1972).

Carruthers, J.R. and Testardi, L.R. "Materials processing in the reduced-gravity environment of space". **Ann Rev Materials Science 13**:247-278 (1983).

Chait, A. "Transport phenomena in space processing: A modeling approach". Presented at **the XXII ICHMT Int'l Symposium on Manufacturing and Materials Processing**. Dubrovnik, Yugoslavia (August 27-31, 1990).

Chait, A. and Arnold, W. "Transient flow behavior on low-*g* vehicles: A numerical study". Presented at the Second Annual FIDAP Users Conference. Evanston, IL (October 2-4, 1988).

Chang, C.J. and Brown, R.A. "Radial segregation induced by natural convection and melt/solid interface shape in vertical Bridgman growth". **J Crystal Growth 63**:343-364 (1983).

Chassay, R.P. and Carswell, B. "Processing materials in space: The history and the future". **AIAA 87-0392**. Presented at the AIAA 25th Aerospace Sciences Meeting. Reno, NV (January 1987).

Chassay, R.P. and Schwaniger, A.J. "Low-*g* measurements by NASA". **NASA TM-86585** (1986).

Clark, P.A. and Wilcox, W.R. "Influence of gravity on thermocapillary convection in floating zone melting of silicon". **J Crystal Growth 50**:461-469 (1980).

Cooke, C., Koenig, M., Lepanto, J., Levine, G., Miller, J., Sargent, D. and Schlundt, R. "SDI Space Shuttle-based experiments for acquisition, tracking, and pointing: Definition of Space Shuttle operational environment". The Charles Stark Draper Laboratory. Cambridge, MA. R-1868 (April 1986).

Coriell, S.R., McFadden, G.B. and Murray, B.T. "Modeling of double-diffusive convection in vertical Bridgman growth". In **Proceedings of the VIIth European Symposium on Materials and Fluid Sciences in Microgravity.** Oxford, UK. (September 10-15, 1989). Also **ESA-SP-295** (January 1990).

Craik, A.D.D. "The stability of unbounded two- and three-dimensional flows subject to body forces: some exact solutions". **J Fluid Mech 198**:275-292 (1989).

Croll, A., Müller, W. and Nitsche, R. "Floating zone crystallization of silicon". Paper D1-WL-MHF-01. In **Scientific Results of the German Spacelab Mission D1**: Norderney Symposium (August 27-29, 1986), pp. 260-264.

Danilewsky, A.N. and Benz, K.W. "InP growth from In solutions under reduced gravity". **J Crystal Growth 97**:571-177 (1989).

Davis, S.H. "The stability of time-periodic flows". **Ann Rev Fluid Mech 8**:57-74 (1976).

Debe, M.K. "Industrial materials processing experiments on board the Space Shuttle Orbiter". **J Vac Sci Tech A 4**:273-280 (1986).

Demel, K. "Implications of acceleration environments on scaling materials processing in space to production" in workshop proceedings of "**Measurement and characterization of the acceleration environment on board the Space Station.**" Guntersville, AL. NASA/Marshall Space Flight Center and Teledyne Brown Engineering, pp. 5-1 to 5-34 (August 11-14, 1986).

Dewandre, T. and Roesgen, T. "Influence of micro-g disturbances on fluid experiments involving bubbles or drops: theory". **Appl microgravity tech I**: 142-150 (1988).

Dewandre, T. and Roesgen, T. "Influence of micro-g disturbances on fluid experiments involving bubbles or drops: applications". **Appl microgravity tech I**: 151-156 (1988).

Drazin, P.G. and Reid, W.H. **Hydrodynamic stability.** Cambridge University Press (1981).

Dressler, R.F. "Transient thermal convection during orbital spaceflight". **J Crystal Growth** 54: 523-533 (1981).

Duh, J-C. "Numerical modeling of enclosure convection". Paper IAF-89-403 from **40th Congress of the Int'l Astronautical Federation**, October 7-12, 1989. Beijing, China. (To be published in **Acta Astronautica.**)

Dunbar, B.J., Giesecke, R.L. and Thomas, D.A. "The microgravity environment of the Space Shuttle Columbia payload bay during STS-32". **NASA TP 3141** (1991a).

Dunbar, B.J., Thomas, D.A., and Schoess, J.N. "The microgravity environment of the Space Shuttle Columbia middeck during STS-32". **NASA TP 3140** (1991b).

Dunbar, B.J. and Thomas, D.A. "'Quick look' post-flight report: The microgravity disturbances experiment performed on STS-32 using the Fluids Experiment Apparatus". NASA Johnson Space Center (April 1990).

Eyer, A., Leiste, H. and Nitsche, R. "Floating zone growth of silicon under microgravity in a sounding rocket". **J Crystal Growth 71**:173-182 (1985).

Eyer, A., Kolbesen, B.O. and Nitsche, R. "Floating zone growth of silicon single crystals in a double-ellipsoid mirror furnace". **J Crystal Growth 57**:145-154 (1982).

Feuerbacher, B., Hamacher, H. and Jilg, R. "Compatibility of microgravity experiments with spacecraft disturbances". **Z Flugwiss Weltraumforsch 12**:145-151 (1988).

Gokoglu, S.A., Kuczmarski, M., Tsui, P. and Chait, A. "Convection and chemistry in CVD -- A 3D analysis of silicon deposition". In **Proceedings of the 7th European Conference on Chemical Vapor Deposition**. Perpignan, France (June 19-23, 1989).

Goldhirsch, I., Pelz, R.B. and Orszag, S.A. "Numerical simulation of thermal convection in a two-dimensional finite box". **J Fluid Mech 199**:1-28 (1989).

Gresho, P.M. and Sani, R.L. "The effects of gravity modulation on the stability of a heated fluid layer". **J Fluid Mech 40**: 783-806 (1970).

Griffin, P.R. and Motakef, S. "Influence of nonsteady gravity on natural convection during microgravity solidification of semiconductors: Part I. Time scale analysis". **Appl microgravity tech II**: 121-127 (1989a).

Griffin, P.R. and Motakef, S. "Influence of nonsteady gravity on natural convection during microgravity solidification of semiconductors: Part II. Implications for crystal-growth experiments". **Appl microgravity tech II**: 128-132 (1989b).

Grodzka, P.G. and Bannister, T.C. "Natural convection in low-*g* environments". **AIAA Paper 74-156** (1974).

Hackler, I.M. Presentation (May 1990).

Hamacher, H., Feuerbacher, B. and Jilg, R. "Analysis of microgravity measurements in Spacelab". Presented at the **Proceedings of the 15th International Symposium on Space Technology and Science**. Tokyo, Japan (1986a).

Hamacher, H., Fitton, B. and Kingdon, J. "The environment of earth-orbiting systems". In H.U. Walter (1987).

Hamacher, H., Merbold, U. and Jilg, R. "Analysis of microgravity measurements performed during D1". In **Scientific Results of the German Spacelab Mission D1**: Norderney Symposium (August 27-29, 1986b), pp. 48-56.

Hamacher, H., Merbold, U. and Jilg, R. "The microgravity environment of the D1 mission". Paper IAF-86-268 presented at the **37th International Astronautical Congress**. Innsbruck, Austria (October 4-11, 1986c).

Hurle, D.T.J. "Convective transport in melt growth systems". **J Crystal Growth 65**:124-132 (1983).

Jacqmin, D. and Duval, W.M.B. "Instabilities caused by oscillating accelerations normal to a viscous fluid-fluid interface". **J Fluid Mech 196**: 495-511 (1988).

Jacqmin, D. "Stability of an oscillated fluid with a uniform density gradient". **J Fluid Mech 219:**449-468 (1990).

Jaluria, Y. **Natural convection: Heat and mass transfer.** Pergamon Press (1980).

Kaldis, E., Cadoret, R. and Schonherr, E. "Crystal growth from the vapour phase". In H.U. Walter, ed. (1987).

Kamotani, Y., Prasad, A. and Ostrach, S. "Thermal convection in an enclosure due to vibrations aboard spacecraft". **AIAA J 19**:511-516 (1981).

Karchmer, A. Private communication (1990).

Kassemi, M. and Duval, W.M.B. "Interaction of surface radiation with convection in crystal growth by physical vapor transport". **J Thermophysics and Heat Transfer.** In press (October 1990).

Kassemi, M. and Duval, W.M.B. "Effect of gas and surface radiation on crystal growth from the vapor phase". **Int'l J of PhysicoChemical Hydrodynamics 11**:735-751 (1989).

Knabe, W. and Eilers, D. "Low-gravity environment in Spacelab". **Acta Astronautica 9**:187-198 (1982).

Koster, J.N. and Sani, R.L., eds. **Low-gravity fluid dynamics and transport phenomena.** Volume 130 in Progress in Astronautics and Aeronautics. AIAA (1990).

Lage, J.L. and Bejan, A. "The Ra-Pr domain of laminar natural convection in an enclosure heated from the side". To appear in **Numerical Heat Transfer** (1990).

Langbein, D. "The sensitivity of liquid columns to residual accelerations". N87-28695 (1987). Also **ESA-SP-256** (February 1987).

Langbein, D. "Fluid physics". In **Scientific Results of the German Spacelab Mission D1**: Nordorney Symposium (August 27-29, 1986), pp. 93-104.

Langbein, D., Großbach, R. and Heide, W. "Parabolic flight experiments on fluid surfaces and wetting". **Appl microgravity tech II**:198-211 (1990).

Legros, J.C., Sanfeld, A. and Velarde, M.G. "Fluid Dynamics". In H.U. Walter, ed. (1987).

Lindenmoyer, A. "Microgravity environment definition and requirements: program director's briefing" (December 4, 1989).

Liu, W.S., Wolf, M.F., Elwell, D. and Feigelson, R.S. "Low-frequency vibrational stirring: a new method for rapidly mixing solutions and melts during growth". **J Crystal Growth 82**:589-597 (1987).

Lu, Y-C, Shiau, J-J, Feigelson, R.S. and Route, R.K. "Effect of vibrational stirring on the quality of Bridgman growth". **J Crystal Growth 102**:807-813 (1990).

Lundgren, T.S. and Mansour, N.N. "Oscillations of drops in zero gravity with weak viscous effects". **J Fluid Mech 194**:479-510 (1988).

Markham, B.L., Greenwell, D.W. and Rosenberger, F. "Numerical modeling of diffusive-convective physical vapor transport in cylindrical vertical ampoules". **J Crystal Growth 51**:426-437 (1990).

Martinez, I. In **Proceedings of the 6th European Symposium on Materials Sciences in Microgravity Conditions**. Bordeaux, France. Also **ESA-SP-256** (1987).

Martinez, I., Haynes, J.M. and Langbein, D. "Fluid statics and capillarity". In H.U. Walter, ed. (1987).

Martinez, I. and Meseguer, J. "Floating liquid zones in microgravity". Paper D1-WL-FPM-04. In **Scientific Results of the German Spacelab Mission D1**: Nordorney Symposium (August 27-29, 1986), pp. 105-112.

McFadden, G.B. and Coriell, S.R. "Solutal convection during directional solidification". **AIAA 88-3635-CP** (1988).

Ménnétrier, C. and Duval, W.M.B. "Solutal convection with conduction effects inside a rectangular enclosure". Submitted to **Int'l J of Heat and Mass Transfer** (1990).

Meseguer, J. "Axisymmetric long liquid bridges in a time-dependent microgravity field". **Appl microgravity tech I**:136-141 (1988).

Meseguer, J., Sanz, A. and Perales, J.M. "Axisymmetric long liquid bridges stability and resonances". **Appl microgravity tech II**:186-192 (1990).

Monti, R. "Gravity jitters: effects on typical fluid science experiments". In J.N. Koster and R.L. Sani, eds. (1990).

Monti, R., Favier, J.J. and Langbein, D. "Influence of residual accelerations on fluid physics and materials science experiments". In H.U. Walter, ed. (1987).

Murray, B.T., Coriell, S.R. and McFadden, G.B. "The effect of gravity modulation on solutal convection during directional solidification". Submitted to **J Crystal Growth** (1990).

Müller, G. "A comparative study of crystal growth phenomena under reduced and enhanced gravity". **J Crystal Growth 99**:1242-57 (1990).

Nadarajah, A., Rosenberger, F. and Alexander, J.I.D. "Modeling the solution growth of TGS crystals in low gravity". **J Crystal Growth 104**:218-232 (1990).

Naumann, R.J. "Complementary use of Space Station and CDSF for microgravity experiments". White paper to Hon. John Boland (June 8, 1988).

Naumann, R.J. "Acceleration requirements for microgravity science and application: Experiments in the Space Station era". White paper to Hon. William Proxmire (June 8, 1988).

Naumann, R.J. "Susceptibility of materials processing experiments to low-level accelerations". In **Spacecraft Dynamics Related to Laboratory Experiments in Space.** Workshop proceedings. NASA Marshall Space Flight Center, Alabama (May 1-2,

1979). Also **NASA Conf Pub 2199**.

Naumann, R.J. and Mason, E.D. "Summaries of early materials processing in space experiments". **NASA TM-78240** (1979).

Olson, J.M. and Rosenberger, F. "Convective instabilities in a closed vertical cylinder heated from below. Part 1. Monocomponent gases". **J Fluid Mech 92**:609-629 (1979).

Olson, J.M. and Rosenberger, F. "Convective instabilities in a closed vertical cylinder heated from below. Part 2. Binary gas mixtures". **J Fluid Mech 92**:631-642 (1979).

Ostrach, S. "Low-gravity fluid flows". **Ann Rev Fluid Mech 14**:313-345 (1982).

Palosz, W. and Wiedemeier, H. "On the mass transport properties of the GeSe-GeI_4 system under normal and reduced gravity conditions". **J Crystal Growth 89**:242-250 (1988).

Perales, J.M., Sans, A. and Rivas, D. "Eccentric rotation of a liquid bridge". **Appl microgravity tech II**:193-197 (1990).

Peterson, L.D., Crawley, E.F. and Hansman, R.J. "Nonlinear fluid slosh coupled to the dynamics of a spacecraft". **AIAA J 27**: 1230-40 (1989).

Polezhaev, V.I., Lebedev, A.P. and Nikitin, S.A. In **Proceedings of the Fifth European Symposium on Materials Sciences under Microgravity.** Schloss Elmau, FRG. **ESA-SP-222** (1984).

Polezhaev, V.I. and Fedyoshkin, A.I. Izvestiya Akad Nauk SSSR, **Mekhanika Zhidkosti i Gaza** 3:11 (1980).

Roux, B., Ben Hadid, H. and Laure, P. "Numerical simulation of oscillatory convection in semiconductor melts". **J Crystal Growth 97**:201-216 (1989).

Radcliffe, M.S., Drake, M.C., Zvan, G., Fowlis, W.W., Alexander, J.I.D., Roberts, G.D., Sutter, J.K. and Bergman, E. In **Proceedings of the American Chemical Society Meeting**. New Orleans (1987).

Ramachandran, N. "*G*-Jitter convection in enclosures". Paper 8-MC-03. Presented at the **9th International Heat Transfer Conference**. Jerusalem, Israel (August 19-24, 1990a).

Ramachandran, N. "Thermal buoyancy and Marangoni convection in a two-fluid layered system -- A numerical study". **AIAA-90-0254**. Presented at the 28th AIAA Aerospace Sciences Meeting, Reno, NV. (1990b).

Ramachandran, N. and Winter, C.A. "The effects of *g*-jitter and surface tension induced convection on float zones". **AIAA-90-0654**. Presented at the 28th AIAA Aerospace Sciences Meeting, Reno, NV (1990). Also **J Spacecraft and Rockets 29:**514-522 (1992).

Regel, L. **Materials science in space.** Halsted Press (1987).

Rindone, G.E., ed. **Materials processing in the reduced gravity environment of space.**

Elsevier Science Publishing Co. (1982).

Rogers, M.J.B. and Alexander, J.I.D. "A strategy for residual acceleration data reduction and dissemination--from orbiting space laboratories". **Advances in Space Research 11**:5-8 (1991a).

Rogers, M.J.B. and Alexander, J.I.D. "Analysis of Spacelab-3 residual acceleration data using a prototype data reduction plan". **J Spacecrafts and Rockets 28**:707-712 (1991b).

Roppo, M.N., Davis, S.H. and Rosenblat, S. "Benard convection with time-periodic heating". **Phys Fluids 27**:796-803 (1984).

Rosenberger, F. and Müller, G. "Interfacial transport in crystal growth, a parametric comparison of convective effects". **J Crystal Growth 65**:95-104 (1983).

Roux, B., Ben Hadid, H. and Laure, P. "Numerical simulation of oscillatory convection in semiconductor melts". **J Crystal Growth 97**:201-216 (1989).

Rouzaud, A., Camel, D. and Favier, J.J. "A comparative study of thermal and thermosolutal convective effects in vertical Bridgman growth". **J Crystal Growth 73**:149-166 (1985).

Rupp, R., Müller, G. and Neumann, G. "Three-dimensional time-dependent modeling of the Marangoni convection in zone melting configurations for GaAs". **J Crystal Growth 97**:34-41 (1989).

Shahani, H., Fredriksson, H. and Smith, R.W. "The effect of gravity on the macrosegregation in tin silver alloys". **Appl microgravity tech II**:10-16 (1989).

Schneider, S. and Straub, J. "Influence of the Prandtl number on laminar natural convection in a cylinder caused by *g*-jitter". **J Crystal Growth 97**:235-242 (1989).

Schoess, J. "Honeywell In-Space Accelerometer STS-32: Final Report." (1990).

Schwabe, D. "Marangoni effects in crystal growth melts". **PCH PhysicoChemical Hydrodynamics 2**:263-280 (1981).

Schwabe, D. and Scharmann, A. "Some evidence for the existence and magnitude of a critical Marangoni number for the onset of oscillatory flow in crystal growth melts". **J Crystal Growth 46**:125-131 (1979).

Schwabe, D., Velten, R. and Scharmann, A. "The instability of surface tension driven flow in models for floating zones under normal and reduced gravity". **J Crystal Growth 99**:1258-64 (1990).

Searby, N. "Effect of science laboratory centrifuge on Space Station environment" in workshop proceedings of "**Measurement and characterization of the acceleration environment on board the Space Station.**" Guntersville, AL. NASA/Marshall Space Flight Center and Teledyne Brown Engineering, pp. 26-1 to 26-17 (August 11-14, 1986).

Sekerka, R.F. and Coriell, S.R. In **Proceedings of the 3rd symposium on Material Sci-**

ence in Space. Grenoble, France. Also **ESA-SP-142** (1979).

Siekmann, J. and Schilling, U. "On the vibrations of an inviscid liquid droplet contacting a solid wall in a low-gravity environment". **Appl micrograv tech II**:17-26 (1989).

Smutek, C., Bontoux, P., Roux, B., Schiroky, G.H., Hurford, A.C., Rosenberger, F. and de Vahl Davis, G. "Three-dimensional convection in horizontal cylinders: numerical solutions and comparison with experimental and analytical results". **Numerical Heat Transfer 8**:613-631 (1985).

"Space Station Freedom Microgravity Environment Definition: Study 3-01" (November 1988).

Space Station Freedom Program Office, Reston, Va. "Space Station Stage Summary Databook" (December 15, 1989).

Space Station Program. "Microgravity environment for baseline and selected alternate configurations". Document No. PSH-520-R88-005. SE&I Report (October 3, 1988).

Spradley, L.W. "Thermoacoustic convection of fluids in low gravity". **AIAA-74-76** (1974).

Spradley, L.W., Bourgeois, S.V. and Lin, F.N. "*G*-jitter convection of confined fluids in low gravity". In L. Steg., ed. (1977).

Steg, L., ed. **Materials sciences in space with application to space processing.** Volume 52 of Progress in Astronautics and Aeronautics. AIAA (1977).

Sullivan, J. Wyle Laboratories. Private communication (1990).

Tatarchenko, V.A. Presented at **28th Proceedings of COSPAR**. The Hague. Netherlands (1990).

Thomas, D. NASA Johnson Space Center. Private communication (1990).

Thornton, W.E. "A method of isolating treadmill shock and vibration on spacecraft". **NASA TM 100 474** (1989).

Tillberg, E. and Carlberg, T. "Semiconfined Bridgman growth of germanium crystals in microgravity". **J Crystal Growth 99**:1265-72 (1990).

Vinals, J. and Sekerka, R. "Effect of *g*-jitter on the spectrum of excitations of a free fluid surface: stochastic formulation". **AIAA-90-0652** (1990).

Wadih, M. and Roux, B. "Natural convection in a long vertical cylinder under gravity modulation". **J Fluid Mech 193**:391-415 (1988).

Walter, H.U., ed. **Fluid sciences and materials science in space: A European perspective.** Springer-Verlag (1987).

Walter, H.U., Belouet, C. and Malmejac, Y. "Industrial potential of microgravity". In H.U. Walter, ed. (1987).

Westphal, G.H. "Convective transport in vapor growth systems". **J Crystal Growth 65**:105-123 (1983).

Wiedemeier, H., Klaessig, F.C., Irene, E.A. and Wey, S.J. "Crystal growth and transport rates of GeSe and GeTe in a microgravity environment". **J Crystal Growth 31**:35-43 (1975).

Wilcox, W.R. "Influence of convection on the growth of crystals from solution". **J Crystal Growth 65**:133-142 (1983).

Witt, A.F., Gatos, H.C., Lichtensteiger, M. and Herman, C.J. "Crystal growth and segregation under zero gravity: Ge". **J Electrochem Soc 125**:1832-40 (1978).

Witt, A.F., Gatos, H.C., Lichtensteiger, M. Lavine, M.C. and Herman, C.J. "Crystal growth and steady-state segregation under zero gravity: InSb". **J Electrochem Soc 122**:276-283 (1975).

Xia, Q. and Yang, K.T. "Linear response of the temperature and flowfields in a square enclosure to imposed wall temperature oscillations". Paper 8-MC-02, presented at the **9th International Heat Transfer Conference**. Jerusalem, Israel (August 19-24, 1990).

Yoo, H-D, Wilcox, W.R. andLal, R. "Modeling the growth of triglycine sulphate crystals in Spacelab 3". **J Crystal Growth 92**:101-117 (1988).

Young, G.W. and Chait, A. "Steady state thermosolutal diffusion in a float zone". **J Crystal Growth 96**:65-95 (1989).

Zappoli, B. "Interaction between convection and surface reactions in physical vapor transport in rectangular, horizontal enclosures". **J Crystal Growth 76**:449-461 (1986).

Zeren, R.W. and Reynolds, W.C. "Thermal instabilities in two-fluid horizontal layers". **J Fluid Mech 53**: 305-327 (1972).

Appendix A

Nondimensional quantities

In general, the choice of appropriate scales for length, temperature, velocity and pressure can allow one to nondimensionalize the governing equations and consider larger classes of problems which are defined by relevant nondimensional quantities (see, e.g., Legros et al., 1987). The ratio of buoyant to inertial forces in thermal convection is expressed by the Grashof number, Gr_T

$$Gr_T = \frac{g\beta\Delta T L^3}{\nu^2} \tag{A.1}$$

where g is the relevant gravitational acceleration; β is the coefficient of thermal expansion; ΔT is the temperature difference; L is a characteristic dimension; and ν is the kinematic viscosity. This properly expresses the buoyant force in the above expression when density can be represented as a linear function of temperature over the range of interest (i.e., Boussinesq approximation). In many materials processes, the density variation in liquids is inextricably linked to the concentration field. When the density variation is primarily controlled by solutal gradients, the solutal Grashof number, Gr_s is, analogously:

$$Gr_s = \frac{g\alpha\Delta C L^3}{\nu^2} \tag{A.2}$$

where the buoyant force is represented in a linearized Boussinesq fashion by $\alpha\Delta C$, the product of the coefficient of solutal expansion and the concentration difference. In situations in which thermal and solutal convection are competitive, the relevant Grashof number appropriately attributes the overall density variation to the buoyant force:

$$Gr = \frac{g\Delta\rho L^3}{\rho\nu^2} \tag{A.3}$$

There are certainly several possible choices for L, including the height of the solutal or velocity boundary layer, the smallest dimension for a rectangular enclosure, the length of the melt region in Bridgman growth, and the radius of the ampoule. Note that all but the last may themselves be functions of time. In some cases, the choice of L is not immediately clear, and there is some variation in the literature, for example, in choosing the diameter of

the cylinder in natural convection or, alternatively, the radius. For cases in which the density variation changes rapidly with space, the appropriate Grashof number may be defined in terms of gradient, i.e., $Ra_t = g\beta(\partial T/\partial x)L^4/\nu^2$, as pointed out by Ostrach (1982).

The Prandtl number relates the importance of the momentum time scale to thermal time scale:

$$Pr = \frac{\nu}{\kappa} \tag{A.4}$$

where κ is the thermal diffusivity. The Rayleigh number, $Ra = Gr * Pr$ or:

$$Ra = \frac{g\beta\Delta TL^3}{\nu\kappa} \tag{A.5}$$

is another way of expressing the relative magnitudes of heat transfer by convection and by conduction.

The nondimensional forcing (i.e., the jitter) can be expressed by the Strouhal number, St:

$$St = \frac{\omega L^2}{\nu} \tag{A.6}$$

where ω is the characteristic frequency of the forcing. The Schmidt number relates viscous to species diffusivity:

$$Sc = \frac{\nu}{D} \tag{A.7}$$

where D is the molecular diffusivity.

In the consideration of free-surface or Marangoni flows, the important parameters are the Bond number Bo:

$$Bo = \frac{\rho g L^2}{\sigma} \tag{A.8}$$

(where ρ is the density and σ is the surface tension) which compares the hydrostatic pressure, tending to maintain a flat surface, to the surface-tension effect, tending to cause a

curved surface. The Marangoni number relates the force associated with surface tension gradient to the viscous force:

$$Ma = \frac{\sigma \Delta T L \left(\partial \sigma / \left(\partial T\right)\right)}{\rho \nu^2} \tag{A.9}$$

A surface tension Reynolds number, Re_s, can also be defined as:

$$Re_s = \frac{\gamma_T \Delta T D}{\mu \nu} \tag{A.10}$$

where γ_T is the surface tension gradient with respect to temperature and μ is the absolute viscosity. For a good discussion of other relevant dimensionless parameters, see Legros et al. (1987).

Appendix B

Merits and simplifications of various types of analysis

B.1 Types of analysis

This appendix attempts to give the reader a basic understanding of different types of analyses used for assessing the effects of g-jitter on materials processing (although the comments can be generalized to other problems as well).

B.1.1 Order-of-magnitude [O(M)] analysis

Dimensional analysis is a simplified approach to providing information on general trends with limited computational effort. Characteristic reference scales for length, time, velocity, etc. are chosen (e.g., boundary-layer height, momentum diffusion time scale, growth rate) which are presumed to reliably define the important physics of the process of interest. These scales are applied to the appropriate governing equations for mass, momentum, species and energy. Characteristic dimensionless groups are then identified which allow the term-by-term comparison of the relative importance, or order of magnitude, of each. For additional information, see, e.g., Monti et al. (1987); Ostrach (1982); Alexander (1990).

The validity of the predictions of such an analysis will depend upon how faithfully the scales chosen represent the transport mechanisms in the problem. Therefore, quantitative reliance on order-of-magnitude analysis alone is extremely dangerous for this class of problems for a variety of reasons. The choice of appropriate characteristic scales may not be immediately obvious due to the inherently multiparametric nature of these problems. The dominant mechanisms for transport (e.g., thermal vs. solutal convection) may change during the course of a single crystal growth (see, e.g., Nadarajah et al., 1990) which means that not only are the scales (such as boundary-layer height) themselves variable in time, but the very criteria on which to choose the relevant scales change during the process. Thus, for many of the materials processes of interest, the relevant scales are unknown *a priori*, leading to estimates which may be orders of magnitude off the mark, even for steady residual gravity (Alexander, 1990; Ramachandran and Winter, 1990). In addition, the single-frequency nature of the disturbance used in O(M) analysis may lead to incorrect predictions when extrapolated directly to a multifrequency and impulsive residual acceleration environment such as will be found aboard the Shuttle and Space Station Freedom. Evidence from the DMOS experiment suggests that fluid response to a such an environ-

ment is additive (see Alexander, 1990). This means that reliance on estimates which are based on a response to a single-frequency disturbance for the simulation of a multiple-frequency environment could dangerously overpredict actual tolerance levels.

The limitations of this approach have been clearly set forth by Alexander (1990) and Ramachandran and Winter (1990), among others. Comparison of Rouzaud et al.'s (1985) and Camel and Favier's (1986) O(M) analysis to the direct numerical simulation of Chang and Brown (1983) in figure B.1 of dopant uniformity in directionally solidified crystals indi-

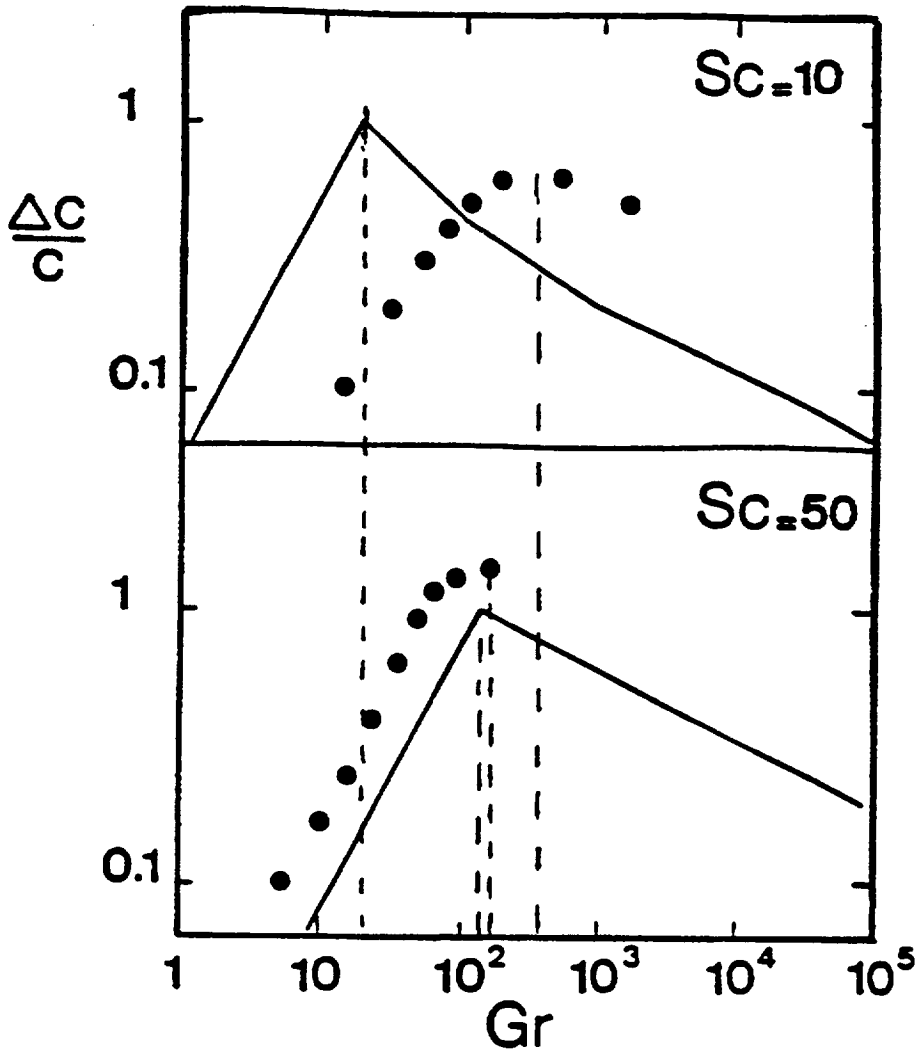

FIGURE B.1. Comparison of order-of-magnitude estimates (solid lines) with direct numerical simulation of Chang and Brown (1983; dots) for lateral solute uniformity in directional solidification as a function of Grashof number (after Alexander, 1990)

cates that, while the radial segregation was predicted by O(M) analysis reasonably well for a Schmidt number of 50, the results were significantly underpredicted for a Schmidt num-

ber of 10. For other cases of growth from the melt, order-of-magnitude results are acceptable in some flow regimes but not in others (Alexander, 1990), or valid in some qualitative trends but unreliable in quantitative prediction of tolerable growth conditions (Nadarajah et al., 1990).

The lesson to be learned here is that O(M) analysis is very useful for what it's good for: an initial qualitative estimate of important parameters and fluid regimes and for establishing general trends in the data. For example, the shape of the frequency tolerance specification curves (figure 2, section 2.1) can be deduced from O(M) analyses. However, without numerical or experimental confirmation, quantitative results should be viewed with extreme caution.

B.1.2 Experimental analysis

Experimental analysis is ultimately the most reliable, but have produced few data points in our existing knowledge base due to:

- Foremost, a lack of *dedicated* experiments, with carefully measured acceleration data and boundary conditions in simple systems. Simple experiments can be designed to separate the many driving forces in a real system to elucidate the effects of residual acceleration.
- Real experiments to date have suffered from:
  - Acceleration measurements have been absent entirely, or not available at the site of the experiment itself;
  - Deduction of g-jitter effects were made from post-mortem analysis of, e.g., the segregation field alone. This can be extremely dangerous since many competing mechanisms affect the segregation behavior;
  - Lack of appreciation of potential g-jitter has resulted in experiments in which "bad" data are attributed to other aspects of the experiment, with no consideration made of the possibly profound implications of the residual acceleration variation. Many of the unsuccessful growth experiments aboard Mir may perhaps be linked to g-jitter, but no systematic studies have been done.

B.1.3 Numerical analysis

This approach is arguably the least costly method. It is perhaps of particular importance to carefully examine the completeness of the numerical model for experiments subject to these sorts of disturbances due to the complexity of the forces involved (see B.2). Three-dimensionality of the body force will almost certainly require a three-dimensional numer-

ical approach for reliable quantitative results. Well-defined physical parameters such as transport properties and/or surface tension as a function of temperature will make all the difference between a useful and relevant numerical simulation and the production of "paper crystals".

The solution of nonlinear partial differential equations require no sweeping changes in approach or outlook to model these flows, even for multiple-frequency problems, e.g., Alexander et al. (1990). However, they may be CPU-intensive especially for high-frequency jitter.

Another use of numerical analysis is in the examination of stability problems in problems involving time-periodic forcing, as by Gresho and Sani (1970); Biringen and Peltier (1990); Davis (1976); Roppo et al. (1984); Murray et al. (1990); Coriell et al. (1989); and McFadden and Coriell (1988). This can be of particular interest for problems which are known to be linearly unstable, e.g., liquid columns, as well as more complex cases such as subcritical bifurcations, etc.

A distinctly different and complementary stochastic approach to this class of problems is under scrutiny by Vinals and Sekerka (1990). This is especially valuable for studying the long-time effects of high-frequency g-jitter and for situations in which the spectrum of excitation is not known, and in which the primary interest is in the averaged or cumulative effects for a real-g spectrum at reasonable computational expense.

B.2 Implications of analysis simplification

It is inevitable that the numerical or analytical study which studies the effects of g-jitter on materials processing will be in some way simplified, due to the complex nature of the forcing and the variety of underlying transport phenomena which dictates the response of a particular system to the forcing. Some of these assumptions severely limit the applicability of a particular study. The following simplifications and some of their corollary shortcomings are routinely employed:

- The characterization of g-jitter as a single-frequency axially directed disturbance can be misleading, because the space environment has been shown to be far more complex (see sections 2.1, 2.2, 2.3). It is comprised of multiple-frequency components at varying levels over a broad range of frequency due to, e.g., structural vibration, machinery

operation, and repetitive astronaut motions. The response of a fluid system to such a system will be different from that obtained due to purely harmonic single-frequency forcing (sections 3.1.2.2, 3.1.3):

- Additive response. Evidence from the DMOS space experiment indicates that the disturbances generated by multiple frequencies may be additive, meaning that single-frequency analyses may underpredict the response (Alexander, 1990; see also section 3.1.2.2);
- Impulsive disturbances may also provoke undesirable long-lasting effects (Alexander et al., 1989; Griffin & Motakef, 1989; see also 3.1.3);
- Random excitation. Systems which are stable to sinusoidal oscillations of gravity may be unstable to random excitation, either temporally or spatially (Biringen and Peltier, 1989; see also 3.1.3.4).

- Three-dimensionality of the body force. It is impossible to ignore that the body force will be three-dimensional in nature (see section 2.3). Enforcing axisymmetry or two-dimensionality on a problem can cause artificial confinement effects (discussed by Roux et al., 1989) or implausible flow modes (Arnold et al., 1990 a, b). For a very low steady background gravity level of 10^{-6} g_0, the prediction of solute nonuniformity by the two-dimensional calculations of Alexander et al. (1989) was comparable to the three-dimensional results. However, raising the steady background level to a still relatively small value of 10^{-5} g_0 showed great variability between the two-dimensional and three-dimensional calculations. In fact, the two-dimensional results overpredicted solute nonuniformity at the interface by as much as 50% relative to the three-dimensional.
- Length of simulation. Due to the large disparity between momentum, heat and mass for typical fluid systems, the response of the velocity field to a transient body force may decay before the disturbance to the solute or thermal field deteriorates. To accurately gauge the effects of g-jitter on the latter fields, it is necessary to carry the simulation to the end of the relaxation phase for the appropriate field.
- Inclusion of species in the analysis of problems such as the directional solidification of a binary or ternary alloy may be very important to the physical understanding of the problem. In fact, solutal or thermosolutal convection may be the predominant drivers of natural convection in a low-g environment, e.g., McFadden and Coriell (1988); Ménétrier and Duval (1990). For alloys in which the solute gradient (due to incorporation or rejection of solute at the interface) causes an increase in density with height, convective instability may occur, even if the temperature gradient is such that the overall net density decreases with height.

- Neglect of radiative heat transfer in high-temperature environments in space may mean ignoring a competitive, or even dominating, mode of heat transfer (e.g., Kassemi and Duval, 1990). In addition, the type of radiation model used can be critical. For example, the gas phase in physical vapor transport can contribute significantly to the transport of radiant heat (Kassemi and Duval, 1989), an effect which is largely ignored in the literature.
- Planar interfaces. The simplification of planar interfaces means that radial temperature gradients (which are almost always present from a practical standpoint due to the mismatch in thermal conductivities between the solid, the melt and the ampoule) are not accounted for properly and therefore neglects the convection which they cause.
- Ill-quantified physical parameters make the difference between a good simulation and a virtual one. For example, the case of directional solidification, the conductivity of the crucible can be the most important determining factor for interface shape (Rouzaud et al., 1985; Brown, 1988). In problems with large thermal variation, the temperature dependence of properties such as thermal conductivity and density are of immense importance in reliably predicting quantitative trends. For some materials of commercial interest, e.g., HgCdTe, little data on these properties are available. Consequently, the researcher may simply use some averaged constant physical properties due to the lack of data or perhaps wishing to avoid the additional computational complexity.
- Extrapolation of results. It may not be straightforward to extrapolate from the results of research which focuses on fluid phenomena to an ultimate and final judgement on the crystal quality without consideration of such things as thermal stresses in the cooldown of the solid which generate increased dislocations.Tatarchenko (1990) discussed the frustration associated with doing intensive ground-based work for GaAs growth, and upon flight discovering that extrapolation of ground-based findings to the space environment was grossly inadequate.
- Effect of other presumed boundary conditions. Numerical simulation of low-Prandtl number fluids in semiconductor melts by Roux and Ben Hadid (1989) near the critical Grashof number range ($1 - 4 \times 10^4$) noted effects of other boundary conditions (adiabatic vs. conducting; rigid vs. free). It is essential that proper boundary conditions be used which reflect the actual experimental (or at least representative) data.

Combined experimental/numerical approaches are just beginning to be available. These complementary approaches will be essential in understanding phenomena under low-gravity conditions.

Appendix C

G-Jitter Bibliography

Following can be found a listing of references with particular application to *g*-jitter, sorted out into various categories:

Reviews/Overviews, Workshop proceedings

[1] _____. "Measurement and characterization of the acceleration environment on board the Space Station." Workshop proceedings. Guntersville, AL. NASA/Marshall Space Flight Center and Teledyne Brown Engineering (August 11-14, 1986).

[2] _____. "Spacecraft Dynamics as related to laboratory experiments in space." Workshop proceedings. NASA Marshall Space Flight Center (May 1-2, 1979). Also **NASA Conf Pub 2199** (1981).

[3] Alexander, J.I.D. "Low-gravity experiment sensitivity to residual acceleration: a review". **Microgravity Sci and Tech 3**:52-68 (1990).

[4] Barmatz, M. "Overview of containerless processing technologies". In G.E. Rindone, ed. (1982).

[5] Carruthers, J.R. and Testardi, L.R. "Materials processing in the reduced-gravity environment of space". **Ann Rev Materials Science 13**:247-278 (1983).

[6] Chait, A. "Transport phenomena in space processing: A modeling approach". Presented at **XXII ICHMT Int'l Symposium on Manufacturing and Materials Processing**. Dubrovnik, Yugoslavia (August 27-31, 1990).

[7] Chassay, R.P. and Carswell, B. "Processing materials in space: The history and the future". **AIAA 87-0392**. Presented at the AIAA 25th Aerospace Sciences Meeting. Reno, NV. (January 1987).

[8] Debe, M.K. "Industrial materials processing experiments on board the Space Shuttle Orbiter". **J Vac Sci Tech A 4**:273-280 (1986).

[9] Langbein, D. "Fluid physics." In **Scientific Results of the German Spacelab Mission D1**: Noderney Symposium (August 27-29, 1986), pp. 93-104.

[10] Monti, R., Favier, J.J. and Langbein, D. "Influence of residual accelerations on fluid physics and materials science experiments." In H.U. Walter, ed. (1987).

[11] Naumann, R.J. "Susceptibility of materials processing experiments to low-level accelerations". **N82-12118**.

[12] Naumann, R.J. "Complementary use of Space Station and CDSF for microgravity experiments". White paper to Hon. John Boland (June 8, 1988).

[13] Naumann, R.J. "Acceleration requirements for microgravity science and application: Experiments in the Space Station era". White paper to Hon. John Boland (June 8, 1988).

[14] Naumann, R.J. and Mason, E.D. "Summaries of early materials processing in space

experiments". **NASA TM** 78240 (1979).

[15] Ostrach, S. "Low-gravity fluid flows". **Ann Rev Fluid Mech 14**:313-345 (1982).

[16] Spradley, L.W., Bourgeois, S.V. and Lin, F.N. "*G*-jitter convection of confined fluids in low gravity." In L. Steg., ed. (1977).

[17] Walter, H.U., Belouet, C. and Malmejac, Y. "Industrial potential of microgravity." In H.U. Walter, ed. (1987).

Books

[18] Koster, J.N. and Sani, R.L., eds. **Low-gravity fluid dynamics and transport phenomena.** Volume 130 in Progress in Astronautics and Aeronautics. AIAA (1990).

[19] Regel, L. **Materials science in space.** Halsted Press. (1987)

[20] Rindone, G.E., ed. **Materials processing in the reduced gravity environment of space.** Elsevier Science Publishing Co. (1982).

[21] Steg, L., ed. **Materials sciences in space with application to space processing.** Volume 52 of Progress in Astronautics and Aeronautics. AIAA (1977).

[22] Walter, H.U., ed. **Fluid sciences and materials science in space: A European perspective.** Springer-Verlag (1987).

Low-gravity environment

[23] Alexander, J.I.D. and Lundquist, C.A. "Motion in fluids caused by microgravitational acceleration and their modification by relative rotation." **AIAA J 26**:34-39 (1988).

[24] Booz, Allen & Hamilton, "Overview of Space Station microgravity requirement". Presented to Dr. J.D. Bartoe, Chief Scientist, Office of Space Station (July 14, 1989).

[25] Chassay, R.P. and Schwaniger, A.J. "Low-*g* measurements by NASA." **NASA TM-86585** (1986).

[26] Dunbar, B.J., Giesecke, R.L. and Thomas, D.A. "The microgravity environment of the Space Shuttle Columbia payload bay during STS-32". **NASA TP 3141**(1991a).

[27] Dunbar, B.J., Thomas, D.A., and Schoess, J.N. "The microgravity environment of the Space Shuttle Columbia middeck during STS-32". **NASA TP 3140** (1991b).

[28] Dunbar, B.J. and Thomas, D.A. "'Quick look' post-flight report: The microgravity disturbances experiment performed on STS-32 using the Fluids Experiment Apparatus". NASA Johnson Space Center (April 1990).

[29] Feuerbacher, B., Hamacher, H. and Jilg, R. "Compatibility of microgravity experiments with spacecraft disturbances". **Z Flugwiss Weltraumforsch 12**:145-151 (1988).

[30] Hamacher, H., Fitton, B. and Kingdon, J. "The environment of earth-orbiting sys-

tems." In H.U. Walter (1987).

[31] Hamacher, H., Merbold, U. and Jilg, R. "Analysis of microgravity measurements performed during D1." In **Scientific Results of the German Spacelab Mission D1**: Nordorney Symposium (August 27-29, 1986), pp. 48-56. Or see: Hamacher, H., Merbold, U. and Jilg, R. "The microgravity environment of the D1 mission". Paper IAF-86-268. Presented at the **37th International Astronautical Congress.** Innsbruck, Austria (October 4-11, 1986).

[32] Knabe, W. and Eilers, D. "Low-gravity environment in spacelab". **Acta Astronautica 9**:187-198 (1982).

[33] Naumann, R.J. "Acceleration requirements for microgravity science and application: Experiments in the Space Station era". White paper to Hon. John Boland (June 8, 1988).

[34] Rogers, M.J.B. and Alexander, J.I.D. "A strategy for residual acceleration data reduction and dissemination--from orbiting space laboratories." **Advances in Space Research 11**:5-8 (1991).

[35] Rogers, M.J.B. and Alexander, J.I.D. "Analysis of Spacelab-3 residual acceleration data using a prototype data reduction plan." **J Spacecrafts and Rockets 28**:707-712 (1991).

[36] Schoess, J. "Honeywell In-Space Accelerometer STS-32: Final Report." (1990).

[37] "Space Station Freedom Microgravity Environment Definition: Executive Summary, Study 3-01" (November 1988).

[38] Space Station Freedom Program Office, Reston, Va. "Space Station Stage Summary Databook" (December 15, 1989).

[39] Space Station Program. "Microgravity environment for baseline and selected alternate configurations." Document No. PSH-520-R88-005. SE&I Report (October 3, 1988).

[40] Stavrinidis, C., Stark, H., Eilers, D., and Hornung, E. "Microgravity quality provided by different flight opportunities." **Microgravity science and technology III**:191-203 (1991).

[41] Thornton, W.E. "A method of isolating treadmill shock and vibration on spacecraft". **NASA TM 100 474** (1989).

Vibration isolation

[42] Grodsinsky, C.M. and Brown, G.V. "Nonintrusive inertial vibration isolation technology for microgravity space experiments". **NASA TM 102386** (1990).

[43] Grodsinsky, C.M. and Brown, G.V. "Low-frequency vibration isolation technology for microgravity space experiments". **NASA TM 1011448** (1989).

[44] Logsdon, K.A., Grodsinsky, C.M. and Brown, G.V. "Development of a vibration isolation prototype system for microgravity experiments". Presented at the **28th Proceedings of COSPAR.** The Hague, Netherlands (June 1990).

[45] Sinha, A. and Kao, C.K. "A new approach to active vibration isolation for microgravity space experiments". **NASA TM 102470** (1990).

[46] Thornton, W.E. "A method of isolating treadmill shock and vibration on spacecraft". **NASA TM 100474** (1989).

Transport phenomena

[47] Amin, N. "The effect of *g*-jitter on heat transfer". **Proc Roy Soc London A 419:**151 (1988).

[48] Bauer, H.F. and Eidel, W. "Linear liquid oscillations in a cylindrical container under zero-gravity". **Appl microgravity tech II**:212-220 (1990).

[49] Biringen, S. and Peltier, L.J. "Computational study of 3-D Benard convection with gravitational modulation." **Phys Fluids A 2**:754-764 (1990). Also **AIAA-89-0068.**

[50] Craik, A.D.D. "The stability of unbounded two- and three-dimensional flows subject to body forces: some exact solutions". **J Fluid Mech 198**:275-292 (1989).

[51] Davis, S.H. "The stability of time-periodic flows". **Ann Rev Fluid Mech 8**:57-74 (1976).

[52] Dressler, R.F. "Transient thermal convection during orbital spaceflight". **J Crystal Growth** 54: 523-533 (1981).

[53] Duh, J-C. "Numerical modeling of enclosure convection." Paper IAF-89-403 from **40th Congress of the Int'l Astronautical Federation** (October 7-12, 1989). Beijing, China. (To be published in **Acta Astronautica**.)

[54] Gresho, P.M. and Sani, R.L. "The effects of gravity modulation on the stability of a heated fluid layer." **J Fluid Mech 40**: 783-806 (1970).

[55] Grodzka, P.G. and Bannister, T.C. "Natural convection in low-*g* environments". **AIAA-74-156** (1974).

[56] Kamotani, Y., Prasad, A. and Ostrach, S. "Thermal convection in an enclosure due to vibrations aboard spacecraft". **AIAA J 19**:511-516 (1981).

[57] Legros, J.C., Sanfeld, A. and Velarde, M.G. "Fluid Dynamics". In H.U. Walter, ed. (1987).

[58] Monti, R. "Gravity jitters: effects on typical fluid science experiments." In J.N. Koster and R.L. Sani, eds. (1990).

[59] Monti, R., Favier, J.J. and Langbein, D. "Influence of residual accelerations on fluid physics and materials science experiments". In H.U. Walter, ed. (1987).

[60] Radcliffe, M.S., Drake, M.C., Zvan, G., Fowlis, W.W., Alexander, J.I.D., Roberts, G.D., Sutter, J.K. and Bergman, E. In **Proceedings of the American Chemical Society Meeting**. New Orleans (1987).

[61] Ramachandran, N. "*G*-Jitter convection in enclosures". Paper 8-MC-03. Presented at the **9th International Heat Transfer Conference**. Jerusalem, Israel (August 19-24, 1990).

[62] Roppo, M.N., Davis, S.H. and Rosenblat, S. "Benard convection with time-periodic heating". **Phys Fluids 27**:796-803 (1984).

[63] Schneider, S. and Straub, J. "Influence of the Prandtl number on laminar natural convection in a cylinder caused by *g*-jitter." **J Crystal Growth 97**:235-242 (1989).

[64] Spradley, L.W. "Thermoacoustic convection of fluids in low gravity". **AIAA-74-76** (1974).

[65] Wadih, M., Zahibo, N. and Roux, B. "Effect of gravity jitter on natural convection in a vertical cylinder." In J.N. Koster and R.L. Sani, eds. (1990).

[66] Wadih, M. and Roux, B. "Natural convection in a long vertical cylinder under gravity modulation". **J Fluid Mech 193:**391-415 (1988).

[67] Xia, Q. and Yang, K.T. "Linear response of the temperature and flowfields in a square enclosure to imposed wall temperature oscillations". Paper 8-MC-02, presented at the **9th International Heat Transfer Conference**. Jerusalem, Israel (August 19-24, 1990).

Interfacial phenomena

[68] Jacqmin, D. and Duval, W.M.B. "Instabilities caused by oscillating accelerations normal to a viscous fluid-fluid interface". **J Fluid Mech 196**: 495-511 (1988).

[69] Jacqmin, D. "Stability of an oscillated fluid with a uniform density gradient". **J Fluid Mech**. In press (1990).

[70] Vinals, J. and Sekerka, R. "Effect of *g*-jitter on the spectrum of excitations of a free fluid surface: stochastic formulation." **AIAA-90-0652.** (1990).

Directional solidification

[71] Alexander, J.I.D. and Ouazzani, J. "A pseudo-spectral collocation method applied to the problem of convective diffusive transport in fluids subject to unsteady residual accelerations." In the **Proc of the 6th Int'l Conf on Numerical Methods in Laminar and Turbulent Flow**, Swansea Wales, U.K. (July 11-15,1989).

[72] Alexander, J.I.D., Amiroudine, S., Ouazzani, J. and Rosenberger, F. "A numerical analysis of the sensitivity of Bridgman-Stockbarger solidification to steady and time-dependent residual acceleration". Submitted to **IUTAM Symposium on Microgravity Fluid Mechanics**. Bremen (1991).

[73] Alexander, J.I.D., Ouazzani, J. and Rosenberger, F. "Analysis of the low gravity tolerance of Bridgman-Stockbarger crystal growth: Part II. Transient and periodic accelerations". **J Crystal Growth 113:**21-38 (1991).

[74] Alexander, J.I.D., Ouazzani, J. and Rosenberger, F. "Analysis of the low gravity tolerance of Bridgman-Stockbarger crystal growth: Part I. Steady and impulse accelerations." **J Crystal Growth 97**:285-302 (1989).

[75] Alexander, J.I.D., Ouazzani, J. and Rosenberger, F. "Analysis of low-gravity toler-

ance of model experiments for Space Station". **NASA Contract NAG8-684 First Semi-Annual Progress Report** (April 14, 1988).

[76] Arnold, W., Jacqmin, D., Gaug, R. and Chait, A. "Convection phenomena in low-gravity processing: the GTE GaAs experiment". **AIAA 90-0409**. Presented at the 28th AIAA Aerospace Sciences Meeting, Reno (1990).

[77] Arnold, W., Jacqmin, D., Gaug, R. and Chait, A. "Three-dimensional flow transport modes in directional solidification during space processing". **J Spacecraft and Rockets 28**:238-243 (1991).

[78] Chait, A. and Arnold, W. "Transient flow behavior on low-*g* vehicles: A numerical study". Presented at the Second Annual FIDAP Users Conference. Evanston, IL (October 2-4, 1988).

[79] Coriell, S.R., McFadden, G.B. and Murray, B.T. "Modeling of double-diffusive convection in vertical Bridgman growth". In **Proceedings of the VIIth European Symposium on Materials and Fluid Sciences in Microgravity.** Oxford, UK. (September 10-15, 1989). Also **ESA-SP-295** (January 1990).

[80] Griffin, P.R. and Motakef, S. "Influence of nonsteady gravity on natural convection during microgravity solidification of semiconductors: Part I. Time scale analysis". **Appl microgravity tech II**: 121-127 (1989).

[81] Griffin, P.R. and Motakef, S. "Influence of nonsteady gravity on natural convection during microgravity solidification of semiconductors: Part II. Implications for crystal-growth experiments". **Appl microgravity tech II**: 128-132 (1989).

[82] Liu, W.S., Wolf, M.F., Elwell, D. and Feigelson, R.S. "Low-frequency vibrational stirring: a new method for rapidly mixing solutions and melts during growth". **J Crystal Growth 82**:589-597 (1987).

[83] Lu, Y-C, Shiau, J-J, Feigelson, R.S. and Route, R.K. "Effect of vibrational stirring on the quality of Bridgman-grown CdTe". **J Crystal Growth 102**:807-813 (1990).

[84] McFadden, G.B. and Coriell, S.R. "Solutal convection during directional solidification." **AIAA 88-3635-CP** (1988).

[85] Murray, B.T., Coriell, S.R. and McFadden, G.B. "The effect of gravity modulation on solutal convection during directional solidification." Submitted to **J Crystal Growth** (1990).

[86] Polezhaev, V.I. "Convective processes at low gravity". In **Proceedings of the 3rd European Symposium on Materials Science in Space.** Grenoble, France. **ESA-SP-142** (1979).

[87] Polezhaev, V.I., Lebedev, A.P. and Nikitin, S.A. In **Proceedings of the Fifth European Symposium on Materials Sciences under Microgravity.** Schloss Elmau, FRG. **ESA-SP-222** (1984).

[88] Polezhaev, V.I. and Fedyoshkin, A.I. Izvestiya Akad Nauk SSSR, **Mekhanika Zhidkosti i Gaza** 3:11 (1980).

[89] Roux, B., Ben Hadid, H. and Laure, P. "Numerical simulation of oscillatory convection in semiconductor melts." **J Crystal Growth 97**:201-216 (1989).

[90] Rouzaud, A., Camel, D. and Favier, J.J. "A comparative study of thermal and thermosolutal convective effects in vertical Bridgman growth". **J Crystal Growth 73**:149-166 (1985).

[91] Tillberg, E. and Carlberg, T. "Semiconfined Bridgman growth of germanium crystals in microgravity". **J Crystal Growth 99**:1265-72 (1990).

[92] Witt, A.F., Gatos, H.C., Lichtensteiger, M. and Herman, C.J. "Crystal growth and segregation under zero gravity: Ge". **J Electrochem Soc 125**:1832-40 (1978).

[93] Witt, A.F., Gatos, H.C., Lichtensteiger, M. Lavine, M.C. and Herman, C.J. "Crystal growth and steady-state segregation under zero gravity: InSb". **J Electrochem Soc 122**:276-283 (1975).

Protein crystal growth

[94] Nadarajah, A., Rosenberger, F. and Alexander, J.I.D. "Modeling the solution growth of TGS crystals in low gravity." **J Crystal Growth 104:**218-232 (1990).

[95] Yoo, H-D, Wilcox, W.R. and Lal, R. "Modeling the growth of triglycine sulphate crystals in Spacelab 3". **J Crystal Growth 92**:101-117 (1988).

Vapor crystal growth

[96] Kaldis, E., Cadoret, R. and Schonherr, E. "Crystal growth from the vapour phase". In H.U. Walter, ed. (1987).

[97] Palosz, W. and Wiedemeier, H. "On the mass transport properties of the GeSe-GeI_4 system under normal and reduced gravity conditions." **J Crystal Growth 89**:242-250 (1988).

[98] Wiedemeier, H., Klaessig, F.C., Irene, E.A. and Wey, S.J. "Crystal growth and transport rates of GeSe and GeTe in a microgravity environment." **J Crystal Growth 31**:35-43 (1975).

Liquid bridges

[99] Alexander, J.I.D. and Zhang, Y. "The sensitivity of a non-isothermal liquid bridge to residual acceleration". Submitted to **IUTAM Symposium on Microgravity Fluid Mechanics**. Bremen (1991).

[100] Bauer, H.F. "Natural frequencies and stability of circular cylindrical immiscible liquid systems". **Appl microgravity tech II**:27-44 (1989).

[101] Langbein, D. "The sensitivity of liquid columns to residual accelerations". In **Proceedings of the 6th European Symposium on Material Sciences under Microgravity Conditions.** Bordeaux, France (Dec. 2-5, 1986). Also **ESA-SP-256** (February 1987); N87-28695.

[102] Martinez, I. and Meseguer, J. "Floating liquid zones in microgravity." In **Scientific Results of the German Spacelab Mission D1**: Nordorney Symposium (August 27-29, 1986), pp. 105-112.

[103] Meseguer, J. "Axisymmetric long liquid bridges in a time-dependent microgravity field". **Appl microgravity tech I**:136-141 (1988).

[104] Meseguer, J., Sanz, A. and Perales, J.M. "Axisymmetric long liquid bridges stability and resonances". **Appl microgravity tech II**:186-192 (1990).

[105] Perales, J.M., Sans, A. and Rivas, D. "Eccentric rotation of a liquid bridge". **Appl microgravity tech II**:193-197 (1990).

[106] Zhang, Y. and Alexander, J.I.D. "Sensitivity of liquid bridges subject to axial residual acceleration". **Phys Fluids A 2**:1966-74 (1990).

[107] Zhang, Y. and Alexander, J.I.D. "Surface tension and buoyancy driven flow in a nonisothermal liquid bridge". Submitted to the **International J for Numerical Methods in Fluids** (Fall 1990).

Float zone

[108] Carruthers, J.R. "Studies of liquid floating zones on SL-IV: the third Skylab mission". **NASA TM 78240** (1974).

[109] Dunbar, B.J. and Thomas, D.A. "'Quick look' post-flight report: The microgravity disturbances experiment performed on STS-32 using the Fluids Experiment Apparatus". NASA Johnson Space Center (April 1990).

[110] Eyer, A., Leiste, H. and Nitsche, R. "Floating zone growth of silicon under microgravity in a sounding rocket". **J Crystal Growth 71**:173-182 (1985).

[111] Eyer, A., Kolbesen, B.O. and Nitsche, R. "Floating zone growth of silicon single crystals in a double-ellipsoid mirror furnace". **J Crystal Growth 57**:145-154 (1982).

[112] Croll, A., Muller, W. and Nitsche, R. "Floating zone crystallization of silicon." D1-WL-MHF-01. In **Scientific Results of the German Spacelab Mission D1**: Nordorney Symposium (August 27-29, 1986).

[113] Müller, G. "A comparative study of crystal growth phenomena under reduced and enhanced gravity". **J Crystal Growth 99**:1242-57 (1990).

[114] Ramachandran, N. and Winter, C.A. "The effects of *g*-jitter and surface tension induced convection on float zones". **AIAA-90-0654**. Presented at the 28th AIAA Aerospace Sciences Meeting, Reno, NV. Also submitted to **J Spacecraft and Rockets** (1990).

[115] Schwabe, D., Velten, R. and Scharmann, A. "The instability of surface tension driven flow in models for floating zones under normal and reduced gravity." **J Crystal Growth 99**:1258-64 (1990).

Drops, bubbles

[116] Dewandre, T. and Roesgen, T. "Influence of micro-g disturbances on fluid experiments involving bubbles or drops: theory." **Appl micrograv tech I**: 142-150 (1988).

[117] Dewandre, T. and Roesgen, T. "Influence of micro-g disturbances on fluid experiments involving bubbles or drops: applications." **Appl micrograv tech I**: 151-156 (1988).

[118] Lundgren, T.S. and Mansour, N.N. "Oscillations of drops in zero gravity with weak viscous effects." **J Fluid Mech 194**:479-510 (1988).

[119] Siekmann, J. and Schilling, U. "On the vibrations of an inviscid liquid droplet contacting a solid wall in a low-gravity environment". **Appl micrograv tech II**:17-26 (1989).

Wetting and sloshing

[120] Langbein, D., Großbach, R. and Heide, W. "Parabolic flight experiments on fluid surfaces and wetting". **Appl microgravity tech II**:198-211 (1990).

[121] Peterson, L.D., Crawley, E.F. and Hansman, R.J. "Nonlinear fluid slosh coupled to the dynamics of a spacecraft". **AIAA J 27**: 1230-40 (1989).

Appendix D

Accelerometers

A brief description of some of the accelerometers which have (or are soon to be) flown on the Shuttle follows. This is *not* meant to be comprehensive, or to provide an exhaustive listing of the capabilities of these accelerometers. The intent is rather to briefly highlight some of the distinguishing features of these instruments which may be commonly used by materials scientists. Three of the accelerometers (OARE, HiRAP and the SAMS) are contrasted in figure D.1 and table D.1.

D.1 The Orbital Acceleration Research Experiment (OARE).

The OARE, sponsored by the Office of Aeronautics and Exploration Technology (OAET), can resolve low-magnitude, low frequency signals and incorporates the Bell MESA sensor with a resolution of 10^{-9} g_0. Other system specifications are shown in table D.1 and figure D.1. Its original purpose was to measure on-orbit atmospheric drag on the Shuttle. It will be mounted in Orbiter's payload bay, but it can also be available for experiment use and as an independent check on the other accelerometers.

D.2 The High-Resolution Accelerometer Package (HiRAP).

The HiRAP, which predates the OARE, was also sponsored by OAET, and is mounted on Columbia's keel. Its location allows it to be used for documentation of transmission of vibrations or cross-checking, although it can also be used to measure atmospheric drag. This accelerometer has provided data during its 10 STS flights. Its system specifications are outlined in table D.1 and figure D.1.

D.3 The Space Acceleration Measurement System (SAMS).

The SAMS, developed at Lewis Research Center, can acquire up to several gigabytes of raw accelerometer data per mission, depending on the mission duration and desired frequency. It can be put in three different locations on the Orbiter (middeck, payload bay, or in the Spacelab module). The accelerometer can be somewhat tailored to experiment requirements by utilizing six different available low-pass frequency bands, as shown in figure D.1 and table D.1. Although it had not been flown at the time of this writing, it soon will be and will support microgravity Spacelab missions conducted by NASA in support of the Microgravity Sciences and Applications Division. This includes the International

Microgravity Lab (IML) series, the U.S. Microgravity Lab (USML) series, the U.S. Microgravity Payload (USMP) series, Spacelab Life Sciences (SLS-1), and two middeck missions per year. It will also be used in cooperation with NASDA on Spacelab J (SL-J).

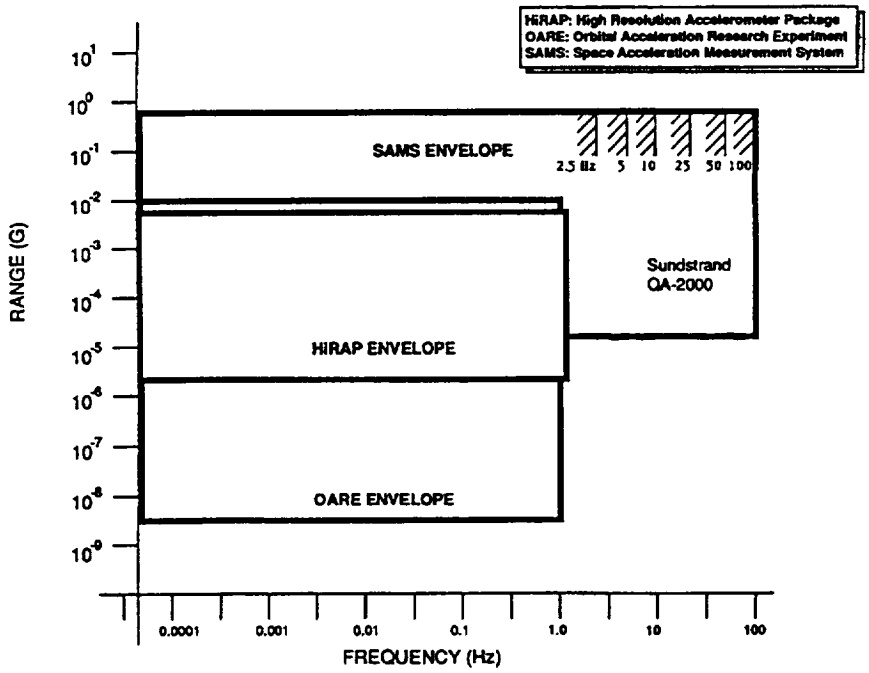

FIGURE D.1. Comparison of operational ranges of three accelerometer systems available for use on the Orbiter (courtesy of R. Delombard)

D.4 Honeywell In-Space Accelerometer (HISA).

The HISA was flown on the middeck of STS-32 in support of the microgravity disturbances experiment (see Schoess, 1990; Dunbar and Thomas, 1990). It provided full three-dimensional resolution of less than 10^{-6} g_0 at a 1.0 Hz sampling rate, and 8.7 x 10^{-6} g_0 at a 50 Hz sampling rate in the measurement range of 10^{-6} to 10^{-2} g_0. For further details and specs, see Schoess (1990).

TABLE D.1. Comparison of three accelerometer systems for use on the Orbiter (courtesy of R. Delombard)

Features	HIRAP	OARE	SAMS (middeck and Spacelab Module)
Data Products Utilization	STS aerodynamic/ atmospheric characterization	STS aerodynamic atmospheric characterization	Acceleration measurements for Principal Investigators
Mission Experience	10 missions to date Next: STS-28 (07/89)	First: STS-40 (SLS-1)	First: STS-40 (05/91) SLS-1
Sensor Location	Orbiter keel close to orbiter CG	Orbiter keel close to orbiter CG	On or near experiments and/or structure
Sensor and Resolution	Bell XI-79: 10 nG	Bell Mesa: 1 nG	Sundstrand QA-2000: 1 μG
Calibration	On-ground On-orbit bias temp. sensitivity	On-ground On-orbit bias and scale factor	On-ground On-orbit zero (Note 1)
Dynamic Range	±8 mG	±10 mG Range A ±1 mG Range B ±0.1 mG Range C	±0.5 G Range A ±0.05 G Range B ±5 mG Range C ±0.5 mG Range D
System Resolution	1 μG	3 nG	15 μG (QA-2000)
Frequency Response	< 1 Hz	< 1 Hz	< 100 Hz, < 50 Hz, < 25 Hz < 10 Hz, < 5 Hz, < 2.5 Hz
Data Storage Medium	STS tape recorder	Solid State/STS tape recorder	Optical disks
Data Recording Interval(s)	During reentry	During on-orbit operations and during reentry	During on-orbit operations
Power Consumption	5 Watts (Note 2)	100 Watts (Note 3)	65 Watts
Weight	2.5 lbs. (Note 2)	117 lbs. (Note 3)	76 lbs.

Note 1: System zero (not including the sensor)
Note 2: Without tape recorder and data handling electronics
Note 3: Without tape recorder

REPORT DOCUMENTATION PAGE

Form Approved
OMB No. 0704-0188

1. AGENCY USE ONLY (*Leave blank*)	2. REPORT DATE	3. REPORT TYPE AND DATES COVERED
	September 1994	Technical Memorandum

4. TITLE AND SUBTITLE

An Examination of Anticipated g-Jitter on Space Station and Its Effects on Materials Processes

5. FUNDING NUMBERS

WU-412-00-00

6. AUTHOR(S)

Emily S. Nelson

7. PERFORMING ORGANIZATION NAME(S) AND ADDRESS(ES)

National Aeronautics and Space Administration
Lewis Research Center
Cleveland, Ohio 44135-3191

8. PERFORMING ORGANIZATION REPORT NUMBER

E-6042

9. SPONSORING/MONITORING AGENCY NAME(S) AND ADDRESS(ES)

National Aeronautics and Space Administration
Washington, D.C. 20546-0001

10. SPONSORING/MONITORING AGENCY REPORT NUMBER

NASA TM-103775

11. SUPPLEMENTARY NOTES

References have been updated and corrected from the May 1991 publication. Responsible person, Emily S. Nelson, organization code 5110, (216) 433-3268.

12a. DISTRIBUTION/AVAILABILITY STATEMENT

Unclassified - Unlimited
Subject Category 29

12b. DISTRIBUTION CODE

13. ABSTRACT ***(Maximum 200 words)***

This study is concerned with the effects of g-jitter, the residual acceleration aboard spacecraft, on selected classes of materials processes. In particular, the anticipated acceleration environment aboard Space Station Freedom (SSF) and its potential effects are analyzed, but the topic is covered with a sufficient level of generality as to apply to other processes and to other vehicles as well. Some of the key findings of this study include:

- The present acceleration specifications for SSF are inadequate to assure a quality level low-g environment.
- The local g vector orientation is an extremely sensitive parameter for certain key processes, but can not be controlled to within the desired tolerance. Therefore, less emphasis should be placed upon achieving a tight control of SSF attitude, but more emphasis should be focused on reducing the overall level of the g-jitter magnitude.
- Melt-based crystal growth may not be successfully processed in the relatively noisy environment of a large inhabited space structure. Growth from vapor or from solution appears more favorable.
- A smaller space structure and/or a free flyer can provide better alternatives in terms of g-jitter considerations.
- A high priority (including budgetary) should be given to coordinated efforts among researchers, SSF designers, and equipment contractors, to develop practical experiment-specific sensitivity requirements.
- Combined focused numerical simulations and experiments with well-resolved acceleration measurements should be vigorously pursued for developing reliable experiment-specific sensitivity data.

Appendices provide an extensive cross-referenced bibliography, a discussion of the merits offered by g-jitter analysis techniques, as well as definitions of relevant nondimensional quantities and a brief description of available accelerometry hardware.

14. SUBJECT TERMS

g-jitter; Space station; Space processing; Low-gravity; Materials processing; Microgravity; Microgravity environment

15. NUMBER OF PAGES

119

16. PRICE CODE

A06

17. SECURITY CLASSIFICATION OF REPORT	18. SECURITY CLASSIFICATION OF THIS PAGE	19. SECURITY CLASSIFICATION OF ABSTRACT	20. LIMITATION OF ABSTRACT
Unclassified	Unclassified	Unclassified	